AD NUMBER
AD866558
NEW LIMITATION CHANGE

TO

Approved for public release, distribution unlimited

FROM

Distribution authorized to U.S. Gov't. agencies and their contractors; Administrative/Operational Use; Jan 1970. Other requests shall be referred to Air Force Materials Lab., Wright-Patterson AFB, OH 45433.

AUTHORITY

AFML/USAF ltr, 12 Jan 1972

RESEARCH AND DEVELOPMENT OF REFRACTORY OXIDATION-RESISTANT DIBORIDES

PART II, VOLUME II: PROCESSING AND CHARACTERIZATION

EDWARD V. CLOUGHERTY

RUSSELL J. HILL

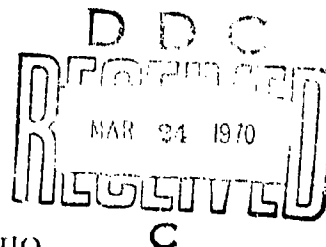WILLIAM H. RHODES

EDWARD T. PETERS

ManLabs, Inc.
and
Avco Corp.

TECHNICAL REPORT AFML-TR-68-190, PART II, VOLUME II

JANUARY 1970

AIR FORCE MATERIALS LABORATORY
AIR FORCE SYSTEMS COMMAND
WRIGHT-PATTERSON AIR FORCE BASE, OHIO

D D C

MAR 24 1970

C

NOTICES

When Government drawings, specifications, or other data are used for any purpose other than in connection with a definitely related Government procurement operation, the United States Government thereby incurs no responsibility nor any obligation whatsoever; and the fact that the Government may have formulated, furnished, or in any way supplied the said drawings, specifications, or other data is not to be regarded by implication or otherwise as in any manner licensing the holder or any other person or corporation, or conveying any rights or permission to manufacture, use, or sell any patented invention that may in any way be related thereto.

This document is subject to special export controls and each transmittal to foreign governments or foreign nationals may be made only with prior approval of the Air Force Materials Laboratory (MAMC), Wright-Patterson Air Force Base, Ohio 45433.

Distribution of this report is limited for the protection of technology relating to critical materials restricted by the Export Control Act.

RESEARCH AND DEVELOPMENT OF REFRACTORY OXIDATION-RESISTANT DIBORIDES

PART II, VOLUME II: PROCESSING AND CHARACTERIZATION

EDWARD V. CLOUGHERTY

RUSSELL J. HILL

WILLIAM H. RHODES

EDWARD T. PETERS

FOREWORD

This report was prepared by the Research Division, ManLabs, Inc. with the assistance of Avco Applied Technology Division, principal subcontractor on this program, under U.S. Air Force Contract No. AF33(615)-3671. The contract was initiated under Project 7350, "Refractory Inorganic Nonmetallic Materials," Task 735001, "Refractory Inorganic Nonmetallic Materials: Non-Graphitic." The work was administered under the direction of the Air Force Materials Laboratory, Ceramics and Graphite Branch, with John R. Fenter acting as project engineer.

This report covers the period from 15 September 1967 to 15 May 1969.

ManLabs personnel participating in this study included E. V. Clougherty, D. Kalish, E. T. Peters, R. A. Yeaton, J. Davis and V. Kousky.

The phases of work performed at Avco Corporation were under the direction of W. H. Rhodes and R. J. Hill with T. Vasilos responsible for the general administration. The personnel associated with the program and their project areas are as follows:

Hot Pressing	P. Jahn and A. Moses
Sintering	J. Centorino
Plasma Spraying	A. J. Delai
Metallography	R. Gardner and R. LeBlanc
Non-Destructive Testing	R. C. Stinebring and B. Killion

Fabrication services were also supplied by Battelle Memorial Institute, Raytheon Research Division and The Boeing Company.

The manuscript of this report was submitted by the authors in November 1969 for publication.

This technical report has been reviewed and is approved.

W. G. RAMKE
Chief, Ceramics and Graphite Branch
Metals and Ceramics Division
Air Force Materials Laboratory

ABSTRACT

Zirconium and hafnium diboride were procured in several 50 to 300 pound quantities. Powder specifications were developed for hot pressing grades of ZrB_2 and HfB_2 for processing of compositions containing additions of SiC and/or C.

Several hundred 2 and 3 inch diameter billets were fabricated and characterized by destructive and nondestructive methods. Extensive thermal, physical, chemical and mechanical property measurements, thermal stress resistance tests and oxidation resistance evaluations were performed for the range of compositions and microstructural variations of grain size and porosity prepared by hot pressing. The sizes of billets fabricated by hot pressing was scaled-up to 6 inches square by 2 to 3 inches high with no reduction in physical and mechanical integrity.

A system of ceramic additives, principally SiC and/or C employed with ZrB_2 and HfB_2 produced compositions which were hot pressed to full density with fine grain sizes of 2 to 10 microns. Compositional variation of SiC and C produced structures of varying oxidation resistance, mechanical properties and thermal stress resistance. The chief effect of the addition of SiC is an improvement in oxidation resistance; the addition of C, a decrease in the bulk elastic modulus. The additions singularly and combined effected improvements in mechanical properties principally by lowering the fabrication temperature to permit full densification without appreciable grain growth. The additions reduce diboride powder specifications for hot pressing with regard principally to allowable metal oxide and carbide impurity content; an in-processing reduction in initial oxygen content is effected by the additives.

Limited examination of other processing procedures performed without obtaining separate powders particularly suitable for individual methods provided information relative to the utilization of methods other than hot pressing. Silicon carbide could not be retained in plasma sprayed coating nor could it be formed along with ZrB_2 as a pyrolytically deposited coating. Pressureless sintering studies carried out with small specimens suggest that additions of reactive activating agents such as zirconium hydride enhance consolidation of ZrB_2 and ZrB_2-SiC compositions. Hot isostatic pressing produced dense, fine grained structures, one half inch diameter by 2 inches long of ZrB_2 and HfB_2 with no intentional additive. Compositions containing SiC and small amounts of carbon (10 volume percent) were also consolidated to near full density with no significant grain growth. Arc casting was successfully employed to produce a structure comprised of a ZrB_2 matrix with a ZrB_2+SiC eutectic and large graphite particles; a sound billet 2 inch diameter by 4 inches long was prepared. Attempts to employ conventional hot pressing to prepare filament and fiber reinforced structures using SiC whiskers, W filaments and Thornel-25 carbon yarn reinforcements were generally unsuccessful. The best results were obtained with the Thornel yarn in a ZrB_2 matrix.

TABLE OF CONTENTS

iv

TABLE OF CONTENTS (CONT)

LIST OF ILLUSTRATIONS

LIST OF ILLUSTRATIONS (CONT)

LIST OF ILLUSTRATIONS (CONT)

LIST OF ILLUSTRATIONS (CONT)

LIST OF TABLES

xi

LIST OF TABLES (CONT)

xiii

I. INTRODUCTION AND SUMMARY

A. Introduction

The diborides of zirconium and hafnium are the outstanding candidates among high melting intermetallic compounds, graphite composites, oxides, and coated refractory metals for applications which require thermochemical stability and oxidation resistance. Earlier studies of diboride compounds provided a good working description of the chemical, physical and thermodynamic properties relevant to material response to high temperature oxidizing environments ([1]*,[2]). Subsequently, extensive data derived from cold gas/hot sample furnace oxidation tests of polycrystalline composites containing ZrB_2 or HfB_2 with various additives designed to impart improved oxidation characteristics without sacrificing high temperature stability identified the SiC addition as the most beneficial composition ([3]). This study also generated mechanical property data for well characterized ZrB_2 and HfB_2 and diboride material response characteristics to hot gas/cold wall arc plasma tests. The results of transverse bend tests showed that strength levels of 40,000 to 60,000 psi were attainable for fine grained, high density ZrB_2 and HfB_2 over the range from room temperature to $1200^{\circ}C$ in inert atmospheres. Results of limited arc plasma testing suggested favorable dynamic oxidation resistance.

The present investigation was undertaken to prepare a number of diboride materials containing either ZrB_2 or HfB_2 as the principal component with selected additives designed to enhance one or more of the following: oxidation resistance, mechanical properties, and thermal stress resistance. Diboride materials, including ZrB_2 and HfB_2 with no additive, were fabricated with microstructural variations of grain size and porosity, principally by conventional hot pressing procedures which are suitable for the production of components such as nose caps, leading edges, vanes and similar objects anticipated for use in high velocity flight or reentry conditions.

The program was broadly divided into three phases: (1) composition and microstructure screening, (2) extensive properties testing, and (3) simulated application evaluations and verification of properties in scaled-up fabrication. In Phase One, oxidation, mechanical, and thermal screening tests of a wide range of compositions and microstructures were used to select a limited number of particularly attractive diboride materials. In Phase Two, the selected compositions and microstructures were fully characterized over a wide temperature range in terms of oxidation resistance, strength, elastic modulus, linear expansion, thermal conductivity, and steady state thermal stress resistance. Finally, in Phase Three, properties were redetermined for materials prepared in scaled-up billet sizes, and several application oriented evaluations including a test of a leading edge configuration subjected to simulated hypersonic flight heating were performed.

---

*The underscored numbers in parenthesis refer to references which are listed at the end of this report.

Processing aspects of this investigation included procurement, characterization and development of specifications for diboride powders and additive materials. Hot pressing was the principal method of fabrication studied and was employed for processing Phase One billets, 2.0 inch diameter by 0.7 inch high, for screening evaluations, Phase Two billets, 3.0 inch diameter by 1.0 inch high, for property measurements on selected diboride compositions and Phase Three billets, 6 inch square by 1.0 to 2.0 inch high, for application evaluations and scale-up studies. Hot pressed billets were examined by nondestructive testing procedures (4); and by several destructive characterization procedures. Density measurements and metallographic analyses were performed for numerous billets to provide grain size and porosity data. X-ray phase identifications, chemical analyses, electron probe microanalyses and quantitative metallographic phase assays were obtained for selected compositions. Fabrication specifications were developed.

Several other processing procedures were examined on a limited basis to ascertain preliminary data relevant to the utilization of methods other than hot pressing to prepare diboride composite structures. The secondary fabrication methods studied included pressureless sintering, press forging, plasma spraying, hot isostatic pressing, pyrolytic deposition and arc casting. Exploratory fabrication studies were also implemented to attempt to prepare fiber and filament reinforced diboride structures. It was anticipated that the structures developed by the secondary fabrication methods would be utilized for particular applications for which hot pressing methods might not be feasible. Tradeoffs in strength, oxidation resistance and possibly thermal stress resistance were anticipated for diboride materials fabricated by methods other than hot pressing. Detailed property evaluations performed for diboride structures prepared by hot pressing were not carried out for structures developed in the secondary fabrication studies. However, several diboride structures were hot pressed with porosity levels in the range 5 to 20% and with compositional variations of the various additives employed. Sufficient characterization data were generated for these structures to gain an assessment of the tradeoff consequences relative to higher density materials of closely controlled composition prepared by hot pressing.

Results of processing studies completed in Part I of this investigation were presented in a previous technical report (5) which contains a complete description of program progress for the first eighteen months of the investigation. The principal activities included the completion of the major powder procurements and the fabrication of numerous diboride compositions for Phase One screening evaluations. A limited number of billets were also fabricated for Phase Two property measurements and Phase Three evaluations. Secondary fabrication studies were also performed.

Separate reports were prepared to describe the studies completed in Part II (6-12).

B.   Summary of Processing and Characterization Study
      in Part I

Zirconium and hafnium diboride powders were procured in several lots ranging from fifty to three hundred pounds. Additive material

2

procurements included silicon carbide powders and fibers, hafnium silicide and boron silicide powders, hafnium metal, hafnium-tantalum alloy and chromium metal powders, tungsten filament, Poco graphite and Cabot Regal carbon powder and Thornel 25 graphite fibers. Extensive powder characterization results were obtained. Tentative powder specifications were developed for ZrB_2 and HfB_2.

Several hundred diboride billets were fabricated with and without one or more of the above additives by conventional hot pressing procedures. The diboride materials fabricated include the following basic compositions which are identified as follows: Material I, ZrB_2 with no additive; Material II, HfB_2 with no additive; Material III, HfB_2 with 20 v/o SiC; Material IV, HfB_2 with 30 v/o SiC; Material V, ZrB_2 with 20 v/o SiC; Material VI, HfB_2 with 4 v/o Hf-Ta alloy; Material VIII, ZrB_2 with 14 v/o SiC and 30 v/o C; Material X, ZrB_2 with 20 v/o SiB_6; Material XI, ZrB_2 with 8 v/o Cr; and Material XII, ZrB_2 with 5 to 50 v/o C.

Additional billets having variations from the basic compositions were also fabricated. The majority of the pressings were Phase One billets, 2.0 inch diameter by 0.7 inch high, although several dozen Phase Two billets, 3.0 inch diameter x 1.0 inch high and about a dozen Phase Three billets, 5.75 inch square by 1.0 to 2.0 inch high, were also prepared. All hot pressed billets were subjected to extensive nondestructive testing evaluations to provide sufficient data for subsequent development of property correlations and flaw identification criteria (4).

Considerable difficulty was encountered in the fabrication of crack free billets of Materials I and II, which do not contain intentional additives. Furthermore, fully dense billets of Materials I and II could not be prepared without significant grain growth. A unique role for ceramic additives in enhancing densification by hot pressing, heretofore not fully understood nor exploited, was found. The incidence of cracking was virtually eliminated for composite compositions of both ZrB_2 and HfB_2; this effect is particularly well documented for additions of SiC and/or C. Numerous diboride microstructures were hot pressed and characterized in terms of chemistry, density, grain size and phase analysis. The various intentional additives to the diborides also resulted in apparent reductions of the impurity phases found in the as-received diboride powders.

An exploratory fabrication effort was initiated to develop secondary methods for producing diboride materials; hot forging, plasma spraying and sintering were studied. The materials fabricated in the sintering and plasma spraying in Part I were not characterized in detail as only low density structures were produced. Attempted press forging of coarse grained Material I was unsuccessful. Three types of reinforcing agents were employed in an attempt to prepare reinforced diboride composites for evaluation in the Phase One screening tests. Composites compositions identified and designated as: (1) Material Vf(5) and Vf(20), ZrB_2 with five and twenty volume per cent SiC whiskers, respectively; (2) Material XIIf(5), ZrB_2 with five volume per cent Thornel 25 carbon filaments, and (3) Material XIIIf(5), ZrB_2 with 5 volume per cent W filaments were fabricated by conventional hot pressing procedures. Experimental difficulties common to reinforced composite fabrications were encountered. Mechanical difficulties were encountered

3

with the SiC whiskers while thermochemical instability was observed with
the Thermal 25 carbon. The behavior of the latter is probably associated
with interaction of the additive with the oxide impurity in ZrB_2. Mechanical
difficulties and chemical reaction with the hot pressing atmosphere were
observed for the W filament - ZrB_2 system. Partial success in fabricating
Material XIIf(5) was obtained but no improvement in mechanical characteristics
were observed.

> C.   Summary of Processing and Characterization Study
>   in Part II

Additional procurements of hafnium and zirconium diboride
were completed. Five lots of zirconium diboride and four lots of hafnium
diboride were employed in the program. Powder specifications were developed
for hot pressing grades of zirconium and hafnium diboride powders for use
with silicon carbide and/or carbon additives. Some variations in hot pressing
characteristics were found among different lots of a given powder; the
available data indicates that these variations are caused by the nature and
extent of impurity phases. Oxidation properties were not affected by the
occurrence of such impurities for the range of conditions employed in the
static and dynamic oxidation evaluations (8). Some indications of reduced
strength at elevated temperatures were obtained for the hafnium based
structures fabricated from a particular lot of hafnium diboride (9).

Two hundred billets were fabricated for Phase One and Phase
Two and twenty large billets were fabricated for Phase Three. A sufficient
number of billets were hot pressed to provide adequate material for screening
evaluations, property measurements and application oriented tests. The
re-orientation of the program toward more applied data generation (6) and
the results obtained in the Phase One screenings (5) led to the elimination
of SiB_6, $HfSi_2$ and Cr as additives and to a reduced consideration of fiber
and filament reinforced compositions. Silicon carbide and carbon were
selected as the principal additive materials to be employed in several compo-
sitional variations to provide polycrystalline two and three phase compositions
based on both ZrB_2 and HfB_2.

The production of ZrB_2 and HfB_2 billets with grain sizes less
than 50μ and relative densities greater than 98 percent was never achieved
in Phase Three and was only partially achieved in Phase Two. Failure to
produce densification was found to be highly dependent upon the starting
powder used and in particular to the type and amount of impurities present
in each of the powder lots.

The carbon and SiC additions reduced diboride powder require-
ments for the production of dense, fine grained composite structures. The
previously well-documented (5) role of SiC for enhancing the hot pressing
characteristics of ZrB_2 and HfB_2 was also found for several compositional
variations of Materials VIII and XII containing ZrB_2 with SiC and/or C.
Similar results were also found for Materials XIV and XV containing HfB_2
with SiC and/or C.

Composite materials based on both ZrB_2 and HfB_2 were
successfully fabricated to essentially 100 percent relative density for Phase

4

Three evaluations. A Material VIII(18,10) composition with 18 volume
per cent SiC and 10 volume per cent C was consolidated into a fully dense billet
six inches square by two and one half inches high. A Material V composition
was hot pressed to 93 per cent density in the first attempt in the form of
a right circular cylinder, five inches o.d. by four inches i.d. by four inches high.

An anomalous grain growth phenomenon was observed for Material
V compositions containing ZrB_2 with five and ten volume per cent SiC
additions; diboride grains of the order of 1000μ were generated with numerous
discrete grains of SiC. Similar but less pronounced effects were observed
for the five and ten volume per cent compositions of C in ZrB_2 based
Material XII. Such phenomena were not observed for HfB_2 compositions with
small volume additions of SiC. The overall phenomenon is not fully under-
stood, but it is believed that the abnormal grain growth occurred in the
presence of a critical composition, size and distribution of second phase
particles. Effective grain size stabilization of diboride composites by
second phase particles can be achieved through proper control of fabrication
variables as well as quantity and characteristics of the selected additive.

A powder mixing problem was encountered in the first scaled
up processings of Material VIII compositions for Phase Three. The submicron
carbon powder employed for the diboride compositions of Material VIII,
XII, XIV and XV agglomerated in the mixing procedures to produce segregated
areas in the microstructures which could be large enough to entrap one or
more SiC grains. Limited examination of slurry mixing procedures did not
alleviate the problem. The adoption of a careful solids mixing procedure
followed by a screening step to remove large aggregates substantially re-
duced the mixing problem so that well dispersed composite structures
containing graphite could be successfully hot pressed.

All billets fabricated were subjected to extensive nondestructive
testing evaluations to provide sufficient data for subsequent development of
property correlations and flaw identification criteria (4). Dye penetrant
testing was employed for detecting gross surface cracking; radiographic
inspection, to show internal voids, porosity and interior cracks; ultra-
sonic pulse echo techniques, to confirm the presence of internal flaws and
ultrasonic velocity measurements, to provide an estimate of modulus
variability within the billet. Such data were employed to select those billets
suitable for metallographic, mechanical and general characterization testing.
The radiographic testing was not, however, applicable to the hafnium based
materials even when a Co(60) γ source was used. In Phase Three, the
material variability maps and the gross flaw locations supplied by NDT were
employed to select the appropriate billet area for machining specimens for the
various application oriented evaluations and property measurements.

The exploratory fabrication effort was generally designed
to provide preliminary information relative to the applicability of forming
methods other than hot pressing for the preparation of diboride materials.
Plasma spraying and pyrolytic deposition were examined as potential methods
for developing diboride coating systems. Pressureless sintering, hot isostatic
pressing and arc casting were investigated provide data relevent to the
consolidation of shaped billets. Hot forging studies were performed to show
potential forming and possibly strengthening of previously consolidated diboride
material. The fabrication of filament and fiber reinforced diboride matrices
was examined to gain preliminary data relevent to the applicability of hot pressing

5

for incorporation of the reinforcements. The feasibility of employing arc welding procedures to develop joining techniques for diboride materials was also examined. The total exploratory effort represented a fraction of the hot pressing effort which was the principal fabrication method employed in the program. Several of the methods studied in the exploratory effort require special powder specifications to fully examine their potential for consolidation of diboride materials. However, the overall objectives of the program and the limited extent of the exploratory effort precluded the procurement of powders other than those employed for hot pressing. The interpretation of the results obtained for the individual fabrication methods in the exploratory effort must consider the limitations imposed by the available starting powders (where applicable) and the relative extent of the study relative to the total fabrication effort.

The plasma spraying produced relatively porous coatings of ZrB_2 and HfB_2 on several metal alloys and hot pressed ZrB_2 and HfB_2 substrates. Attempts to develop diboride-silicon carbide coatings were unsuccessful; no SiC was retained in coatings sprayed with mixtures of the diboride and silicon carbide powder. Some improvement in coating density and adherence characteristics were however noted for the coatings obtained by spraying the powder containing silicon carbide.

Dense diboride coatings (20 mils) were pyrolytically deposited on Poco graphite substrates with the earlier reported grain growth which culminates in the formation of surface crystallites for ZrB_2 and HfB_2(2). Attempts to prepare coatings of ZrB_2 with SiC as in Material V were unsuccessful but the gaseous charge for the anticipated deposition of ZrB_2 and SiC did produce a dense, fine grained coating (40 mils thickness) of ZrB_2 and B_4C. Further attempts to incorporate stable silicon bearing compoinds in deposited coatings also failed.

Sintering studies were primarily performed for ZrB_2 and ZrB_2 plus SiC with additions of Zr or ZrH_4 to promote densification. Some reduction in temperature and time requirements to produce a given density (above 90 per cent) were achieved for relatively small billets which were found substantially free of elemental zirconium. The lack of a supply of closely sized, fine powder particles hindered the development of dense structures below $2000^{\circ}C$.

Hot isostatic pressing characteristics were determined for ZrB_2, HfB_2 and several composite compositions. The billets were fabricated at $1700^{\circ}C$ and 36,000 psi for two hours in the form of cylinders for ZrB_2 and HfB_2 with no intentional additives and for the diboride composites. The beneficial effect of carbon in enhancing densification of diborides in conventional hot pressing was not observed in the isostatic pressing system for Material VIII(14, 30) and XII(20). Compositions of Material VIII(18, 10) with 10 volume percent carbon could be fabricated to near full density. The encapsulation of the billets required for this fabrication method effectively produced a closed system which would prohibit any gas producing reactions which may occur and be necessary for the enhanced densification observed in conventional hot pressing.

6

The first attempted casting of ZrB_2 based Material VIII composition by employing the methods developed for the production of the refractory hypereutectic carbides (13) produced a sound billet with a ZrB_2 matrix which contained a ZrB_2 plus SiC eutectic and large graphite grains. Evaluation of furnace oxidation characteristics showed a level of performance equivalent to that found for hot pressed Material VIII.

Hot forging was successfully performed on dense, fine grained discs of Material V and VIII. A flat cylinder (three inches diameter by one eighth inch thick) was forged into a hemispherical cap. Mechanical property measurements provide strength levels of the same magnitude as obtained for the hot pressed structures prior to forging.

A limited experimental effort failed to produce a sound HfB_2 structure with W filament reinforcement. Hot pressing at $1900^{\circ}C$ effected complete carburization of the filament. The need for lower temperature fabrication processes as noted in the previous study (5) was again apparent.

Limited arc welding experiments showed that sound bonding could be achieved for ZrB_2 and Material V to Nb and Ta but not to Mo; Material XII showed poor wetting action. Successful self bonding experiments were also conducted for ZrB_2.

7

II. MATERIALS IDENTIFICATION, PROCUREMENT AND CHARACTERIZATION

A. Introduction and Background

The quantities of zirconium and hafnium diboride required for a program of this magnitude, and the apparent nonexistence of powder specifications for particular processing methods led to a procurement procedure in which fifty to one hundred pound lots of diboride powder were purchased and characterized by preliminary chemical analyses and a determination of hot pressing characteristics. Initially, it was anticipated that powder suppliers chosen from among the major powder manufacturers would be able to reproduce production lots in the indicated quantities. The processes employed for the manufacturing of the diborides generally use the metal oxide as the source of metal and boron carbide, elemental boron, or a combination of boron oxide and carbon as the source of boron (14). Accordingly, the price of diboride powder and the impurity levels found in these materials are determined to a large degree by the price and availability of the metal oxide; eighty to ninety weight percent of the diborides of zirconium and hafnium is comprised of the metal.

The ceramic and metallic additives required to formulate the range of compositions studied in this program were generally obtained according to manufacturers specifications.

B. Material Identification

Diboride materials in this program included ZrB_2 or HfB_2 with no intentional additive, and several composite materials based on either ZrB_2 or HfB_2 with one or more additives designed to impart improvement in strength or oxidation resistance or thermal stress resistance, or any combination of these properties. The phase constitution and base composition of all the materials considered for this program are identified by a Roman numeral designation, as shown in Table 1. Compositional variations within a given identified material were also examined; representative designations for such variations are provided in Table 2.

The billet identification system extends the above designation to include the pressing number and the size of the billet. Reinforcing agents such as W filament, Thornel C yarn and SiC fibers are also identified by an extension of the original designation. Several billet designations are explained in Appendix I to familiarize the reader with this system.

C. Material Procurement and Characterization

1. Chemical and Spectroscopic Analyses

Qualitative and quantitative analyses were performed for all diboride powder starting materials and for hot pressed billets of Materials I and II as well as several compositions containing SiC and/or C. Qualitative and semi-quantitative analyses for metallic elements were obtained

8

by emission spectrographic methods employing facilities at the Jarrell-Ash Co. or Kent Laboratories both of Waltham, Massachusetts. Routine spectrographic analyses were also obtained at ManLabs with a laboratory instrument developed by Applied Research Laboratories, Inc., Glendale, California which proved useful for screening operations. Quantitative chemical analysis of diborides for Zr, Hf and B and silicon carbide for Si and C were obtained with minor variations by methods described in Kriege's compilation (15). The sodium carbonate fusion method suggested by the latter for the B determination in ZrB_2 and HfB_2 was not employed for ZrB_2 as the pyrohydrolysis method (16) was found to be more reliable. The higher temperatures found necessary for pyrohydrolysis of HfB_2 hindered the applicability of this method and resulted in the adoption of the fusion method (15). The base metal content of ZrB_2 and HfB_2 were determined after solution in persulfuric acid by precipitation of the base metal tetramandelate followed by ignition to the dioxide. The method does not distinguish between Zr and Hf, hence results are reported as the sum of the two base metals. This distinction is particularly relevant for the analyses of Hf base materials as the extreme and costly methods used to produce Zr-free Hf materials were not specified in this program. Such material was procured and tested in an earlier study and it was found that 1 to 3% zirconium in hafnium did not significantly affect oxidation resistance (2). The C content was determined by the combustion method at $1200^\circ C$. Oxygen analyses were initially obtained by vacuum fusion methods and subsequently by inert gas fusion and activation analysis. The vacuum fusion results were always lower than inert gas fusion and activation analyses which gave oxygen contents consistent with observed metal oxide impurity content found by X ray and other methods. The activation analyses were obtained from Gulf General Atomic Corp. Earlier (5) oxygen results obtained by activation analyses were generally higher than those obtained by inert gas fusion. However, procedures developed at General Atomic to correct for interferences caused by boron produced adjustments which brought the results of the two methods into accord. Oxygen results obtained for billets and powders are provided in Appendix II. The inert gas fusion analyses as well as metal, boron and carbon analyses for selected samples were performed in the Materials Science Department of MIT. The majority of the wet chemical analyses for selected samples were performed at ManLabs.

The results of elemental chemical analyses are employed to calculate a phase assay consistent with X-ray phase identification and powder density. The calculated powder assay can be compared with a metallographic phase assay obtained from a dense hot pressed structure. It is conceivable that the phase content observed for a hot pressed diboride structure would reflect the occurrence of reactions involving impurity phases and the hot pressing atmosphere. A comparison of calculated powder assay and calculated and observed phase assays obtained for diboride compositions with additives reflect the occurrence of reactions between additives, hot pressing atmosphere and impurity phases.

2.   Diboride Powders

Several lots of ZrB_2 and HfB_2 were procured from powder manufacturing companies. The earlier report (5) describes the procurement and characterization of four principal lots of ZrB_2 powder designated 102, 103, and 105 which were purchased as 100 pound lots, and

9

I07 which was purchased as a 400 pound lot. The relative and the total amounts of carbon and oxygen impurities varied from lot to lot; the hot pressing characteristics did not vary significantly. A fifth lot of ZrB2 designated I08 was obtained in the latter part of the program. Procurement difficulties for HfB_2 powder were reported in two earlier reports (2, 5); such difficulties have persisted throughout this program. In all, four principal lots of HfB_2 designated I105, II06B, II09, and II10 have been purchased. Pronounced variations in nonmetallic and metallic impurities were found from lot to lot, and particularly large variations in identifiable impurity phases were found in two lots from one supplier. For HfB_2, the hot pressing characteristics of the individual powder lots also varied considerably. In general, the enhancement in fabrication effected by the SiC and carbon additives diminished the significance of the variations found among the various powders.

The powder characterization data for the five lots of ZrB_2 and the four lots of HfB_2 are provided in Tables 3 through 11. The minor variations found for I02, I03, I05, and I07, and the higher oxygen content measured in I07 are consistent with the observed hot pressing characteristics. The large amounts of Ti, Si, O and C in I08 exceed the limits of the tentative powder specifications developed earlier (5). The significance of the specifications was demonstrated by the unusual hot pressing characteristics found for the I08 powder. In particular, undesireable reactions which apparently took place in preliminary hot pressings of formulations of I08 and SiC lead to substantial billet distortion. Revised powder specifications for a hot pressing grade of ZrB_2 are provided in Table 12. The larger variations found in powder characterization data for I105, II06B, II09, and II10 serve to demonstrate the need for requiring a supplier to meet powder specifications such as the tentative list provided earlier (5). The latter included specification of overall boron to hafnium (or hafnium plus zirconium) ratio to less than two (2.0). The occurrence of a significant quantity of the low density phase in II10 identified as B_4C and the observed enhancement of grain growth in the hot pressing of the II10 powder, and compositions of II10 with up to 5 volume percent SiC confirm the need to maintain the overall composition to avoid the presence of B_4C. Revised powder specifications for HfB_2 are provided in Table 12. The new powder specifications for ZrB_2 and HfB_2 were developed on the basis of available mechanical, thermal and oxidation results, as well as hot pressing characteristics. The limited amount of effort extended to fabrication methods other than hot pressing precluded the development of appropriate diboride powder specification for these methods. As a matter of fact, interpretation of the results obtained in the investigations of methods such as sintering and plasma spraying must take into account the relevance of the powders employed.

It should be emphasized the best available powders of ZrB_2 and HfB_2 which were employed to fabricate polycrystalline structures of varying density and grain size do not provide single phase materials. The principal identifiable impurity was ZrO_2 or HfO_2; metal carbides, metal oxycarbides and boron carbide were also found and identified. Such impurities constituted from one to ten volume percent of the material.

10

3.   Additive Materials

         The additives required to formulate the compositions
shown in Table 1 include silicon carbide powder and fibers, hafnium metal
powder, hafnium-tantalum alloy powder, hafnium silicide powder, boron
silicide powder. Poco graphite powder and Thornel 25 graphite fibers,
amorphous submicron carbon powder, chromium powder and tungsten fila-
ment. Procurement information for the additive materials and character-
ization results were provided in the previous report (5). Since the SiC
powder and the amorphous submicron carbon powder were the principal
additives employed in Phases Two and Three, specifications for these
materials are provided in Table 13.

4.   Fabricated Diborides

         The original plans for the fabrication effort included
the procurement of hot pressed billets from one or more sources other than
Avco. The latter was the principal subcontractor in this study and, among
other things, performed a broad research and developmental hot pressing
effort. The earlier reported cracking difficulties encountered in the hot
pressing of ZrB_2 and HfB_2 to full density without intentional additives lead
to the initiation of procurements of 2.0 inch diameter by 0.7 inch high billets
(Phase One billet size) from The Carborundum Company which were described
in the previous report (5). A single ZrB_2 billet of 6.0 inch diameter by 2.0
inch high (Phase Three billet size) was purchased from the U.S. Borax
Research Corp. The billet was subjected to complete NDT evaluation by
the techniques described in Section III-C and found to be free of surface
cracks and internal flaws. The metallographic characterization is provided
in the description of the hot pressing of ZrB_2 billets for Phase Three
evaluations.

D.   Billet Characterization

1.   General Procedures

         All billets fabricated by hot pressing which were
visably free of surface flaws were subjected to a preliminary surface grinding
followed by a determination of density by the immersion method and several
nondestructive test measurements to assess overall billet uniformity and
integrity. Selected billets in Phase One were examined in further detail
which included one or more of the following, metallographic analysis for
grain size, phase assay, porosity, further NDT in a diametric slice from
the center of the billet, chemical analysis, X-ray diffraction and electron
probe microanalysis, thermal screening and oxidation screening. Subsequently
in Phase Two and Phase Three, billet density and NDT measurements were
coupled with metallographic, chemical and X-ray analyses for characterization
and specimens for various property measurements or evaluations were obtained.

2.   Nondestructive Testing

         Techniques employed for these evaluations are des-
cribed in detail in the report submitted at the completion of Part II of the

11

NDT program at Avco (4).

Effective NDT methods were found for characterization of the diborides-material systems, monitoring material variability, predicting mechanical properties and detecting flaws, such as cracks, porosity, voids and inclusions. A list of the tests used, the variable detected and the material property monitored is provided in Table 15.

Additions of materials such as SiC and/or graphite to the diborides affect the mechanical properties in different ways. These effects can be conveniently and nondestructively monitored using the techniques employed.

Radiographic testing and gamma radiography (using a Co^{60} source of 10 mC intensity) could not be effectively employed for compositions containing hafnium; a stronger radiation source is required.

3. Metallographic and Chemical Analyses

Metallographic analyses generally comprised examination of polished structures with light microscopy methods in as polished and etched conditions. A cut-away drawing of a billet showing the diametrical and axial sections employed for metallographic analysis in Phase One and Phase Two is provided in Figure 1. In some cases the design of special test specimens did not allow the indicated sectioning and samples were taken from other locations. For Phase Three billets two corings were obtained for metallographic analysis, one located 1 inch from the edge along the center line and one from the center of the billet. The cores were cut into four pieces and mounted to provide in-depth axial and horizontal sections. Photomicrographs were obtained at appropriate magnifications to show impurity phases, grain size relations and particulate mixing. A brief description of polishing procedures and recommended etching solutions is provided in Table 14.

Porosity measurements were obtained by comparison of billet immersion density, phase constitution and the quantitative metallographic phase assay for voids.

Grain size values were obtained from the average measurements about a central point in three directions (two mutually orthogonal and a third at a 45°Angle to the former) in a polished and etched section. Fifteen grain intercepts were measured in each direction with a Hurlbut Counter. Grain size measurements were performed for the diboride phase.

Metallographic phase assays were determined by traversing a distance of 1.6 mm on a polished section with the Hurlbut Counter. The measuring procedure produced an identification and determination of diboride, silicon carbide, carbon and impurity phases and voids. An assessment of the degree of polishing pull-out was gained by comparing void content with porosity provided the chemistry and phase constitution were well characterized.

Chemical analyses were obtained by the methods described in II.C.1. The solid specimens were crushed to powder in a hardened steel "diamond" mortar until all of the sample passed through - 200 mesh sieve. Emission spectrographic analyses showed that no significant

12

amount of Fe impurity was introduced by this procedure.

Selected metallographic specimens were examined by electron probe microanalytical methods. The analysis of fine grained polycrystalline materials which contain both low atomic number elements such as B, O and C and high atomic number elements such as Hf, and Zr presented several experimental difficulties which have hindered the full utilization of this potentially powerful analytical tool. The techniques of measurement and the types and limitations of data which can be obtained are described in detail.

a.   Electron Probe Microanalysis

Electron probe microanalysis provides a chemical analysis from specimens as small as a few cubic microns in volume. For this purpose, a finely focused electron beam impinges onto a specimen area of interest located within the surface of a metallographically prepared specimen through a 300X light magnification system. The electrons diffuse into the specimen a short distance at which point interaction with orbital electrons (associated with the atoms of the specimen) occurs and causes ionization. X-rays produced in this way are characteristic of the elements present within the field of electron diffusion. The depth of electron penetration, i.e., the electron distribution is dependent primarily on the accelerating voltage of the electron beam and upon the average atomic number of the specimen. At 30kv, which has been used throughout this work, the depth of electron distribution in Cu is 2 to 3 microns, whereas in C it is about 8 microns. The characteristic X-rays of a particular wavelength (λ) are dispersed from a crystalline grating (with a mean spacing of d) at an angle θ, where $\lambda = 2d \sin \theta$. Knowledge of characteristic wavelengths of the various elements allows one to identify the chemistry of the specimen. The X-ray line intensities, when appropriately corrected for matrix absorption, secondary fluorescence and various electron effects, can be used to determine compositions.

A Philips AMR/3 Electron Probe Microanalyser has been employed in these studies. The apparatus is equipped with two scanning dispersive spectrometers which can simultaneously analyze for any element between sodium Atomic No. 11 and uranium Atomic No. 92. One of the spectrometers is specially equipped with thin windows and stearate film overlay on the mica analyzing crystal to extend its analysis range to include the light elements, boron Atomic No. 5 to sodium Atomic No. 11.

Various qualitative data collection procedures can be employed, as follows:

(1)   Spectral scans - The specimen is held stationary under the electron beam and the spectrometers are scanned over a range of 2θ values to identify the various elements present.

(2)   Distribution scans - The spectrometers are set to specific X-ray lines and the specimen is traversed under the beam, presenting a record of X-ray intensity versus distance.

13

(3)   Scanning display - The electron beam is scanned across an area of the specimen by means of orthogonal deflection coils. The monitored signal (which can be any X-ray line, specimen current or back scattered electron current) is used to modulate the brightness of a cathode ray tube having a sweep synchronous with the electron beam. In this manner, one can obtain qualitative chemical information related to an area on the specimen surface.

For a quantitative analysis, it is necessary to know the relationship between X-ray intensity and concentration of the element being measured. This relationship can be determined by experimental, semiempirical or theoretical procedures. To obtain a specific theoretical accuracy, integrated time point counting procedures are employed with all data corrected for background noise and counter linearity.

Several factors influence light element analysis of the diboride samples. As previously mentioned, the volume of material analyzed corresponds to a few microns in extent. When the grain size of a specimen is also a few microns in extent, as is the case for most of the diboride materials, it is not certain that the analysis is confined to one particular grain. The largest appearing second phase particles are those that have centers coinciding with the surface of the specimen; a 5 micron particle would extend 2.5 microns below the surface. The electron distribution could extend 4 or 5 microns below the surface, and the analysis would include both the particle and some of the underlying matrix. The depth of penetration can be decreased to a few microns by decreasing the beam voltage to 15kV; however, the X-ray intensities would be decreased below a practical value. To insure that the analysis is confined to a given phase, the analyzed grain should be at least 10 microns and only the largest appearing grains should be employed.

The X-ray intensities of B, C, O and N from a sample containing a heavy element, such as Zr or Hf, are very low. Reliable measurements require at least 50 second counting times to provide favorable statistics. In addition, several other complications arise. A carbon contamination spot is formed on almost all materials at the point of the electron beam impingement. This phenomena causes interference with the measurement of carbon; such analyses require data collection for several times (i.e., 10, 20, 30, 40 and 50 seconds) in order to provide data for extrapolation to zero time. Other experimental interferences arise from the occurrence of the ZrM_α line at the same wavelength as the $C K_\alpha$ line. The $Zr L_\alpha$ (3rd order) is relatively close to the $O K_\alpha$ line but interference can be avoided by taking suitable precautions. Oxygen and nitrogen intensities are very weak due to substantial absorption by the detector window.

14

III. HOT PRESSING

A. Introduction

Conventional hot pressing was originally selected as the principal fabrication method to prepare high density structures of ZrB_2 and HfB_2 and the oxidation resistant diboride compositions developed earlier (3). It was anticipated from results obtained for dense structures prepared by high pressure hot pressing (3) that the conventionally hot pressed structures would be characterized by strength properties of the order of 40,000 to 60,000 psi at room temperature and 25,000 to 40,000 psi at $1400^\circ C$. Several other methods of fabrication were studied at significantly reduced levels to determine the potential for development of diboride structures in the form of coatings and shaped billets and filament reinforced structures with diboride matrices.

The additives chosen to increase oxidation resistance and/or thermal stress resistance were not originally considered as potentially advantageous to fabrication. From previous studies it was anticipated that the SiC and C additives could be employed without introducing harmful interaction between the diboride matrix and the additive. Interaction difficulties were anticipated for the W and Hf-Ta alloy additives.

B. Fabrication Apparatus and Procedures

Fabrication of two and three inch diameter billets in Phase One and Phase Two were performed for the most part with a conventional hot pressing apparatus employing a 50 kilowatt low frequency induction heating power supply and a 75 ton Dake press. Other presses are identified in Appendix I. At the beginning of the program a period of 1.5 to 2 hours, depending upon billet diameter, was required to reach fabrication temperatures of $2000^\circ C$. Equipment modifications during the program reduced this heat up time to 30 to 40 minutes. All Phase One and Phase Two billets after D0786 (see Appendix I for billet fabrication and material composition identification) were processed with the faster heating rate using the modified power supply.

Phase Three billets including 4, 5 and 6 inch diameter and 5-3/4 inch square by 1 to 2 inch high sizes were hot pressed with a 250 kilowatt low frequency power supply; initially, a 125 ton press was employed and subsequently a 400 ton Rogers press. The heat up time for the larger billets was of the order of two hours.

For the diboride-additive systems studied, powders of the desired proportions are placed in a suitable container with spherical plastic mixing aids and agitated through a 30° angle for 20 minutes. The powder mixture is screened through a 10 mesh sieve to remove the mixing aids and any large particulate agglomerates and transferred to the hot pressing mold. The powder is uniformly spread in the cavity, then a pressure of 500 psi is applied and the heating cycle is started. Power is applied to raise the temperature to the desired level for fabrication as stated above for different sizes. Next, the

load is increased to produce the desired fabrication pressure on the consolidating powder. The fabrication temperature and pressure are maintained for periods 60 to 360 minutes, depending upon composition, mass of powder, geometry of mold and desired density. A piston travel measuring device is used to assess the degree of powder shrinkage. The cooling cycle begins after the desired time at temperature and pressure is achieved. The power is shut off and the pressure is reduced to ambient after the measured temperature falls below 1800°C. The hot pressing assembly is subsequently removed from the press and allowed to cool. A period of 24 to 48 hours is required to complete the cooling cycle of two inch diameter to six inch square billets. The billets are removed from the hot pressing assembly and prepared for examination by nondestructive testing procedures.

Several powder mixing techniques were investigated in anticipation of the larger quantities of powders required for Phase Three, 7 to 15 pounds/billet for ZrB_2 base compositions to attempt to improve the 1 to 2 pound capacity of the above method. However, the gross delaminations encountered in pressing of billets VIIIQ2400L and R27L, prepared by a liquid slurry mixing method, attest to the utility of the above shaker method. Billets VIII07F D0956K, D0965K and D0967K and VIII(18,10)07F R33L and R35L were also prepared from slurried powder mixtures. These billets did not delaminate, but extensive segregation was found in the microstructures. The oily surface impurity peculiar to the Regal graphite, Table 13, could be responsible for the difficulty in mixing the composites containing carbon.

Chemical reactions between the graphite furnace and the diboride powder were observed in the Part I study (5). The following die liners were tested as reaction limiting diffusion barriers: (a) boron nitride wash on graphite sleeve, (b) tungsten foil, (c) pyrolytic graphite paper, (d) silicon carbide wash and (e) pyrolytic graphite paper with an inner BN wash coating. The pyrolytic graphite paper with an inner boron nitride wash coating is the most effective diffusion barrier for temperatures up to 2100°C. Above 2100°C, reaction zones are very apparent and approach the width of those found without a diffusion barrier, about 3/16 inch. Many billets pressed below 2100°C showed microstructural evidence, in terms of grain size, porosity level, or phase distribution, of an interaction with the BN layer, but the effects are minor compared with results obtained without such diffusion barriers. The diboride compositions containing SiC and/or C revealed markedly smaller reaction layers than Materials I and II. In fact, the vast majority of the billets of these additive containing materials exhibited no evidence for a die wall interaction.

The tables of fabrication conditions for the various material compositions processed provide time at the stated fabrication temperature and pressure. The reported temperatures are measured optically with a Leeds and Northrup Micro Optical Pyrometer and are uncorrected for deviations caused by the lens and mirror arrangement, the emissivity and the position of the sight hole relative to the billet, Figure 2. A photograph of a hot pressing assembly is shown in Figure 3.

C.   Fabrication Conditions and Results

Hot pressing processing procedures were performed as described above. Processing conditions including maximum temperature, pressure and time at maximum temperature are provided in tables for each diboride-additive system employed; available characterization data including density and grain size are also tabulated. The latter and other characterization data including representative microstructures, quantitative metallographic phase assays, chemical analyses and electron probe microanalyses (for selected structures) are presented and discussed for individual material compositions.

The billet identification system employed is described in II. B and Appendix I. The powder components and base compositions are shown in Table 1; representative compositional variations within a given material are described in Table 2. The pycnometric densities for all as-received powders, the calculated powder mixture densities for the composite materials and the maximum experimental billet bulk densities obtained by hot pressing are listed in Table 16.

1.   Material I

Fabrication conditions and billet densities for pressings of Material I required in Part II are provided in Table 17. Available grain size results are also tabulated. The billets employed for Phase Two property measurements, Phase Three evaluations and special NDT measurements are identified.

Earlier processing data and results for Material I were provided in the previous report (5).

Fluid energy milling in air was employed to break up powder aggregates; this effect was shown in the increase in finer sized particle in the Part I study (5). Hot pressing characteristics were also enhanced and no significant impurity pick up was found. The fluid energy milling was incorporated into the powder specifications, Table 12. Exploratory examination of vibratory milling was performed as an alternate powder particle size reduction method. Extensive impurity phase pick up was observed for powder processed in an alumina coated vessel. Material I billets fabricated with this powder (designated V) at 2100°C were extensively cracked; sound billets processed at 1950°C were not fully dense, Table 17. Extensive impurity phase is evidenced in the microstructure provided in Figure 4.

The hot pressing characteristics of the ZrB_2 powder lots 102, 103, 105A, 107 and 108 varied somewhat; differences in chemistry and particulate aggregation were found for the powder lot which showed different processing characteristics. Comparison of relative billet density with processing temperature for equivalent pressure and time variables for Material I fabricated from 105A, Figure 5, shows behavior similar to that displayed by 103 but different from that observed for 102 (5). Inspection of powder characterization data for these powders in Tables 3, 4 and 5 reveals lower carbon contents, 0.02 to 0.03 weight per cent for 103 and 105A relative to 0.38 per cent found for 102A. Such processing data are not available

17

for I07 and I08; higher carbon content, 0.2 to 0.3 per cent, was found for I07. Powder lots I03 and I07 have high oxygen contents, 1.1 to 1.2 per cent where as I05A has considerably less, 0.15 per cent. Material I pressings for Phase Two included both a 100 per cent dense and a 90 per cent dense structure as shown in Table 17. All of the Phase Two Material I structures were fabricated from the I07 powder which had been procured as a 400 pound production lot. Fine grained, fully dense Material I could not be obtained in the Phase Two processings of 3.0 inch diameter by 1.0 inch high billets; average grain sizes of 18 to 56μ were measured for the fully dense structures, Figure 6. Microstructures for the billets employed for the 90 per cent dense Material I for Phase Two are provided in Figure 7; the actual densities varied between 85 to 90 per cent.

Quantitative metallography was employed for three Phase Two billets; the results provided in Table 18 are consistent in part with the results of chemical analyses performed for powders and for hot pressed billets. The results of the latter are provided in Appendix III. The void contents from the metallographic analyses are consistent with porosity levels from bulk billet densities except for I07F D0700K; the apparent high void content for the latter is probably caused by polishing pull-out which is difficult to avoid in coarse grain structures. The metallographic features of I07F D0700K are shown in Figure 6.

Impurity phase identification in Material I is based in part on chemical analysis of powder starting material and hot pressed billets; oxygen and carbon are common nonmetallic impurities. Light microscopy provides limited resolution among oxide and carbide phases as such materials are observed in diboride microstructures as gray phases with differing color intensity. Silicon carbide is found with similar color characteristics. The fine grain sizes of the impurity phases precludes effective use of electron microprobe analyses as discussed in II.D.3.a. Earlier metallographic analyses of Material I microstructures from a lot of powder designated I05, revealed the presence of substantial quantities of impurity phases in agreement with chemical analyses. This lot of powder was not employed to any significant extent in the program and was replaced by a lot designated I05A, Table 5. Metallographic analysis of samples from billet I05 D0450 revealed a large quantity (20 to 25 per cent) of secondary phase particles ranging in size from 1 to 5 microns. Most of the particles were orange, the others being dark grey. An X-ray diffraction pattern of the sample yielded peaks consistent with the ZrC phase in addition to the ZrB_2 pattern. Electron probe microanalysis was employed to provide a qualitative chemistry for the various phases (Table 19).

Attempts to prepare fully dense Material I in Phase Three processing of 6 inches square by 1 to 2 inches high were not successful. Both I07 and I05A powders were employed in the Phase Three processings. These results appear to conflict with the successful fabrication of a 6 inch diameter by 2 inch billet of fine, grain size (8.6μ) with 96 to 97 per cent density by U.S. Borax Research Corp. The powders employed for the pressing were not available for the thorough characterization which was obtained for powder lots employed in the program. Detailed metallographic analysis and ultilization of electron microprobe analysis which is limited by the fine grain size of the impurity phase found in this structure provided results consistent

18

with the identification of ZrO_2 as the chief impurity. A photograph of the hot pressed billet and a representative microstructure are provided in Figure 8. This billet was employed to prepare a simple structural element for evaluation at Bell Aerosystems in one of the leading edge tests (6, 11). Representative microstructures of Material I fabricated in Phase Three processing but which were not employed for the leading edge evaluations are provided in Figure 9. The billet fabricated from I05A fractured into two pieces approximately 3 inches by 6 inches by 1 inch during hot pressing; the microstructure in Figure 9 shows the large grain size, 29μ. Original plans to employ this billet for a simple structural element had to be changed as a piece of the material fractured during final machining operations. The choice to use one of the pieces fractured during processing was based on NDT measurements which did not detect any flaws.

The I08 powder lot was procured near the end of the program; the powder characterization data provided in Table 7 shows significantly high oxygen (1.87 percent) and carbon (1.12 percent) levels and a higher silicon level (0.27 percent) than previously found. The titanium and iron levels are not excessive. This powder was not employed for Material I processings; results obtained in attempts to fabricate Material V with a 20 volume percent addition of SiC led to serious processing difficulties as explained in the next section.

2.   Material V

Fabrication conditions and billet densities for pressings of Material V required for Part II are provided in Table 20. Available grain size results are also tabulated. Billets employed for Phase Two property measurements and Phase Three evaluations are identified.

Earlier processing data and results for Material V were provided in the previous report (5). The present results confirm and extend the earlier findings regarding the enhancement of fabrication of ZrB_2 by SiC; several 6-inch square billets in Phase Three and the singularly attempted hollow right circular cylinder, 5-inch o.d., 4-inch i.d., 5-inch high, were successfully fabricated. Material integrity is characterized by a high level of confidence as evidenced by NDT findings, Appendix IV, and material performance in several application oriented evaluations (12) which required test specimens of a range of sizes up to that of the simple structural element (11).

The specification for zirconium diboride powder for hot pressing of the SiC and/or C compositions, including Material V (Table 12), is less restrictive than requirements for ZrB_2 with no intentional additive. Enhanced fabricability of ZrB_2 powder was evidenced for I02, I03, I05A and I07 powders; no difficulties were experienced except the grain growth anomaly found for 5 and 10 volume percent additions, as detailed below. The successful fabrications of Material V compositions with the above four lots of ZrB_2 were

contrasted by the difficulties experienced with the I08 powder lot. Extensive billet growth developed during pressing, particularly at the edges of a six-inch square billet. The powder characterization data, Table 7, show carbon (1.12%), oxygen (1.87%) and silicon (0.27%) impurities and free boron oxide (0.71%): the levels of these impurities far exceed any found in the first four powder lots. This powder was not employed to fabricate any billets for property determinations.

A considerable number of quantitative metallographic phase analyses were performed for Material V microstructures, Table 21, as part of a study to identify the reactions between the SiC additive and the powder impurity phases, particularly the metal oxide. It is believed that such reactions play an important role in the observed enhanced fabricability; identification of such reactions would be of value in the analysis of the grain growth anomaly described below.

The phase analyses of 100 percent dense Material V02A billets were analyzed statistically in order to establish a reliable value for the difference in second phase content (SiC plus impurity phases) in the Material V powder mixture and in the hot pressed billets. The impurity phases present in I02A powder and I02A billets could not be distinctly identified in hot pressed V02A; all of the second phase was counted as SiC. A mean value of 21.3 volume percent second phase was obtained for ten billets of Material V02A with a standard deviation of 3.3 volume percent. The powder mixture of Material V02A, 80 volume percent I02A and 20 volume percent SiC, contains about 26 volume percent second phases including the SiC additive and the ZrO_2 and ZrC impurities in the I02A powder, Table 3. X-ray diffraction measurements provided identification of $ZrSi_2$ in several of the hot pressed Material V microstructures. A decrease in total second phase volume and the presence of a silicide in the microstructure is consistent with the occurrence of a reaction between the SiC additive and the ZrO_2 impurity as follows:

$$ZrO_2 + 2SiC \rightarrow ZrSi_2 + 2CO(g) \tag{1}$$
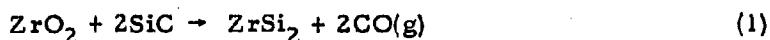
which results in the following phase proportion changes in volume percent, v/o,

$$ZrB_2 + SiC + ZrO_2 + ZrC \rightarrow ZrB_2 + SiC + ZrC + ZrSi_2$$

$$74.9 \text{ v/o} + 20 \text{ v/o} + 3.5 \text{ v/o} + 1.6 \text{ v/o} \rightarrow 77.0 \text{ v/o} + 16.4 \text{ v/o} + 1.6 \text{ v/o} + 5.0 \text{ v/o} \tag{2}$$
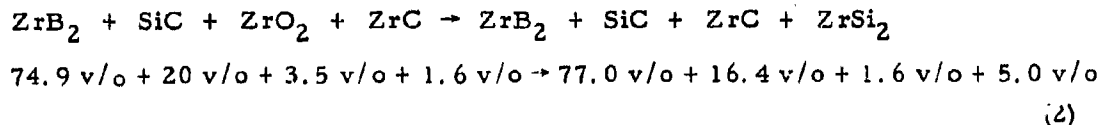
It is known that there is essentially no solubility of SiC in ZrB_2 (17) and less than one percent solubility of ZrC in ZrB_2 to 2200°C (18). At 1300°C, there

is no solubility of ZrC in $ZrSi_2$ nor is there solubility of $ZrSi_2$ in SiC. There is an indication of a very slight solubility of ZrC in SiC (17). However, both $SiC + ZrSi_2$ and $SiC + ZrC$ are in equilibrium at some temperature between 1300° and $1600^\circ C$; a four phase reaction plane occurs (17) with:

$$ZrSi + SiC \; \rightleftarrows \; ZrSi_2 + ZrC_{1-X} \qquad (3)$$
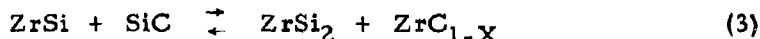
It appears likely that the ZrC and $ZrSi_2$ would be stabilized by the excess of SiC, forcing the reaction to the right hand side of Eq. (3). Virtually none of the ZrC or $ZrSi_2$ can be dissolved in the SiC or ZrB_2 even at the pressing temperatures of $2000^\circ C$ and above. Consequently, all phases should exist as discrete particles or grains and be subject to identification by X-ray or electron probe microanalyses. The phase quantities in Eq. (2) are in reasonable agreement with the metallographic phase distribution in Material V02A, Table 21. The results for V07F D0703K are also in accord with an analogous phase computation based on the I07F powder, Table 6, which has an impurity phase assay of 4.7 volume percent ZrO_2 and 2.0 volume percent ZrC. The results for V07F R26L which were used for Phase Three evaluations show an apparent high ZrB_2 content, 84.4 volume percent and a low SiC content, 14.2 volume percent, but the billet density is 5.54 g/cc which is essentially the maximum density observed for fully dense Material V. The absence of any significant amount of porosity in the microstructure of this billet, Figure 13, confirms the high billet density and also supports the composition of 20 volume percent SiC based on the powder mixture. The result in Table 21 for V07F R26L is thus not interpreted as evidence for a powder mixing error and the composition of billet V07F R26L is the same as the average of Material V billets.

In order to more thoroughly understand the phase changes occuring during the fabrication of Material V, a special series of billets containing large amounts of the ZrO_2 and ZrC impurity phases together with SiC and, in some cases, ZrB_2, were prepared (5). Starting compositions and characterization results are presented in Table 22. X-ray diffraction analysis yielded the presence of both $ZrSi_2$ and ZrC phases in samples that initially contained ZrO_2; no oxide phases were identified by X-ray diffraction.

Samples of the special compositions and ZrC and ZrO_2 standards were prepared metallographically and analysed by electron probe microanalysis methods. None of the samples gave any indication for the presence of an oxide phase. Based upon the characteristic light blue optical fluorescence produced by electron bombardment of ZrO_2, it is estimated that a very small amount (less than 1 volume percent) would have been detected if present. Attempts to provide quantitative analyses of the phases present in addition to SiC were precluded by the very small grain size of these phases (2 to 6 microns); grain definition was not sufficiently clear to reproducibly sample a specific phase. Consequently, X-ray distribution scans were obtained by monitoring Si and Zr X-ray signals as

the specimen was traversed beneath the focused electron beam. Within the limits of resolution, the signals yielded opposite behavior, i.e., an increase in Si intensity was accompanied by a decrease in Zr intensity, and vise versa. The observed data are not consistent with the presence of a zirconium silicide phase as identified by X-ray diffraction analysis. This difference is attributable to either a loss of the $ZrSi_2$ phase due to pullout during metallographic preparation or insufficient resolution by the electron probe microanalysis method.

An apparent grain growth anomaly was found in certain billets of Material V which contained large grains of ZrB_2 either constituting the majority of the microstructure or dispersed within a polycrystalline matrix of normal grain size. The larger grains are about two orders of magnitude larger than the normal grains. Billets in which large diboride grains formed in Material V are listed in Table 23. An example of the morphology of the large tabular grains is shown for billet V(5)02A D0531 in Figure 10 and a polarized light micrograph, Figure 11 shows the grain boundary phase. A survey of the fabrication conditions producing large grains in Material V showed that they occur under the following conditions:

(a) in low volume SiC additions to ZrB_2;
(b) for more than one ZrB_2 powder batch;
(c) for both 2-inch and 3-inch diameter billets;
(d) regardless of prepressing history.

A modification of the induction heating power supply reduced the heat-up time necessary in hot pressings from ca. 75 minutes to ca. 20 minutes. The higher heating rate for reaching the fabrication temperature was used on all pressings starting with billet III(10)09F D0786. Billets pressed with the rapid heat-up rate, but otherwise under conditions which previously produced anomalously large grains, no longer contain such large grains; e.g., billets D0788, D0796K, D0828, D0828 in Table 21.

Evidently, the addition of low volume amounts of SiC induces excessive secondary grain growth during which the diboride grain boundaries sweep past the SiC particles. The resulting microstructures contain large diboride grains with included SiC grains. A certain amount of impurity phase in addition to the SiC is often found surrounding the large grains in a greater concentration than around the normal small matrix grains, Figure 11, perhaps due to the reduction in total grain boundary area.

Hillert (19) has mathematically treated the problems of normal and abnormal grain growth in the presence of second phase particles in a two dimensional array of grains. Without going into the details of the model, it is suggested that there are always two grain size limits for particle limited normal grain growth. Normal grain growth can only

22

occur below the lower limit, but all defective grains are locked above this limit. Between the two limits a large grain would be able to grow abnormally. The risk of developing a large grain to precipitate abnormal growth is much higher if the two grains size limits slowly move to larger sizes by coalescence or dissolution of the second phase particles. Abnormal grain growth is avoided by forming an average grain size so much larger than the upper limit that it will remain larger even when the limit moves to larger values during heat treatment. Another way to avoid abnormal grain growth would be to decrease the distance between the two size limits. According to the model presented, this is achieved with larger volume fractions of second phase particles, stable second phase particles and large particle sizes. Consequently, grain size stabilization of ceramics by second phase particles will depend on the particle size, composition and quantity of the additive phase in a particular system. Similar abnormal grain growth situations to that in Material V are encountered in Materials XII and IX; these will be briefly discussed in subsequent sections. The influence of impurity phase reactions with SiC may be to contribute to the shifting of the grain growth limits which Hillert describes and thereby promote abnormal grain growth. The low additions of SiC, 5 and 10 volume percent, are evidently in the proper range of second phase particle content such that abnormal grain growth may be nucleated. Finally, because of the induction period required for secondary grain growth to occur and the narrow range of temperature required, fast heating rates are not conducive to secondary grain growth.

All of the Material V structures for Phase Two and Phase Three were fabricated with the 107F ZrB_2 powder. Fine grained fully dense structures were prepared with no difficulty; the 90 per cent dense structures for Phase Two property measurements were achieved with minor difficulty. Accordingly, the "90 per cent structures" actually included materials from 88.5 to 91.5 per cent dense. No mixing problems were encountered for Material V and no scale-up problems were evidenced in Phase Three. The successful fabrication of a 5 inches o.d. by 4 inches i.d. by 5 inches high cylinder of Material V also shows the absence of scale-up problems; a 93 per cent density with no flaws (detectable by NDT) was fabricated in the first pressing of this shape. The microstructures of the fully dense Material V billets employed in Phase Two and Phase Three are provided in Figures 12 and 13. Microstructures of the billets employed for the 90 per cent dense structures of Material V in Phase Two are provided in Figure 14. The quantitative metallographic phase analyses were discussed above; results for Phase Two structures, V07F D0703K and V07F D0850K, and Phase Three structure, V07F R26L are included in Table 21. A macrophotograph of the cylindrical billet of Material V pressed to shape with surfaces machined to a ground finish is provided in Figure 15.

3. Material VIII

Fabrication conditions and billet densities for pressings of Material VIII with 14 and 30 volume per cent SiC and C respectively and compositional variations with 5, 10 and 15 volume per cent carbon and the remaining ZrB_2 and SiC in the ratio 4 volumes ZrB_2 to 1 volume SiC are

23

provided in Table 24. Available grain size results are also tabulated. Billets employed for Phase Two property measurements and Phase Three evaluations are identified.

Preliminary processing data and results for Material VIII were provided in the previous report (5). Mixing problems encountered in the preliminary work can be avoided by utilizing the dry solids mixing technique described in III.B. Grain growth problems were not encountered in Material VIII. The total second phase constitution varied from 44 to 24 volume per cent which is considerably more than the 5 to 10 volume per cent levels of SiC in Material V which did show the grain growth anomaly. The Material VIII composition with 18 volume per cent SiC and 10 volume per cent C required shorter pressing times for full density than did the original Material VIII composition. The superior mechanical (9) and oxidation (8) properties of Material VIII(18, 10) led to the selection of this composition for the leading edge evaluation in Phase Three. The reduction in the carbon content also reduced mixing difficulties. Cabot Regal carbon, Table 13, proved to be the best carbon additive with respect to the physical and mechanical properties of the hot pressed material. The very fine powder particle size and the oily binder hindered mixing with the ZrB_2 and SiC. A twenty minute agitation in the mixer with the lucite balls was employed and the resultant powder mixture was sieved to remove agglomerates. As described in III.B. some agglomerated material is removed during sieving. The presence of carbon is clearly shown by the bulk billet density, the elastic modulus values and the different processing characteristics. Billets of Material VIII employing the Regal carbon additive were fabricated to high density in sizes up to 5 inch diameter and 6 inch square. Structures with very small grain sizes were obtained.

The microstructures of Material VIII and Material VIII(18, 10) employed for Phase Two property determinations are provided in Figures 16 and 17; only fully dense structures were examined. Billet VIII07F D0761K, 4.64 g/cc, was also employed in Phase Two property measurements; the microstructure is similar to that shown in Figure 16 for VIII07F D0767K, 4.65 g/cc. The effect of porosity in thermal and mechanical properties was obtained from 90 per cent dense structures of Material I and Material V. Metallographic features in Figures 16 and 17 show the extremely fine grained diboride matrix with the SiC clearly visible and uniformly dispersed. The carbon appears as discrete grains of less than 1 micron to aggregated particles approaching 10 to 20 microns. The larger particles are more common in Material VIII which is formulated with 30 volume per cent SiC. An apparent SiC grain growth within a graphite aggregate was found in VIII07F D0760K, Figure 16. The magnitude of the carbon content is difficult to assess by metallographic phase analyses. The results of such measurements provided in Table 25 indicate 3.8 volume per cent carbon in VIII(18, 10)07F D0919K which was employed for mechanical property measurements in Phase Two. The small size of the carbon particles in Material VIII(18, 10) clearly limits the use of light microscopy to accomplish quantitative metallographic phase assays. As indicated above the free carbon content is evidenced from elastic modulus and density data (9).

Several billets of Material VIII and Material VIII(18, 10) were fabricated in Phase Three. Both compositions were employed for the

24

application oriented evaluations (12), but only Material VIII(18,10) was used to provide a simple structural element for simulated hypersonic flight testing as a leading edge (11). Representative microstructures of Phase Three Material VIII and Material VIII(18,10) are provided in Figure 18. The microstructure of VIII(18,10)07F R33L shows the poor mixing relative to VIII(18,10)07F R40L. The former billet was fabricated from a mixture prepared by a slurry procedure, the latter, by the dry solids mixing procedure. The previously cited simple structural element was obtained from VIII (18,10)07F R40L.

4. Material X

The originally planned composition for Material X was 20 volume per cent SiB_6 with the remainder ZrB_2. A limited number of 2 inch diameter Phase One screening billets were prepared and evaluated. The processing results were quite different from those found for Material V and VIII and subsequently found for Material XII. The hot pressing conditions and results are provided in Table 26; metallographic phase analysis results, in Table 27. The hot pressing at 1900° and $2000^\circ C$ appears to have caused significant reaction between the additive and the diboride powder (and its impurities). The density of the powder mixture was 5.24 g/cc; the final billet densities for the pressings at 1900° and $2000^\circ C$ were 5.53 and 5.81 g/cc. Liquid phase formation was noted in the $2000^\circ C$ processing. Representative microstructures for billets hot pressed at 1700°, 1800°, 1900° and $2000^\circ C$ are provided in Figure 19. Oxidation (8) and mechanical (9) screening performed for Material X showed little improvement relative to Material I and substantial reduction in oxidation resistance and strength relative to Material V. No structures of Material X were advanced to Phase Two.

5. Material XII

The originally planned composition for Material XII was 50 volume per cent graphite with the remainder ZrB_2; earlier results (5) for this composition showed a substantial reduction in oxidation resistance relative to Material I. Compositional variations of Material XII employing 5, 10, 15 and 20 volume per cent carbon were examined in Part II. The processing conditions and results are provided in Table 28. The Regal carbon, Table 13, employed for Material VIII was used for Material XII except for three pressings as noted in Table 28. A graphite powder obtained by milling Poco graphite was employed as indicated. The Regal product is commercially available and following the screening evaluations of oxidation resistance (8) and strength (9) was employed for all Material XII fabrications. Carbon agglomeration was noted for Material XII; the dry solids mixing was employed.

The microstructures of Material XII(5) and Material XII(10) fabricated with Poco graphite in 2 inch diameter billets are provided in Figure 20. The carbon particles are considerably coarser than are those produced in similar compositions with the Regal carbon. The Phase Two structures of Material XII(20) are provided in Figure 21; only fully dense structures were examined. The carbon aggregation problems are evident in the microstructures. The principle effects of the carbon additive are

enhancement of densification resulting in the production of fully dense
structures with grain sizes less than 5 microns and reduction in metal
oxide impurity in the ZrB_2 powder. The observed carbon aggregation
did not adversely affect the strength of Material XII(20) for which the
observed results are consistent with the fine grain size (9).

The reaction of the carbon additive with the metal
oxide and the resulting increase in billet density to 5.40 g/cc relative to
the calculated density for the powder mixture, 5.21 g/cc is consistent
with the following reaction scheme

$$ZrO_2 + 3C \rightarrow ZrC + 2CO(g) \qquad (4)$$
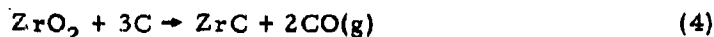
which is analogous to that proposed for Material V. Extensive metallo-
graphic phase analyses were not performed for Material XII; the small
size of the major portion of the carbon additive preclude accurate assess-
ment of phase assay by light microscopy. Microstructures of Material
XII revealed that anomalously large grains were found in certain samples,
Table 29, under the following conditions:

(a)   in low volume carbon additions to ZrB_2;

(b)   for more than one ZrB_2 powder batch;

(c)   for all carbon materials used.

As in the case of Material V, it was found that a fast heat up rate during hot
pressing prevented the formation of large grains; billet XII(5)05A D0635
has small grains. The difference between Material V and XII with respect
to the development of the large grain morphology is that Material V forms
large regular tabular grains whereas Material XII forms irregularly shaped
grains, Figure 22. The carbide and carbon phases were swept past by the
moving grain boundary in the same manner as was the SiC in Material V.
The impurity phase in Material XII is found as discrete particles and is not
segregated along the grain boundaries. It is proposed that the absence of
grain boundary $ZrSi_2$ in Material XII, as compared to Material V, accounts
for the different large grain shapes. The same nucleation mechanism for
abnormal grain growth is applicable in both materials.

The Phase Three pressing of fully dense Material
XII(20) was processed with no difficulty. A representative microstructure,
of the billet, XII(20)07F R56L is provided in Figure 23. This billet was
used to provide a simple structural element for simulated testing for
leading edge applications (11). The carbon aggregation noted for the Phase
Two structures, Figure 21, was evidenced in the Phase Three structure.
The observed strength properties are consistent with the fine grain size (9)
as previously observed in Phase Two testing.

26

6. Material II

Fabrication conditions and billet densities for pressings of Material II prepared in Part II are provided in Table 30; available grain size data are also tabulated. Three powder lots of HfB_2 were employed in Part II; a fourth lot was used in Part I (5). The four lots of HfB_2 possess different powder chemistry and different identifiable impurity phases. Although oxidation characteristics were insensitive to the powder variability (8), the processing characteristics of each powder were markedly different. Metallographic phase assays are provided in Table 31 for billets prepared from each of the powder lots procured in Part II. Identification of impurity phases in powders were presented in II.C.2.; characterization data, in Tables 8 through 11. A considerable number of Material II pressings were performed in the 3 inch diameter billet size but the extensive cracking problems and the inability to prepare fully dense, fine grained structures precluded the selection of a Material II structure for Phase Two property measurements. No Material II was fabricated in the Phase Three billet size.

Fabrication of Phase Two billets of Material II06B was complicated by a high incidence of cracking, Table 30. The microstructures of billets made from the II06B powder indicate that a surface reaction takes place during hot pressing between the die walls and the billet and between the punches and top and bottom of the billet. Two rings of material with different microstructures were found around the billet circumference. The outer ring is about 5/16 inch wide and consists of grains about 3 times the size of the grains in the center of the billet. The outer grains have rounded edges and show evidence of a second phase having been in the liquid state which is different from the II06B impurity phase. The inner ring is about 3/16 inch wide and consists of grains about one fourth the size of the center grains. This second ring of grains contains the impurity phase found in the center of the billet, but the impurity is segregated into discrete areas. Finally, the center of the billet contains a moderate grain size of about 12μ with a 5 v/o impurity phase evenly dispersed, Table 31. The top and bottom of the billets also have the two boundary areas of different morphology but to a lesser extent than about the circumference. The cracking present in the II06B billets originates at the outer larger grain size area and penetrates up to 1/2 inch into the center of the billet. The cracks run straight and usually follow a radial direction. There is clearly an anisotropy of contraction present which results in the surface becoming crazed much like a glaze on cooling. The addition of only 5 volume per cent SiC eliminates the surface cracking and uniform crack free billets are produced as in billet III(5)06B D0778K, Table 32. A representative microstructure of Material II06B is shown in Figure 24.

Fabrication of dense Phase Two billets of Material II09F required a $2200^{\circ}C$ fabrication temperature and time at temperature in excess of 200 minutes and was accompanied by extensive grain growth. An average grain diameter of 60 microns was obtained for II09F D0697 pressed in a 2 inch diameter billet at $2200^{\circ}C$ for 150 minutes. The impurity phase in II09F

27

is shown in the microstructure of II09F D0784 which should be fully dense (10.33 g/cc) relative to the powder density (10.39 g/cc), Table 16. Examination of this microstructure, Figure 25, clearly shows porosity. The presence of porosity would be consistent with the occurrence of reactions during hot pressing which increase the magnitude of the density of the starting material. The available powder characterization data, Table 10, and the microstructures of hot pressed billets suggest that the titanium impurities are present in solid solution as a mixed metal diboride composed principally of hafnium. An etch microstructure of II09F is provided in Figure 26.

Fabrication of dense Phase Two billets of Material II10 also required a 2200°C fabrication temperature and times at temperature in excess of 200 minutes as noted above Material II09F. Extensive grain growth enhanced by liquid phase formation produced average grain diameters of 80μ, II10 D0934K. A representative microstructure for Material II10 is provided in Figure 27. The available powder and billet characterization data show that the grain boundary phase characteristic of dense II10 Material is B_4C. The absence of metallic constituents in the grain boundary phase was confirmed by electron probe microanalysis. Liquid phase formation in the temperature range required for hot pressing of dense II06B is also consistent with the above identification of the impurity phase as B_4C; Rudy (18) reported liquid phase formation at 2050°C for small concentrations of B_4C with HfB_2.

7.   Material III and IV

Fabrication conditions and billet densities for pressings of Material III and IV performed in Part II are provided in Table 32. Available grain size data are also tabulated. The three lots of HfB_2 powder, II06B, II09F and II10 were employed for these fabrications. Billets selected for Phase Two property measurements are identified. Earlier processing data for these compositions were reported for the II05 powder (5).

The experimental difficulties described for Material II processings were completely eliminated by the addition of 20 and 30 volume percent SiC in Materials III and IV, respectively. Additions of 5 and 10 volume percent SiC also provided enhancement of densification and can be considered as alternate means to produce a slightly modified Material II. The 5 volume percent addition would provide a dense structure fine grained structure with total non-diboride phase content of the same magnitude which obtains from ordinarily procured HfB_2 powder. The enhancement of densification of HfB_2 in Materials III and IV is analogous to that found for ZrB_2 in Material V; no grain growth anomaly was observed in the Material III(5) and III(10) pressings. The chemical effect of SiC addition to HfB_2 was studied in some detail for the II10 powder. The beneficial processing effect of SiC for this powder is not readily understood as beneficial reactions between B_4C and SiC are not anticipated.

Billets III(5)06B D0915 and III(5)10 D0918 were fabricated to provide structures detailed analyses pertinent to the SiC interaction phenomena. Billets fabricated with significantly larger quantities of SiC are discussed below but the larger amount of SiC in such materials renders impurity phase identification difficult. The billet prepared from II06B HfB_2

28

exhibited a random distribution of a dark grey phase dispersed in a HfB_2 matrix. The grey phase was identified as SiC by means of electron beam scanning display X-ray images of Si, a characteristic orange-gold optical fluorescence under electron bombardment and a substantially higher specimen current than observed for adjacent HfB_2 grains. The sample also contained 5 volume percent voids. The billet prepared from Il10 HfB_2 powder exhibited a very large HfB_2 grain size (70 to 100μ) with 10 to 15 volume percent of a grey grain boundary phase. The morphology of the grain boundary phase was similar to that produced in hot pressed billets of the Il10 powder with no additive. In both cases the grain boundary phase appears to have been liquid during processing, but the wetting action appears to be different. Electron probe microanalysis of the grain boundary phase revealed that it was actually a mixture of SiC and B_4C phases, which could not be distinguished metallographically. Under electron bombardment, the B_4C phase yields a pale yellow-green optical fluorescence which can be easily distinguished from the orange-gold fluorescence from SiC. X-ray intensities of B and Si were collected from the areas attributed to the SiC and B_4C phases, with the following results:

	X-ray Intensity	
III(5)10 D0918	Si	B
B_4C phase	90	790
SiC phase	17,380	100
HfB_2 grain	60	230

These results confirm the chemistry of the phases. The relative amount of SiC in these billets was determined by X-ray fluorescence methods employing a He path and EDDT analysing crystal. Compared with billet III06A D0672, which was assumed to contain 20 v/o SiC, the X-ray intensity measurements of Si would indicate 4.5 volume percent SiC in III(5)06B D0915 and 5 to 6 volume percent SiC in III(5)10 D0918. The microstructural features of these two billets are shown in Figures 28 and 29.

The larger amount of SiC in the base Material III and Material IV compositions stabilize the grain growth for the Il10 powder. The compositions selected for Phase Two property measurements were chosen to provide dense, fine grained structures of Material III10 and Material IV09F. The metallographic phase analysis results for several Material III compositions with the three HfB_2 powder lots and for Material IV09F are provided in Table 33. The two billets prepared with 20 volume percent SiC and the Il10 powder, III10 D0825 and III10 D0941K, show 17 and 13 volume percent SiC respectively indicating significant chemical interaction during processing. A better accord between powder proportions and billet phase analyses was found for pressing with the Il09F powder.

29

The Phase Two structures for dense Material III10 and Material IV09F are provided in Figures 30 and 31, respectively. The B₄C grain boundary phase is not identifiable; fine grain structures were obtained with no difficulty. No cracking problems were encountered.

The fabrication data in Table 32 show processing conditions for one Phase Three billet, Material III10R52L. The billet density, 9.03 g/cc, was lower than obtained for fully dense structures of III10 in Phase Two processing. For example, a density of 9.21 g/cc was obtained for 3 of the 4 Phase Two structures, Figure 30. NDT testing, Appendix IV, found indications of small sized flaws and porosity. Flaw patterns were found in machined sections of this billet and no extensive Phase Three evaluations were performed. A photomicrograph of the structure of III10 R52L is provided in Figure 32.

8.   Material IX

Fabrication conditions and billet densities for two pressings of HfB_2, 09F, with 23 volume percent $HfSi_2$ as an additive are provided in Table 34. Processing conditions employed for an attempted fabrication with the II10 powder are also tabulated. Fabrication with the 09F powder at 1900° and 2000°C produced identical billet densities of 10.75 g/cc. Metallographic phase analyses, Table 35, show substantial reduction in additive phase content during processing and Brukl (17) reported no solubility of $HfSi_2$ in HfB_2.

The microstructural features of 1X09F are shown in Figure 33; the large tabular grains occur in random locations. The larger grains are generally surrounded by extremely fine grains. Evidence for liquid phase formation is found in the microstructure; Brukl reported incipient melting temperatures of 1576°C in the pseudo binary system, $HfSi_2$-HfB_2 (17). The microstructural features are similar to those found in the Material V structures which contained anomalously large grains; the presence of $ZrSi_2$ formed by reaction of SiC with ZrO_2 impurity was proposed for Material V.

An attempt to prepare Material IX with the II10 powder failed; the billet fractured into several pieces during processing.

9.   Material XIV

Fabrication conditions and billet densities of Material XIV fabricated primarily with the II09 HfB_2 powder are provided in Table 36. The two inch diameter billets were fabricated with 14 and 30 volume percent SiC and C respectively analogous to the ZrB_2 Material VIII composition. A representative microstructure is provided in Figure 34. Phase Two billets of Material XIV were fabricated with 18 and 10 volume percent SiC, respectively. The overall effects of SiC and C were essentially the same as observed for ZrB_2 compositions; fine grain sized structures were produced with nearly full density. Phase Two

30

structures of Material XIV(18,10)09F are provided in Figure 35. The fine grain size of the major portion of the graphite precludes accurate assessment of graphite phase content by light microscopy. The results of metallographic phase analyses in Table 37 reflect this difficulty. The presence of carbon in levels significantly greater than the 2.2 volume percent shown in Table 37 is demonstrated by the billet density and mechanical properties (9). Mixing problems are more severe for the HfB_2 base compositions; the carbon aggregation was also encountered for Material XIV and Material XIV(18,10).

The XIV(18,10)09F composition was fabricated to full density in a Phase Three size billet but extensive property measurements and evaluations were not preformed.

10. Material XV

Fabrication conditions and billet densities for pressing of Material XV with 5 and 20 volume percent C are provided in Table 38. Two inch diameter billets were fabricated with II06B, II09F and II10 powder; billets for Phase Two and Phase Three were fabricated only with the II10 powder. The grain size control found in Material XII(20) was observed in Material XV(20), although the impurity phase content of the II10 powder is substantially different from that found for the I07 powder. Graphite aggregation was found for Material XV(5) and XV(20); the grain growth problem observed for XII(5) and XII(10) was not encountered for XV(5). The results of the metallographic phase analysis, Table 39, reflect the previously cited difficulties in identifying and assessing accurate carbon content.

The Phase Two structures of Material XV(20)10 are provided in Figure 36.

The Phase Three structure of Material XV(20)10 is shown in Figure 37. The billet was fabricated to full density with no difficulty. Material for this billet was used to provide a specimen for evaluation of leading edge configurations in a simulated hypersonic flight environment (11).

D. Discussion

1. Ceramic Additives

The system of ceramic additives developed for ZrB_2 and HfB_2 was reduced to SiC and/or C. These additives, singularly and combined, function to lower fabrication temperatures, control grain growth, eliminate processing difficulties and increase material integrity. In addition, oxidation resistance (8), mechanical properties (9) and thermal stress resistance (11) are substantially improved with no effective reduction in thermal stability (8). The use of these additives relaxes powder specifications for hot pressing grades of ZrB_2 and HfB_2 and lowers material costs and bulk densities.

31

Mixing problems were encountered with the carbon additive; some carbon aggregation is produced but the aggregate size is not significantly larger than the average diboride grain size. Elimination of this mixing problem could possibly further enhance mechanical properties and thermal stress resistance.

2.   Usefulness and Limitations of NDT

During the course of the program it was demonstrated that NDT techniques could supply important information for hot pressed billets. Two separate kinds of information can be generated: quantitative property data and qualitative information regarding physical integrity.

Ultrasonic velocity and gamma radiometric techniques supplied quantitative data showing variations in elastic modulus and density within a billet or specimen, Figures 38 and 39. The variation of dynamic moduli obtained from NDT sound velocity and density measurements with billet densities for compositional variations of Materials VIII and XII is provided in Figure 40. Comparisons of destructive test results and predicted moduli based on NDT showed excellent correlations, Table 40. As a result, the numbers of destructive test samples needed for characterization of billets can be reduced and more reliance can be placed on nondestructive tests. Such information can also be used by the process engineer to make adjustments in mixing and hot pressing techniques to achieve more homogeneous and consistent billets. As the processing scale-up progressed from 2 inch diameter billets to 3 inch diameter and 6 inch square billets, the variability in modulus and density was determined by NDT techniques and the fabrication processes were modified to minimize material variability.

The ultrasonic pulse echo, radiographic, dye penetrant and thermoelectric techniques gave qualitative information on the billet defect content and inherent properties associated with the powder supplier. Numerous billets were fabricated and employed for property testing (8, 9) and application oriented evaluations (11, 12). Billets were evaluated using the techniques listed above and the NDT test data were supplied with a map showing the location of defect areas and their extent, Figure 41. This inspection information was employed to select portions of a billet for test specimens with the minimum number of gross flaws. As part of the characterization process, flaws were evaluated by metallographic and visual techniques. In general, flaws detected by NDT consisted of pore clusters, voids, inclusions, cracks and laminar segregation of constituents, Figures 42 through 44. Representative NDT data for a 6 inch square billet of Material VIII(18,10) are provided in Figures 45 and 46.

The principal limitations of the currently developed NDT methods involve the absence of reliable correlations to predict bend

strength and the lack of sufficient data resolution to properly identify all defects in the hot pressed diboride billets. Some information regarding the type of defect was obtained by using a combination of measurements such as X-ray and ultrasonic pulse-echo. However, certain defects such as voids, high density inclusions, laminar segregation and cracks can not be adequately identified.

The NDT techniques development and testing was performed under a separate Air Force Contract; complete discussion of these techniques are given in a separate report (4). NDT data for diboride billets fabricated in this program are provided in Appendix IV.

3. Reproducibility of Process Conditions

An important aspect of this program was to obtain sufficient process control so that duplicate microstructures and compositions could be fabricated. Previous experience indicated that density would be the most difficult parameter to reproduce, hence this property was considered as the primary measure of reproducibility.

A number of Phase One pressings of Materials I, III and V with comparable temperature-pressure-time cycles are presented in Table 41. In several cases the observed degree of process control appears satisfactory, e. g., compare I02A D0289 with I02A D0290; III05 D0385 with III05 D0386 and V02A D0395 with V02A D0397. In other comparisons the variations in density could be caused by differences in the relatively short fabrication times, e. g., compare I03A D0324 with I03A D0328 and III05 D0400 with III05 D0444. However, some comparable pressings afforded more than the expected 1 to 2% density variations, e. g., compare I03A D0311 with I03A D0314 and I03A D0330 with I03A D0339. The process control variations appear to be less satisfactory for Material I than for Materials III and V.

The hot pressing process was examined in detail to determine whether the process control could be improved. Temperature is the most difficult parameter to accurately and precisely measure. In the temperature range geing employed, the precision of optical temperature readings is approximately +20°C. Billets prepared with an intentional difference of 50° in the pressing temperature can have significantly different microstructures. In addition to the process variation introduced by the degree of precision in the temperature measurement, the formation of a deposit within the temperature sight tube renders temperature control to $\pm$20°C difficult.

The pressing time at temperature is by far the easiest parameter to control. Some variation in heating rate can be encountered, which would give different effective total pressing time if the heating rates were different within 200° to 300°C of the hot pressing temperature.

33

Pressure can be controlled with an automatic pressure release valve. It is somewhat difficult to read the pressure scale accurately since relatively low loads of 4 to 6 tons of a total 75 tons available in the press are required for the 2 inch diameter billets. This limitation is less severe for larger billets in Phase Two and Phase Three. A load variation of +500 pounds between runs is possible. Data were collected on the effect of pressure on the densification of Material II, Table 42. It was concluded that a change in pressure from 4,000 to 6,000 psi produced minor variations in density, but at some lower pressure between 2,500 to 4,000 psi a threshold pressure was found necessary to obtain a uniform densification rate.

Several other parameters were also considered for process control. The densification rate was used with limited success as a measure of progress in the densification process. Another technique often employed in hot pressing to obtain a less than fully dense billet is to construct the die so that, for a given quantity of powder, the pressure train comes against a physical stop, usually a flange in the piston, at the desired density level. However, this technique is not effective at the high temperatures required for the fabrication of the diborides. In the 2000° to 2200°C temperature range, the graphite furnace parts creep at a fast rate and this alters the initial geometry employed to define the stop point.

Another important variable recognized in this program is the hot pressing furnace itself. Three furnaces were employed and any variation in their thermal characteristics could manifest itself in the same manner as a variation in hot pressing temperature. The point of temperature measurement (a cavity in the die wall) is approximately 2 inches from the billet; consequently, different rates of heat loss down the pressure train will affect the billet temperature. Carbon blocks are incorporated in the pressure train as thermal insulators. As these blocks graphitize, their thermal conducti ity changes which probably results in a variation in temperature at the billet relative to the temperature at the die wall.

An experiment was designed to illustrate the importance of furnace construction as a process parameter. Three furnaces were completely rebuilt in as nearly the identical manner as possible. Two pressings were conducted in each furnace with the I03A powder under identical fabrication conditions, the results of which are presented in Table 43. It appears that, in spite of the precautions, furnace 1A behaves differently from furnace 3A. It is difficult to form any conclusions concerning furnace 2A because of the low density for billet I03A D0368. It is not clear whether errors in the measurement of temperature and pressure, variations in heating rate or furnace construction led to the variations in density in Table 43. However, these experiments point out that the expected level of control presently available for hot pressing the diborides is about $\pm 1.7\%$ relative density, although greater variations can occur.

34

For production of high density billets in Phase Two, the method found to give most reproducibility was to press at temperature and constant pressure until the piston movement was equivalent to the creep rate of the graphite at that temperature. This procedure took into account differences in temperature between various furnaces, but often resulted in apparently anomalous pressing times between furnaces. When billets had to be made at low densities, 90%, it was difficult to reproduce these conditions. Billets of this nature were made using the same furnace and punches and under identical conditions. This is not to say that the same furnace after having aged, would subsequently provide billets reproducible with the ones pressed previously. Thus, for each less than fully dense billet, a trial pressing would be necessary to establish the conditions necessary and appropriate for a given furnace at a given time. Further, such a trial pressing would be necessary for each billet composition, e.g., Material V or VIII, etc.

This procedure was employed to measure the progress of densification and was an accurate measurement of the rate at which the billet approaches theoretical density. Each composition required a specific fabrication temperature which was kept as low as possible, commensurate with obtaining a fully dense material but with a fine grain size. For billets having the silicon carbide and/or graphite additives, this temperature remained well below 2200°C. However, to approach full density with the Material II powders, temperatures of 2200°C together with very long pressing times were required (over 300 minutes). The result was excessive grain growth (to almost 100 microns). Similar difficulties were encountered for Material I.

Using this method, billets could be consolidated in 3 inch diameter sizes (Phase Two) to within $+1\%$ density differences if compositions containing silicon carbide and/or graphite were desired and fully dense billets were required; less than fully dense billets needed special calibration. When no additives were present, reproducibility fell to more than 2% for zirconium diboride and it was not possible to determine for hafnium diboride since fully dense, even moderately fine grain materials could not be produced. The grain growth problems encountered for Material II is not entirely a processing equipment difficulty as the impurity phase content of the HfB_2 powder, particularly the II09F and the II10 powders also effects grain growth as discussed in III.C.5.

The reproducibility of Phase Two structures for fully dense Materials I, III, IV, V, VIII, VIII(18,10), XII(20), XV(18,10) and XV(20) is provided in III.C; satisfactory density control was achieved but some grain size variations were obtained for Material I. The grain size control effected by the SiC and/or C additive could substantially reduce processing specifications to control final grain sizes. The reproducibility of the 90% dense structures of Materials I and V was not equivalent to that obtained for full density as discussed in III.C.1 and III.C.2. Better reproducibility for this structure was obtained for Material V. These results are consistent with the above remarks concerning difficulties in controlling densities less than 100 percent.

35

4.   Scale-Up Problems

        The scale-up problem in the pressing of the 6
inch squares in Phase Three were primarily encountered for the
Material VIII compositions containing 10 to 30 volume percent
graphite. Powder mixing and out-gassing during processing were
the chief difficulties and with suitable operating procedures, fully
dense billets were prepared with structures equivalent to those pre-
pared in the 3 inch diameter billets. The scaled-up fabrication of
the diboride powders with no intentional additives also provided some
difficulty. Material I07F could not be hot pressed to greater than 95
percent density. Material I05A was hot pressed to full density but
excessive grain growth developed and the billet fractured into two
pieces during processing. The cracking and grain growth difficulties
encountered for Material II in Phase Two precluded any processing in
Phase Three.

        The pressings of the Material VIII compositions
required several hundred minutes at the fabrication temperature and
considerable time (often as long as 4 hours) was required during the
heat-up cycle to allow excessive gas evolved, presumably CO, to burn out
of the carbon black insulation. The evolution of the CO is believed to
be associated with the reactive hot pressing system which effectively
functioned during the processing of the composite compositions. Failure
to allow adequate degassing times before applying the full processing
pressure affords laminated billets. The mixing problems were discussed
in III-B.

IV.   EXPLORATORY FABRICATION

A.   Introduction

The exploratory fabrication effort was designed to provide preliminary information relative to the applicability of forming methods other than hot pressing for the preparation of selected diboride compositions. Extensive material characterization and property evaluations were not planned for any materials other than hot pressed structures but the range of porosities and grain sizes for the hot pressed structures is sufficient to estimate property trade-offs which would result for material fabricated by any of the exploratory methods.

The entire exploratory effort represented a fraction of the hot pressing study which was the principal fabrication method employed in the program. Several of the methods studied in the exploratory effort require special powder specifications to fully examine their potential for consolidation of diboride materials. However, the overall objectives of the program and the limited extent of the exploratory effort precluded the procurement of powders other than those employed for hot pressing. The interpretation of the results obtained for the individual fabrication methods in the exploratory effort must consider the limitations imposed by the available starting powders (where applicable) and the relative extent of the study relative to the total fabrication effort.

Plasma spraying and pyrolytic deposition were studied as potential methods for developing diboride coatings of compositions which displayed superior oxidation resistance. Pressureless sintering, hot isostatic pressing and arc casting were examined as potential methods for shape forming. Hot forging of previously consolidated billets was investigated as a potential forming technique and for thermomechanical processing data for the diboride materials.

A study of the applicability of hot pressing to form filament and fiber reinforced diboride structures was performed. Feasibility arc welding studies were initiated to examine diboride joining characteristics.

Exploratory fabrication studies were initiated in Part I of this program; preliminary results of plasma spraying, sintering, hot forging and hot pressing of filament and fiber reinforced materials were reported earlier (5).

B.   Plasma Spraying

Plasma spraying studies were performed at Avco to examine the potential of this technique for producing coatings of diboride materials on metal or diboride surfaces. Although optimization of this method would include development of a special powder specification, the experiments were conducted with powder lots obtained for the hot pressing studies.

37

Plasma spraying experiments performed in Part I were restricted to a ZrB_2(I02A) charge sprayed onto several substrates using an Avco Model PG-100 with argon carrier gas. Substrates included silica phenolic, stainless steel, copper and aluminum. The coatings were extremely porous and contained a significantly higher impurity phase content, presumably metal oxide, than is observed in hot pressed structures of I02A.

Two series of exploratory plasma spraying fabrications were performed in the Part II study. In the first group, ZrB_2 powder, I02A, was sprayed onto hot pressed HfB_2 and ZrB_2 and Type 303 stainless steel substrates. The spraying was performed inside an argon atmosphere dry box, using argon as a carrier gas. Qualitative remarks for these coatings are provided in Table 44. Low density materials were formed in all coatings. Previous work at Avco with spraying heavy metal carbides has generally resulted in densities of 60 to 75%; the upper limit of this range is approached only when the spraying conditions and the powder particle size are optimized. The I02A coatings which adhered to a substrate appeared the most dense by visual observation, however, metallographic examination showed that all samples were no more than 50 to 70% dense. The more porous I02A coatings were easily removed from the substrate by surface abrasion. The relatively porous coatings also appeared to be laminated. The I03A powder was found to be unsuitable for spraying; considerable clogging of the spray gun was encountered with this powder. The particle sizes of the two ZrB_2 powders are similar and it is not clear why the powders behave differently.

The second series of exploratory plasma spraying HfB_2 base powders, II06B and III05A, were sprayed onto substrates of TZM alloy, Ta, and hot pressed Material I and II, Table 45. All coatings were applied in an argon atmosphere in order to minimize oxygen pickup.

X-ray analysis of the coating from II06B powder provided identification of only HfB_2. Coatings from Material II and III were generally dense and little difficulty was encountered in the spraying operation. The most dense and adherent coatings were obtained with Material III sprayed onto TZM alloy and Ta substrates. Coatings obtained from a charge of III05A(HfB_2+SiC) sprayed onto Ta and TZM were examined by X-ray diffraction, chemical analysis and metallography. The X-ray data revealed HfB_2 as the principal component with minor amounts of HfC and cubic HfO_2 in each coating. No SiC was detected in any of the samples. It is concluded that the SiC readily vaporized in the high temperature plasma and that only the higher melting low vapor pressure diboride and impurity phases remain in the coating. The absence of silicon in the coating sprayed from Material III powder was confirmed by chemical analysis. Although the SiC vaporized during the spraying operation, the presence of SiC in the powder charge could be responsible for the superior coating characteristics of Material III05A as compared with Material II06. The SiC could function as a fugitive carrier material. Other materials are known to function this way in plasma spraying systems. Although the coatings obtained with the III05A powder charge were superior to other diboride coatings obtained to date, metallographic examinations showed excessive porosity and layered microstructures.

38

The plasma spraying studies were terminated as it was obvious that considerably more effort would be required to optimize material compositions and powder characteristics to provide material with structures approaching 85 to 90% densities.

C. Pyrolytic Deposition

Pyrolytic deposition procedures were employed to attempt to produce coatings of Material V on Poco graphite. The latter was selected on the basis of chemical compatibility with the furnace atmosphere, and the diboride material composition and also on the basis of physical compatibility. The Poco graphite and the diboride materials have CTE values in the range 6.5 to 8.0 x 10^{-6} in/in/°C (10). The pyrolytic deposition experiments were performed by the Raytheon Research Division. Earlier pyrolytic deposition of ZrB_2 (2) and to a limited extent HfB_2 (3) was also performed in a previous program at Raytheon. The pyrolytic coatings of ZrB_2 and HfB_2 formed in the earlier work were characterized by a columnar grain structure which could result in the formation of gross surface crystallites. The ZrB_2 was, however, successfully fabricated to coating thicknesses approaching 0.100 inches; the HfB_2, to 0.80 inches.

The initially chosen conditions for a ZrB_2 deposition in the present work produced the surface crystallites, Figure 47; metallographic analysis revealed a ZrB_2-B eutectic, Figure 48. Attempts to prepare a ZrB_2+SiC coating analogous to Material V produced a dense coating of 0.040 inches thickness with no evidence of surface crystallization, Figure 49. Chemical, metallographic and X-ray fluorescence failed to reveal SiC or any Si bearing compounds in this coating. Metallographic analyses showed an extremely fine grained structure which was difficult to resolve by light microscopy, Figure 50. Electron micrographs provided in Figure 51 show typical areas of the two phase composite structure composed of ZrB_2 and B_4C. The stabilization of B_4C appears to override chemical composition adjustments in the gas feed, CH_4, BCl_3, $SiCl_4$, $ZrCl_4$ and H_2. Attempts to prepare a coating without the CH_4 and adjusting the feed compositions to prepare SiB_4 or $ZrSi_2$ also failed to produce a coating containing Si in any compound.

In view of the overriding destabilization of Si bearing compounds in the diboride pyrolytic deposition atmospheres, the effort was terminated. The apparent role of the B_4C in controlling the grain growth phenomena in ZrB_2 could be employed to advantage in other systems. The role of B_4C or possibly any stable second phase in stabilizing grain growth in the pyrolytic coatings is analogous to the role of SiC and/or C in controlling grain growth in hot pressed diboride structures.

D. Sintering

The sintering effort was the principal study in the exploratory effort. Sintering methods were studied to provide data relevant to a consolication procedures which are basically less expensive than hot pressing and more suitable to shape forming.

39

Sintering studies in Part I of this program (5) showed than an argon atmosphere was preferred to vacuum as considerable weight loss, 28 percent, was observed for ZrB_2, IO3A at 2200°C in 150 minutes. Generally, low density billets were produced in several sintering runs conducted in the temperature range, 2000° to 2200°C. Results from a previous program (3) demonstrated that a ZrB_2 powder with an overall B/Zr = 1.89 mixed with Zr metal powder to bring the stoichiometry to B/Zr = 1.7 could be sintered to high densities at considerably lower temperatures than was required for the ZrB_2 powder with no additive. The major portion of the sintering work in Part II was a continued study of the effect of the addition of elemental zirconium to enhance densification of ZrB_2 and the ZrB_2-SiC composite, Material V.

Zirconium was added in two ways -- as -325 mesh metal powder and as ZrH_2 powder. The initial work in Part II was accomplished with the Zr powder, and precautions against a pyrophoric reaction had to be taken during the mixing operations. Sintering billets are identified by the ZrB_2 powder mixture e.g., IO3A, VO2A, followed by the additive material in parenthesis, e.g., (Zr), and the experiment number B1, B2, etc. Billets after Experiment B44 were formulated with the more stable ZrH_2 compound. Powders were cold pressed with a polyvinyl alcohol pressing aid. Uniaxial pressing was employed for all the 1/2 inch diameter billets and the majority of the 1 inch diameter billets; isostatic pressing, for one 1 inch diameter billet. The sintering was accomplished in a tungsten mesh element furnace under an argon atmosphere. The cold compacted billets were placed on a HfB_2 pedestal which was supported by a tungsten holder. Separation of the billet and the HfB_2 surface was achieved by a sprinkling of large particle size ZrB_2 obtained by crushing a hot pressed billet of ZrB_2. The sintering conditions and results are listed in Table 46.

Billets B13 through B17 were sintered near the Zr-ZrB_2 eutectic, 1695°C (3) in order to examine the possibilities of enhancing sintering by liquid phase formation or by the reaction of the added Zr and ZrB_2 to form ZrB in a matrix of ZrB_2. These samples were characterized by low bulk densities with a homogeneous pore distribution. A density of 83% was achieved after sintering at 1700°C for four hours, B17. A two step sintering process was then explored in which the ZrB_2 - Zr powder mixture was first heated to 1700°C, held for one hour, then heated to 2200°C and held for four hours, B20 and B21. These billets sintered to approximately full density, and a typical microstructure is shown in Figure 52. Quantitative metallography and X-ray phase identification results are presented in Table 47 for the fully dense IO5A (Zr1) B20; the secondary phases were identified as ZrB, ZrO_2 and Zr. The metallographic phase identifications are supported by earlier X-ray and metallographic results for a billet sintered at 1700°C, 500°C below the temperature employed for billet B20. A 1 inch diameter by 1 inch high billet was sintered to near full density at 2200°C without the 1700°C pre-treatment, billet IO3A(Zr1)B26. Bend test data in Table 48 show low temperature strengths reasonably consistent with Material I grain size, density, strength correlations; the observed strengths at 1400° and 1800°C are lower than observed on analogous hot pressed structures of Material I (9).

40

Experiments were conducted with an 8 w/o and a 4 w/o
Zr addition to ZrB₂ to provide overall compositions with B/Zr = 1.8
and 1.9, respectively. The 8 w/o Zr mixture was sintered to densities
equivalent to those obtained for the 14 w/o Zr addition; the 4 w/o addi-
tion, to 95% density. It was necessary to sinter 100°C higher to even
achieve full density for the 4 w/o addition. The tabular grain micro-
structure shown in Figure 53 for the material with the 8 w/o addition is
consistent with the presence of a liquid phase during sintering. Linear
grain boundaries are intersected by other grain boundaries without any
change in angle which cannot be rationalized with surface energy con-
siderations except by the presence of a second phase. The elemental
Zr phase was not identified in the unetched section; the second phase
responsible for the sintering activity is probably ZrB. The average
grain intercept is 12 microns. The microstructure for the 4 w/o addition,
also exhibited evidence for the presence of ZrB although a finer grain
size was obtained, Figure 54.

Attempts to sinter a 1 inch diameter billet of ZrB₂ with the
8 w/o Zr were not completely successful; although high densities were
achieved a central crack developed in the specimens. The 1 inch diameter
specimen from B48 showed one central crack which is similar to results
obtained for B40. The former was cold compacted with isostatic pres-
sure to reduce density gradients relative to the billets cold compacted by
uniaxial pressing. Clearly, scale up sinterings present a new set of
problems which will have to be investigated.

A number of experiments were conducted with Material V
employing a Zr metal addition. A low relative density and considerable
loss of SiC were noted after sintering at 2200°C with the normal pedestal
arrangement. Later runs were conducted at 2000°C, B34 and B35, both
inside and outside a tungsten crucible, respectively. Specimen B34 was
difficult to extract from the crucible although it gave the highest density
for this composition. Specimen B35 exhibited a SiC depleted surface layer
while the center section has the microstructure illustrated in Figure 55.
The observed porosity and the bulk density of 5.37 g/cc suggest that some
SiC was lost from the overall mixture. Consequently, the true maximum
possible density would be higher than that for hot pressed Material V,
5.50 g/cc. A number of successful 1/2 inch diameter specimens were
fabricated, but 1 inch diameter specimens were cracked.

The metal additions and the SiC additive clearly enhance
sintering to high densities without significant grain growth. Optimization
of starting material powders, particularly ZrB₂ would be the first step
in the scale up of the process to produce billets of sufficient size to pro-
vide meaningfuly characterization data.

41

Several diboride powders and several SiC and/or C diboride compositions were fabricated in the isostatic hot pressing facility at Battelle Memorial Institute. The processings were performed under the exploratory fabrication effort to obtain preliminary data for a method which is more suitable than conventional hot pressing for shape forming. Isostatic pressing is presently not economically favorable for processing refractory materials relative to conventional hot pressing.

The first experiments were performed with Material I03A and a Material V composition which was prepared at Battelle with I03A and SiC powders supplied by ManLabs. In the procedure employed for the first pressing of Material V, the specified compositions were blended with carbon tetrachloride containing 2 percent parawax in a polyethylene container using alumina balls to disperse the powder. The carbon tetrachloride was removed by evaporation while continuously stirring the mix. The specimen was then cold isostatically pressed at 100,000 psi and ground into specimens 1/2 inch diameter by 2 inches long. The specimen was then vacuum outgassed to remove the parawax and other volatiles and sealed in tantalum tubes by electron beam welding under vacuum. After pressing,the materials were decanned by grinding. The Material I03 and Material V03 (prepared as above) were fabricated at 1650°C and 36,0000 psi for one hour. Material I was 90% dense and Material V was close to full density. Detailed electron microprobe data were obtained for Material V as mechanical property results, Table 49, were not in accord with strength-grain size-porosity levels obtained for hot pressed structures of Material V (9). Representative microstructures of the isostatically hot pressed Materials I and V are shown in Figures 56 and 57, respectively. The measured strength values are 40 to 50 percent lower than would be predicted on the basis of the microstructure in Figure 57. Metallographic analysis provided a ZrB_2 grain size of 2 to 20 microns, with an average of about 5 microns. The microstructure exhibited numerous very small boride grains, which are possibly the result of diboride grain fragmentation during pressing. Considerable bridging of SiC grains was also noted.

There was occasional evidence for the presence of a fine-grained (0.5 to 1μ diameter) impurity phase within the diboride matrix. This phase was characterized by a slightly yellow hue of color compared to the diboride. An X-ray diffraction pattern of the sample yielded ZrB_2 and SiC diffraction data with a slight indication for the presence of a small amount of ZrC. There was no X-ray evidence for ZrO_2 or a metal silicide phase. Electron probe microanalysis procedures were employed, utilizing scanning display and X-ray distribution procedures. An X-ray distribution scan for Si and Zr was carried out over a distance of 1000 microns; Si and Zr intensities were precisely reversed over the distance, precluding the presence of a $ZrSi_2$ phase. The yellow phase

42

was located at several positions along the distribution scan; the phase yielded a Zr intensity comparable to that of ZrB_2 and did not contain any silicon. It is speculated that this phase is either ZrN or a modified composition of ZrC. Scanning display pictures of the specimen were consistent with the finding of the distribution scans. The SiC phase was observed to yield a dark orange (and sometimes bright green) light fluorescence in contrast to the yellow-gold fluorescence usually observed for SiC. In addition, several observations were made of light blue fluorescence, which is associated with ZrO_2. Metallographic inspection; of these areas revealed pits. It is difficult to distinguish porosity voids from pullout areas previously occupied by ZrO_2 by metallographic techniques but the measured room temperature elastic modulus of 74.5×10^6 psi indicates very little porosity. The low strengths observed for the Material V03A could result from the SiC bridging caused in turn by the mixing procedure; the presence of ZrO_2 and other composites which are not present in conventionally hot pressed Material V could also contribute to the observed strength properties.

Subsequently, eight diboride powders including several SiC and/or C containing compositions premixed at ManLabs were isostatically hot pressed at Battelle. The liquid mixing was not employed; the dry powders were compacted isostatically at 100,000 psi. The latter procedure is not satisfactory; considerably handling difficulties were encountered. The fabrication conditions were 1700°C, 2 hours and 36,000 psi. The resulting billet densities are compared with the powder densities and the calculated powder mixture densities and with the maximum densities observed for conventially hot pressed structures in Table 50; the isostatic pressings were performed in duplicate. All the billets, 1/2 inch diameter by 2 inches long were processed in a single fabrication run.

The results obtained for the diboride powders II09F, II10, II06B and I07F with no additives show that densities in excess of 95 percent of the powder density can be achieved for all powders except II10 which contains B_4C as the principal impurity phase. Representative microstructures for II09F, II10, II06B and I07F are provided in Figures 58, 59, 60 and 61. The near full density achieved for I07F contrasts the 90% density achieved for I03A processed 50°C lower and one hour less at the fabrication temperature; this behavior could be a powder variation. As with the sintering and other exploratory fabrication methods, no particular attention was relegated to obtaining special powders. The average isostatic billet density of 5.63 g/cc for V(5)07F for the 5 volume percent SiC addition to ZrB_2 is less than anticipated from the previous pressing of the 20 volume percent addition of 1650°C. The microstructure of V(5)07F provided in Figure 62 shows approximately 1% porosity which indicates that the calculated powder density could be erroneously high as a consequence of reactions which take place during processing in an essentially closed system. The beneficial effect of carbon additions found in the conventional hot pressing was not observed for the isostatic pressings as shown by the relatively low billet densities for VIII(14,30) and XII(20); representative microstructures are provided in Figures 63 and 64, respectively. Near full

43

density was obtained for VIII(18, 10), Figure 65, which contains substantially less carbon than VIII(14, 30) and XII(20).

The variations in billet densities encountered in several of the duplicate pressings were believed to be associated with the difficulties encountered in the cold impacting. Optimization of powder specifications for this process and development of improved cold compacting would improve the suitability of this method for the diborides with no additives and for modest amounts of SiC and SiC with C additions. The encapsulation of the billets required for this fabrication method effectively produce a closed system and prohibit any gas producing reactions which may occur and be necessary for the enhanced densification observed in conventional hot pressing for the carbon containing composites.

F. Arc Casting

Arc casting experiments were performed in the concluding part of the program to prepare diboride compositions containing SiC and C. The method does not require special powders to enhance consolidation; as a matter of fact solid materials can be employed as starting materials. The method can be developed into a shape forming fabrication technique. Carbon contamination is introduced by the electrodes but the carbon composition in the resulting billet can be controlled by adjusting the charge composition. It is conceivable that a Material V composition of ZrB_2 and SiC could be fabricated from ZrB_2+Si in the charge. The details of the procedure and the apparatus are presented elsewhere (13); the experiments were conducted at Battelle Memorial Institute.

A 5.9 lb ingot was obtained from approximately 15.4 lbs of solid charge material consisting of a Material VIII hot pressed billet which had been discarded due to excessive porosity and material variability. A radiograph of the arc cast billet showed the center section to be sound; however, the ingot was porous both at the top and bottom sections. This porosity is related to the casting of a smaller volume of charge material than desirable. The castings were prepared with less difficulty than had been experienced for the hypereutectic carbide. A photograph of the ingot is provided in Figure 66. The melting of 15 lbs of this material took approximately 10 minutes. Two or three times larger heats can probably be melted in the present facility. The microstructure consists of primary ZrB_2 grains, a eutectic mixture of SiC and ZrB_2, and graphite flakes. The continuous phase is ZrB_2 as shown in Figure 67. The diboride structure appears to contain more carbon than the Material VIII charge which contained 30 volume per cent carbon. Oxidation screening results described elsewhere (8) show a level of oxidation resistance equivalent to that of the charge composition of Material VIII.

G. Hot Forging

Thermomechanical processing of diboride materials by hot forging or press forging (20) was employed in the exploratory fabrication effort as a potential technique for strengthening and/or forming of hot pressed

44

or otherwise prefabricated structures. The experiments were performed
at Avco; the previous work with oxide materials was also performed at Avco (20).

Several attempts were made to hot form thin sections of
hot pressed Material I into a 30° right angle cone configuration; all of the
forgings were terminated by brittle fracture without gross plastic deformation.
The first experiment employed a 2 inch diameter by 0.082 inch thick section
of a porous billet and was unsuccessful; examination of the piece revealed
that no deformation took place before the piece split into four segments.
The next forming experiments were attempted with high density sections
prepared from billet I05A D0650K (26μ grain size). A 3 inch diameter by
0.060 inch section of this billet was hot forged at 2150°C and postforming
inspection revealed no signs of material deformation before fracture. The
forging assembly was changed to another press to provide greater control of
the initial deformation rate. Another attempt was made to forge a 3 inch
diameter by 0.080 inch section of billet D0650K at 2200° to 2250°C. Molten
material was extruded from the press during forging and metallographic
examination indicated that the pseudo-binary eutectic between ZrB_2 and
graphite (2390°C) (17) was reached, Figure 68. These runs indicated that
the feasible temperature limit for forming operations for a coarse grained
Material I is 2200°C (as measured in this furnace assembly). The complete
lack of deformation at 2150°C suggested that lower temperatures were in-
advisable. Hot forging deformation of Material I appears to require very
low strain rates and temperatures of 2150° to 2200°C. A third slice of
billet D0650K, 3 inch diameter by 0.080 inch thick was then hot forged at
2150°C using 30° angle conical dies to 1/4 inch deflection in the center during
seven minutes. The disc broke during the operation. No grain growth was
observed during the forging cycle.

The high temperature deformation studies performed in the
mechanical properties measurement program (9) show Material I can be
deformed in this temperature range employed for the press forging. The
high temperature deformation data was obtained in the last part of the program
and was not available at the time the press forging experiments were per-
formed. The available data strongly suggest that fully dense Material I
with a 25 micron grain size could be successfully hot forged by lowering
the piston travel rate; that is, lowering the effective strain rate. Further-
more, a 95 per cent dense Material I which would have a 5 to 10 micron
grain size could also be forged at an appropriately adjusted deformation
rate. These conclusions are based on the observed grain size dependence
found in the high temperature deformation studies (9); the Material I
structures with finer grain sizes deform more readily than coarser grained
structures.

A dense fine grained Material V structure was selected for
additional experiments. Two discs of billet V07F D0761K were obtained with
a 3 inch diameter by 0.070 inch thick and were successfully hot forged.
The forging was performed in a graphite die assembly at 2125°C with a rate
of piston movement of 7.9×10^{-3} in/min. One disc was forged into an
approximately conical shape with the center offset to approximately 1/2 inch.
Two additional discs of billet D0761K, 3 inch diameter by 0.080 inch thick
were also hot forged. The center of the disc was deformed by 0.6 inch with
a piston movement rate of 6.85×10^{-3} inch/min. During the run the load on
the die increased from 78 to 300 pounds. The increased load was presumably

45

due to the shortening of the effective lever arm as the slice continued to deform around the hemispherical die. A typical strain versus time curve is shown in Figure 69. The next 0.080 inch thick disc was forged to a roughly hemispherical shape with a 1 inch deformation in the center but the center 1 inch diameter section tore away from the main body. No grain growth took place in the Material V samples during forging. A photograph of a forged disc is shown in Figure 70.

High temperature deformation studies for a dense fine grained Material V structure was also completed late in the program (9). The dense Material V with a grain size of 7 to 10 microns was found to be more readily deformed than a dense Material I with a grain size of 26 microns; the mechanical behavior of Material V is more complex than was observed for Material I.

A dense fine grained Material VIII structure was also forged by the same procedure employed for Material V. A 3 inch diameter by 0.070 inch thick disc was prepared from billet VIII07 D0803K and forged at 2140°C with a 300 psi average pressure. The deformation versus time for Material VIII is shown in Figure 71. The observed successful forging is consistent with the fine grain size observed for all the Material VIII structures.

Strength data obtained from the deformed sections of discs of Material V and VIII, provided in Table 51, do not show a strength enhancement. An apparent strength reduction was observed for Material V at 1400°C.

H.   Filament and Fiber Reinforced Structure

The major portion of the reinforcement study in the exploratory fabrication effort was performed in Part I of this program, and was based in large part on systems recommended in Krochmal's review article (21). A detailed discussion of the results obtained for the three types of reinforcing agents employed in attempts to prepare reinforced diboride composites for evaluation in screening tests is presented in a previous report (5). Composite compositions identified and designated as follows: (1) Material V, ZrB_2 with five and twenty volume per cent SiC whiskers, Vf(5) and Vf(20) respectively; (2) Material XII, ZrB_2 with five volume per cent Thornel 25 carbon filaments, XIIf(5) and (3) Material XIII, ZrB_2 with 5 volume per cent W filaments were examined with hot pressing as the fabrication procedure. The attempted processings were characterized by experimental difficulties common to reinforced composite fabrications. Mechanical difficulties were encountered with the SiC whiskers while thermochemical instability was observed with the Thornel 25 carbon. The behavior of the latter is probably associated with interaction of the additive with the oxide impurity in ZrB_2. Mechanical difficulties and chemical reaction with the hot pressing atmosphere were observed for the W filament - ZrB_2 system. Similar difficulties were observed for a W filament HfB_2 system prepared for hot pressing by winding three mil tungsten wire with 200 wires per inch in five layers with about 15 mils of plasma sprayed HfB_2 from a HfB_2+SiC charge between each layer on a tungsten foil coated carbon mandrel. The loss of SiC from the charge was expected; it was anticipated that a better HfB_2 coating would be obtained.

The final composite was hot pressed at 1900°C and 2500 psi for 105 minutes. The composite was very brittle on removal from the die and a cross section showed complete carburization of the tungsten, Figure 72.

Partial success in fabricating Material XIIf(5) was obtained in Part I for billet XIIf(5) D0644 prepared by winding the continuous yarn on a mandrel and cutting round mats of the windings. Mats were loading consecutively with layers of boride resulting in continuous aligned layers of Thornel yarn in the pressing. Reaction was reduced at least in the center of the Thornel yarn by not separating the yarn into its constituent filaments. A representative microstructure is provided in Figure 73. The average room temperature bend strength measured from three specimens of billet D0644 was 30,000 psi indicating no improvement in properties as compared to 100% dense Material XII(5) which has a room temperature bend strength in excess of 50,000 psi. A second billet of XIIf(5) with the Thornel reinforcement was prepared; same filament clustering was observed. The average diboride grain size was 5 microns. Strength data from room temperature to 1800°C in Table 52 are generally lower than would be expected for a Material XII(5) composition of the same grain size. Full co-operative effects typical of functional composites was not realized almost certainly due to the stresses not being transferred fully to the graphite filaments. This is because each filament of the yarn is not in contact with the boride. This would only be possible if the yarn were separated into its filament constituents. However, under such circumstances the filaments are degraded under the hot pressing conditions. Thus, the principal problem in forming filament boride composites revolves around chemical compatibility of the filament material and the diboride during hot pressing. It is clear that processes employing lower fabricating temperatures must be developed.

I.   Joining Characteristics

A limited study of diboride joining characteristics was performed at the Boeing Company (Seattle) in the final stages of the program.

The experiments were performed in air with conventional arc welding equipment. Butt welds were made between slabs approximately 0.25 in by 0.5 in by 0.1 in. Table 53 summarizes weld data and Figure 74 shows welds between some zirconium diboride compositions and some refractory metals. Welds between zirconium diboride and tantalum and niobium were pore free and of good appearance. Welds to molybdenum often contained a few pores and occasionally the diboride was cracked perpendicular to the weld. Flexural strengths for these welds varied between 15,000 and 30,000 psi including specimens (Mo-ZrB$_2$ welds) that contained short longitudinal cracks in the diboride. Zirconium diboride containing a silicon carbide addition was welded to tantalum and molybdenum. Welds contained many fine pores and an occasional larger pore. Porosity was generally heaviest at the weld-diboride interface. Flexural strengths were lower, 16,000-24,000 psi, presumable because of the porosity in the weld. The zirconium diboride compositions containing carbon could not be welded to tantalum or molybdenum. The liquid did not appear to wet the junction satisfactorily and the solidified melt contained many pores. These welds broke apart during normal handling. Trials to weld zirconium diboride to graphite and stainless steel were mostly unsuccessful. POCO Graphite and

47

Graph-i-tite G were used. The weld to the POCO graphite contained many fine pores and broke during handling. The weld to Graph-i-tite G contained fewer pores but its flexural strength was only 1800 psi. The weld to 321 stainless steel broke during handling.

The results suggest that suitable joining techniques can be developed by this method for the eventual application of the diboride materials which will of necessity require several joining methods, some chemical and others physical.

V. CONCLUSIONS

1. Manufacturing capability is available within present powder production technology to produce ZrB_2 powder in 100 to 400 pound quantities which meets specifications developed in this program for hot pressing grades to be employed with SiC and/or C additives. Production capability for HfB_2 powder is not similarly advanced as demonstrated by variability from lot to lot of 50 to 100 pound quantities. Limited availability of hafnium oxide of suitable composition as a starting material for production of HfB_2 and an apparent reaction variability in the production process contribute to procurement difficulties of HfB_2.

2. The system of ceramic additives, SiC and/or C function to enhance the hot pressing characteristics of ZrB_2 and HfB_2 powder by lowering the fabrication temperature needed to consolidate the powders to full densification. The additives employed in suitable quantities also provide a grain size control, eliminate processing difficulties encountered in the processing of ZrB_2 and HfB_2 with no intentional additives and increase the physical integrity of the material. Polycrystaline diboride composite materials comprised of ZrB_2 with discrete particles of SiC and/or C can be hot pressed in sizes up to 6 inches square by 2 to 3 inches high without reduction in properties and performance obtained from 2 and 3 inch diameter billets, provided adequate mixing is achieved and proper modifications of processing cycles are employed. Nondestructive testing procedures are available for assessing material integrity and variability. Hot pressing of hollow cylindrical shapes of the composite materials of 4 to 6 inches o.d. by 3 to 5 inches i.d. by 4 to 6 inches high appears feasible for production of dense structures. The larger sized billets could also be fabricated with HfB_2 base compositions providing suitable diboride powder were procured.

3. Present hot pressing technology and powder production capability are adequate to extend the sizes of billets fabricated and the quantities of ZrB_2 procured to 8 inches diameter by 4 inches high billets and 500 to 1000 pound powder lots. The system of ceramic additives provide fabrication enhancement such that processing of shaped billets other than cylinders should be attainable if moderately simple shapes of near uniform thickness are desired.

4. Loss of SiC from powder charges for plasma spraying and preferential formation of B_4C over SiC in pyrolytic depositions from gas stream containing volatile chlorides of boron, silicon and zirconium and methane prohibit the immediate use of such methods to produce coatings of diboride compositions containing SiC. Diboride powder specifications for plasma spraying were not developed in this program but attainment of 90 percent dense coatings appears feasible.

5. Technology for pressureless sintering of a ZrB_2 and SiC composition with Zr of ZrH_2 added as a reactive activating reagent was not developed to any significant extent. The available ZrB_2 powder was not well suited for sintering studies. Scale-up problems typical for this fabrication method are expected for the diboride compositions with SiC and/or C additives.

49

6.   Hot forging is a feasible method for limited shaping of flat thin sections of billets hot pressed or otherwise consolidated. Hot forging capability demonstrated for dense fine grained structures of Material V and VIII could be extended to similar structures of Material XIII(20) and the hafnium analogs with the same techniques, and also to fine grained, 95 percent dense structures of Materials I and II. The strain rate dependence observed for deformation processes at high temperatures in the mechanical properties study (9) strongly suggest that fully dense coarser grained structures of Materials I and II could be successfully hot forged at significantly lower strain rates than employed in this study for Materials V and VIII.

7.   Hot isostatic pressing is a feasible fabrication method for consolidating Materials I and II and the SiC composites to near full density within present processing technology. Grain growth is minimized by the high processing pressure (36,000 psi) and the low processing temperature (1650°C). Additions of small amounts of carbon detract somewhat from the processing characteristics, however, Material VIII(18,10) can be consolidated to near full density. The method can be employed to advantage for shape forming but appropriate canning procedures and improved cold compacting techniques have to be developed.

8.   The carbon containing compositions can be fabricated by the arc casting procedure. Fabrication by this method eliminates the solid particulate requirements of most ceramic processing methods and could prove to be advantageous for shape forming.

9.   The need for lower temperature fabrication processes and reinforcement protective systems for successful formation of functional, filament or fiber reinforced diborides was demonstrated.

10.   Tradeoffs in strength, oxidation resistance and possible thermal stress resistance for diboride materials fabricated by methods other than hot pressing can be estimated from extensive characterization and property data generated for hot pressed structures of 5 to 20 percent porosity.

11.   Considerable confidence can be placed on the fabrication of diboride compositions with SiC and/or C by hot pressing to produce monolithic ceramic bodies of sizes and material integrity for applications such as nose cones and leading edges as well as other hardware items which require the strength, thermal stress resistance and oxidation and corrosion resistance of the diboride compositions.

50

REFERENCES

1. Kaufman, L. and Clougherty, E. V., "Investigation of Boride Compounds for Very High Temperature Applications", RTD-TDR-63-4096, Part I, December 1963.

2. Kaufman, L. and Clougherty, E. V., "Investigation of Boride Compounds for Very High Temperature Applications", RTD-TDR-63-4096, Part II, February 1965.

3. Kaufman, L. and Clougherty, E. V., "Investigation of Boride Compounds for Very High Temperature Applications", RTD-TDR-63-4096, Part III, March 1966.

4. Stinebring, R. C., Shultz, A. W. and Orner, J. W., "Investigation of Nondestructive Methods for the Evaluation of Graphite Materials", AFML-TR-67-128, Part II, December 1968.

5. Clougherty, E. V., Kalish, D. and Peters, E. T., "Research and Development of Refractory Oxidation Resistant Diborides", AFML-TR-68-190, May 1968.

6. Clougherty, E. V., "Research and Development of Refractory Oxidation Resistant Diborides, Part II Volume I: Summary", AFML-TR-68-190, Part II, Volume I, December 1969.

7. Clougherty, E. V., Hill, R. J., Rhodes, W. H., and Peters, E. T., "Research and Development of Refractory Oxidation Resistant Diborides, Part II Volume II: Processing and Characterization", AFML-TR-68-190, Part II Volume II, November 1969.

8. Clougherty, E. V. and Peters, E. T., "Research and Development of Refractory Oxidation Resistant Diborides, Part II Volume III: Thermochemical Stability Characteristics", AFML-TR-68-190, Part II Volume III, November 1969.

9. Rhodes, W. H., Clougherty, E. V. and Kalish, D., "Research and Development of Refractory Oxidation Resistant Diborides, Part II Volume IV: Mechanical Properties", AFML-TR-68-190, Part II Volume IV, November 1969.

10. Clougherty, E. V., Wilkes, K. E., and Tye, R. P., "Research and Development of Refractory Oxidation Resistant Diborides, Part II Volume V: Physical, Thermal, Electrical and Optical Properties", AFML-TR-68-190, Part II Volume V, November 1969.

11. Clougherty, E. V., Niesz, D. E., and Mistretta, A. L., "Research and Development of Refractory Oxidation Resistant Diborides, Part II Volume VI: Thermal Stress Resistance", AFML-TR-68-190, Part II Volume VI, November 1969.

51

12. Clougherty, E. V., Mistretta, A. L. and Anthony, F. M., "Research and Development of Refractory Oxidation-Resistant Diborides, Part II Volume VII· Application Evaluations and Design Considerations", AFML-TR-68-190, Part II Volume VII, November 1969 (Secret Report).

13. Foster, E. L., et al., "Development of a Subscale Manufacturing Process for the Fabrication of Hypereutectic Transition Metal Carbide Composites", AFML-TR-68-255, September 1968.

14. Powell, C. F., "Borides", in High Temperature Technology, John Wiley and Sons, Inc., New York, N. Y. (1956), I. E. Campbell, Editor in Chief.

15. Kriege, O. H., "The Analysis of Refractory Borides, Carbides, Nitrides and Silicides", LA-2306, Los Alamos Scientific Laboratory of the University of California.

16. Kebler, R. W. and Walsh, P. M., "Research on Physical and Chemical Principles Affecting High Temperature Materials for Rocket Nozzles", Union Carbide Research Institute, Tarrytown, New York, Final Report (1965), Contract No. DA-30-069-ORD-2787, Volume III, Appendices 6 and 7.

17. Brukl, C. E., "Ternary Phase Equilibria in Transition Metal-Boron-Carbon-Silicon Systems", AFML-TR-65-2, Part II, Volume X, 1966.

18. Rudy, E., Windisch, St., "Ternary Phase Equilibria in Transition Metal Boron-Carbon-Silicon Systems", Part II, Volume XIII, December 1966.

19. Hillert, M., "On the Theory of Normal and Abnormal Grain Growht", Acta Met. (1965), 13, 227-238.

20. Heuer, A. J., et al., "Microstructure Studies of Polycrystalline Refractory Oxides", AVSSD-0211-67-RR(1967).

21. Krochmal, J. J., "Fiber Reinforced Ceramics: A Review and Assessment of Their Potential", AFML-TR-67-207, October 1967.

POLISHED SURFACE
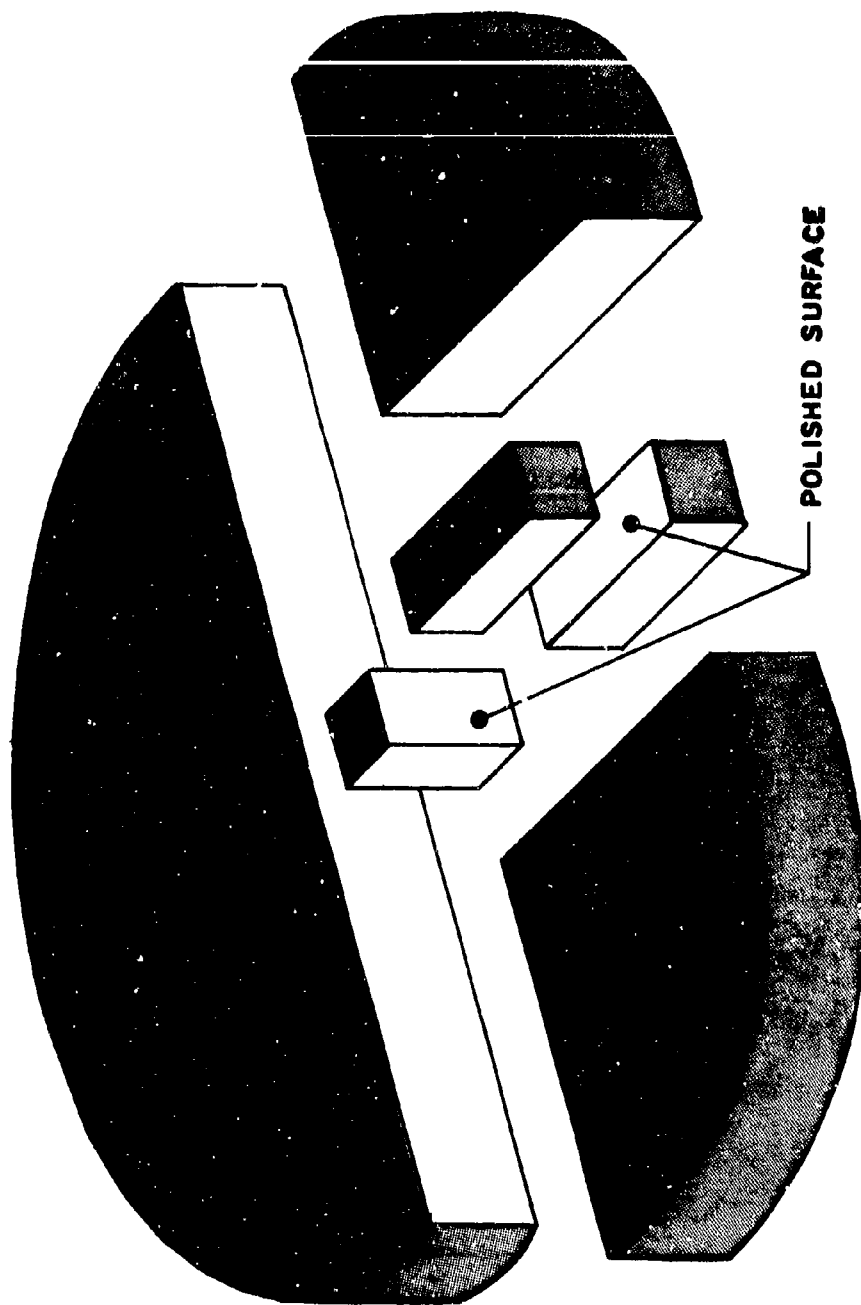
Figure 1. Cut-away Drawing of Sections for Metallographic Analysis in Phase One and Phase Two.

Front surface mirror

Optical Pyrometer

Rigid Platform

Attached to Moving Piston
0-1 Inch Dial Indicator

Pistons to
Hydraulic Ram Head

Asbestos Ring

Quartz Lens

Piston

Argon Flushed Water
Cooled Sight Tube For
Temperature Measurement

Graphite
Retaining
Tubes

Induction Coil

Inner Graphite Sleeve*

Boron Nitride Impreg-
nated Graphite Cloth

Piston*

Diboride Billet

Graphite Mold

Carbon Black Insulation

Carbon
Insulating
Plates

Water Cooled Steel
Support Plate

Transite
Support Plate

*Coated with boron nitride slurry

Figure 2. Schematic Drawing of Graphite Hot Pressing Assembly.

54
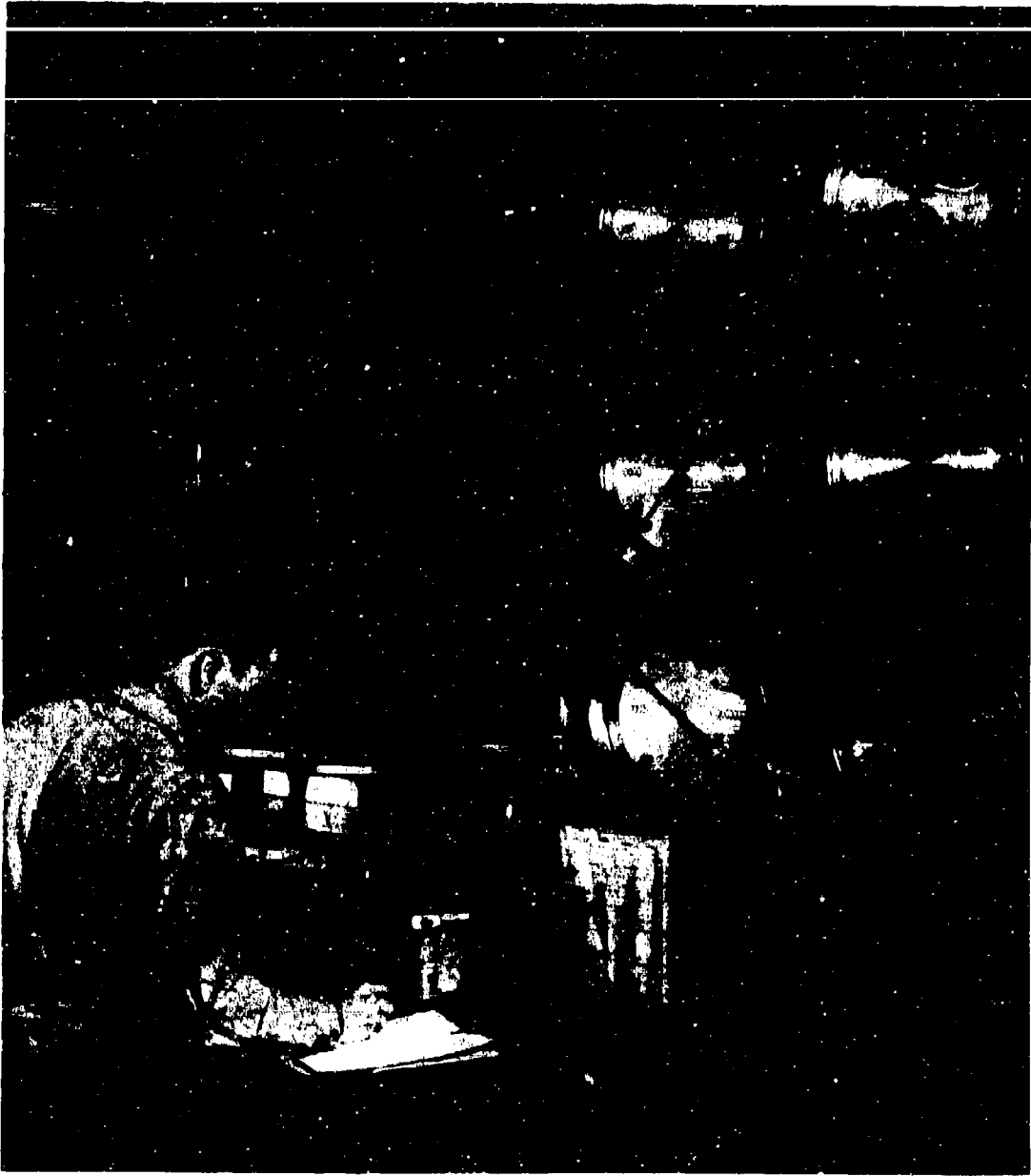
Figure 3. Hot Pressing Assembly, 125 Ton Press.
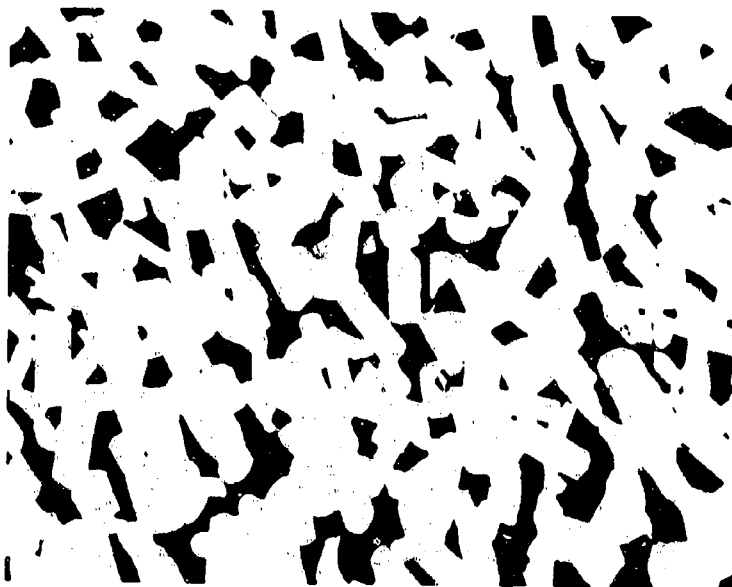
Avco Plate
No. 4808

As Polished   500X

Figure 4. Microstructure of Billet I02AV D0645
           Pressed with Vibratory Milled Powder.

56
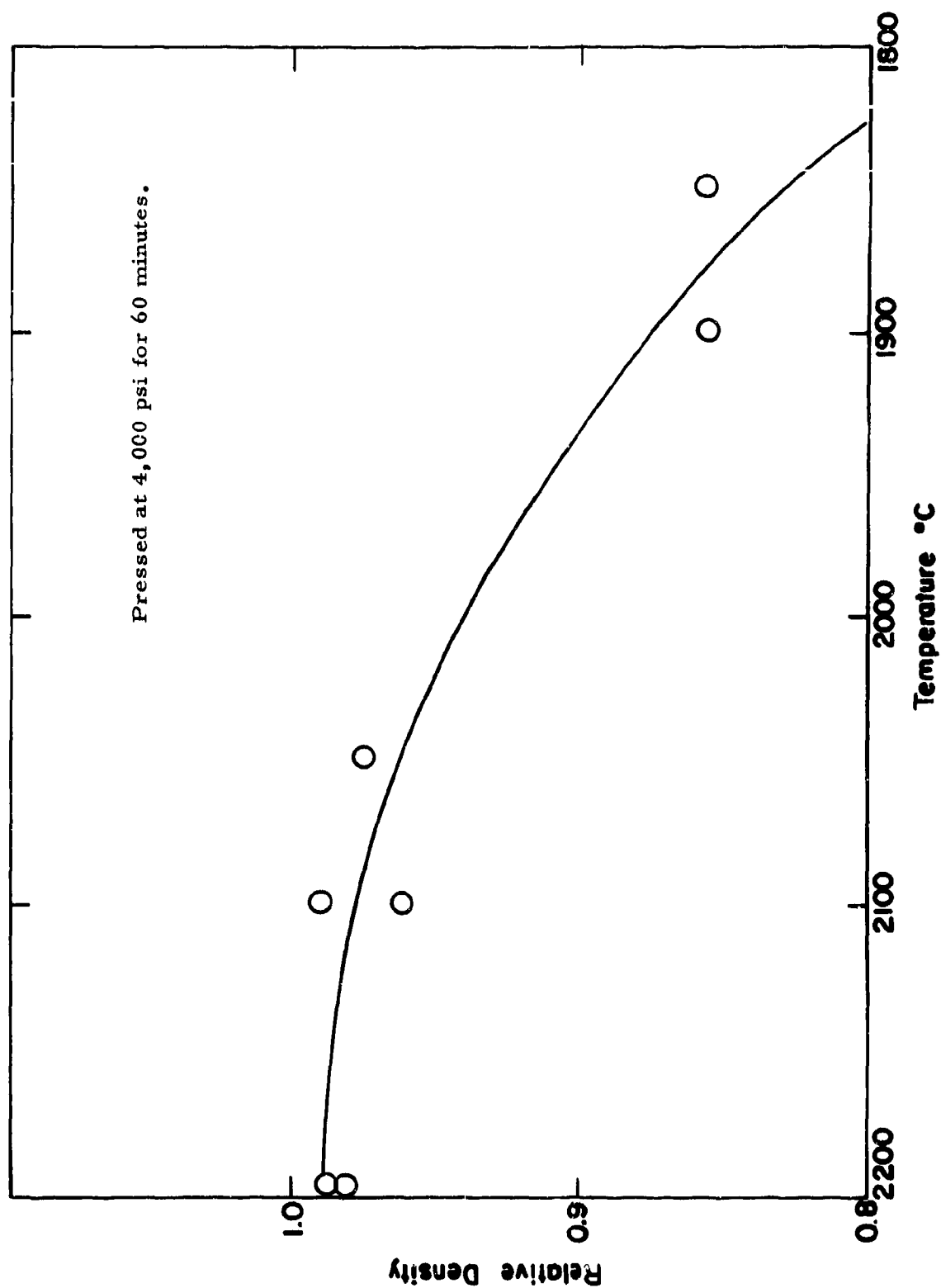
Figure 5. Densification as a Function of Temperature for Material 105A.
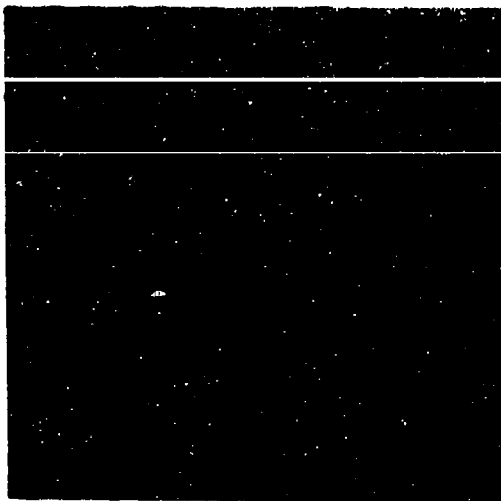
ManLabs Plate No. 4584-W
Etched   500X
       I03A D0619K
       6.02 g/cc, 100%
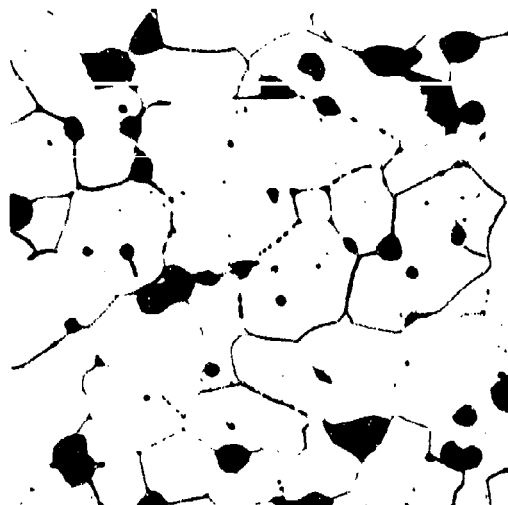
ManLabs Plate No. 5271
Etched   500X
       I07F D0700K
       5.91 g/cc, 99%
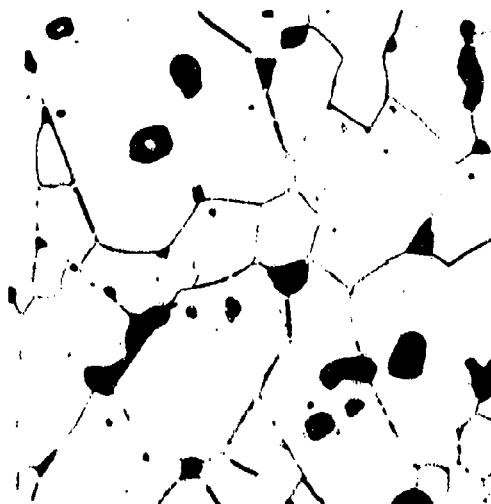
ManLabs Plate No. 5269
Etched   500X
       I07F D0701K
       5.93 g/cc, 99%

Figure 6. Phase Two Structures for Fully Dense Material I.
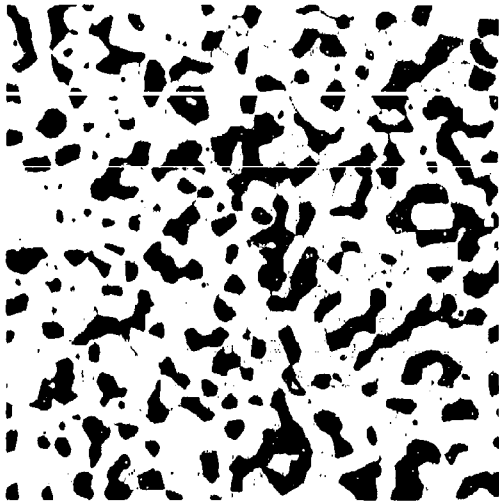
ManLabs Plate No. 4933-1
Etched   500X
        I07F D0940K
        5.03 g/cc, 85%
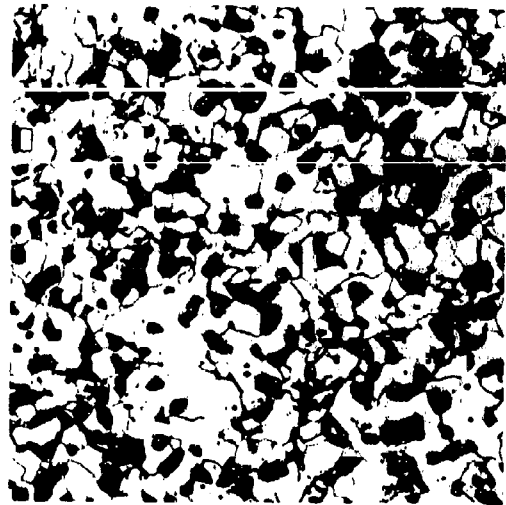
ManLabs Plate No. 5656
Etched   500X
        I07F D0905K
        5.40 g/cc, 90.6%
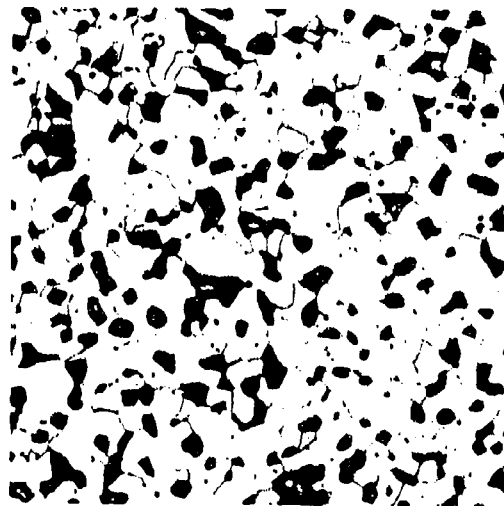
ManLabs Plate No. 5658
Etched   500X
        I07F D0936K
        5.21 g/cc, 87.3%

Figure 7. Phase Two Structures for Ninety PerCent Dense Material I.

59
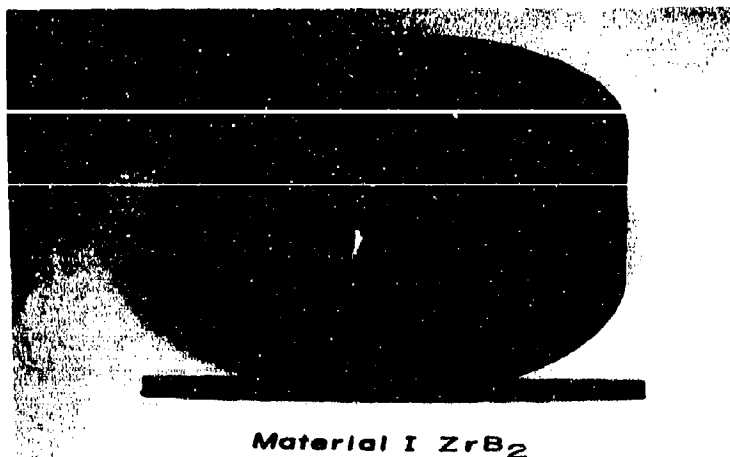
Material I ZrB$_2$

Billet I0001M
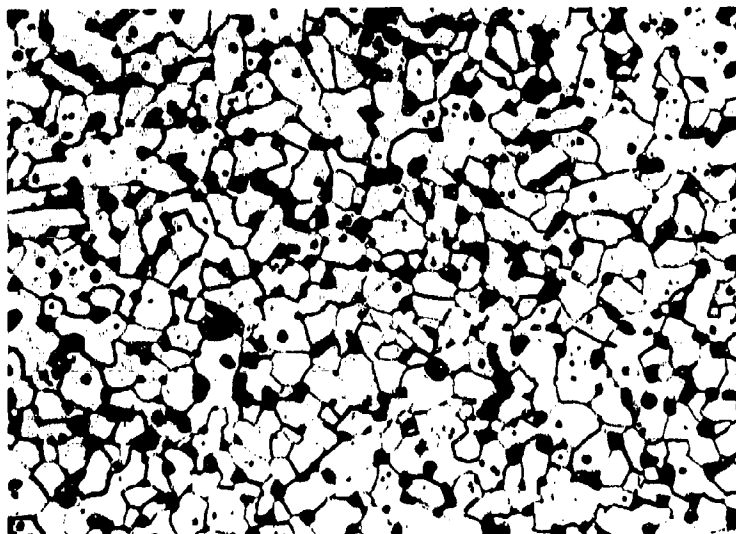
ManLabs Plate No. 5435
Etched   5.80 g/cc, 96.7%   500X

Figure 8. Phase Three Material I Billet Fabricated
by U.S. Borax with Representative
Microstructure.

60
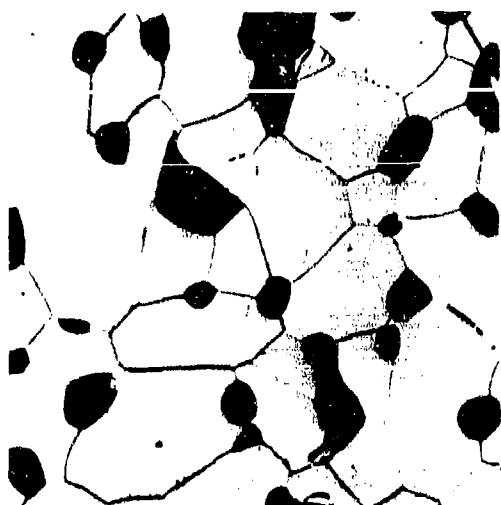
ManLabs Plate No. 5660
Etched   500X
            107F R37L
            5.32 g/cc, 88%

ManLabs Plate No. 5434
Etched   500X
            107F R38L
            5.46 g/cc, 90.5%
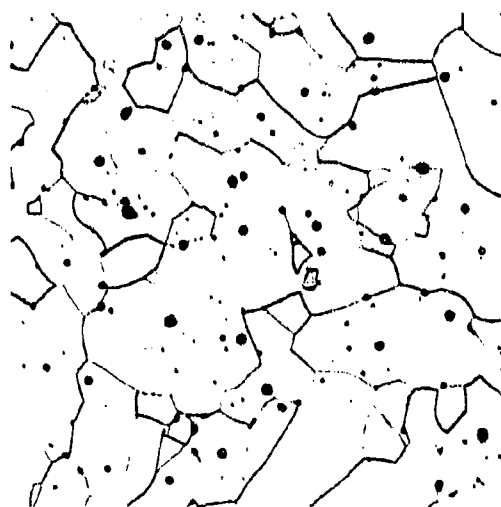
ManLabs Plate No. 5420
Etched   500X
        105A R44L
        6.10 g/cc, 100%

Figure 9. Representative Microstructures of Material I Fabricated
           in Phase Three Processing Study.

61

Etched   500X

Avco Plate No.
4491-A

Figure 10. Morphology of Large Grains Found in Billet
V(5)02 D0531.

Etched - Polarized Light   500X
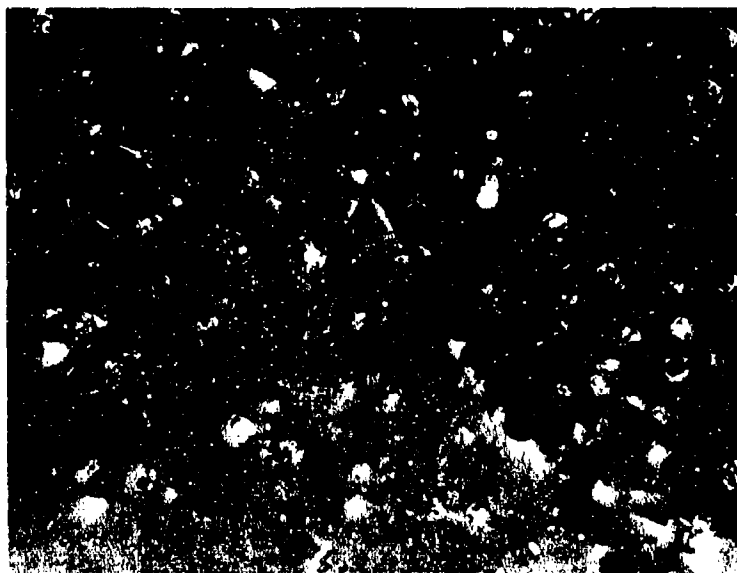
Avco Plate No.
4725-R

Figure 11. Morphology of Large Grains Found in Billet
V(10)07 D0721K.

62
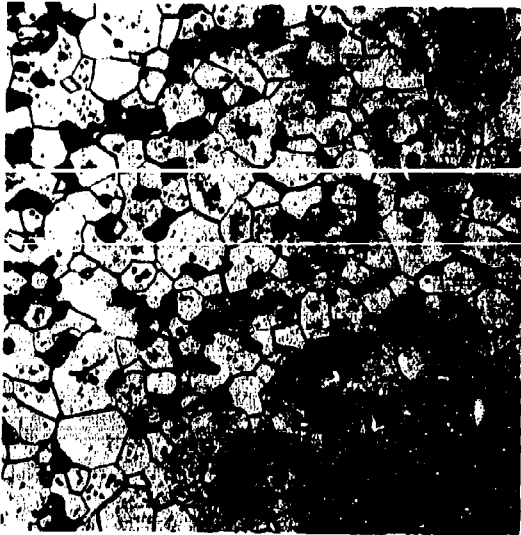
Avco Plate No. 4539C
Etched   500X
    V07F D0580K
    5.56 g/cc
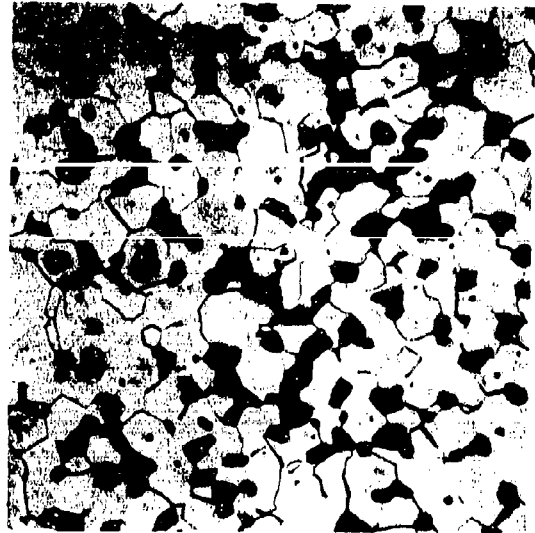
Avco Plate No. 4751-A
Etched   500X
    V07F D0703K
    5.51 g/cc
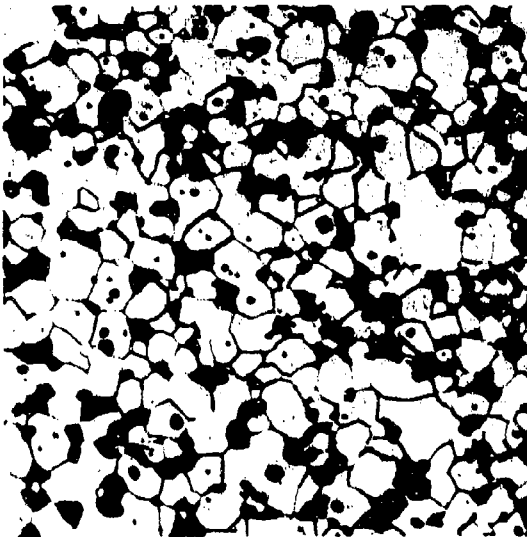
ManLabs Plate No. 5275
Etched   500X
    V07F D0706K
    5.50 g/cc
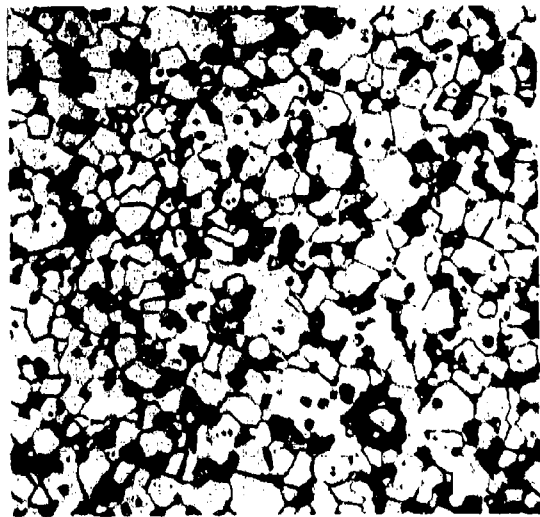
ManLabs Plate No. 5830
Etched   500X
    V07F D0902K
    5.52 g/cc

Figure 12. Phase Two Structures for Fully Dense Material V.

63
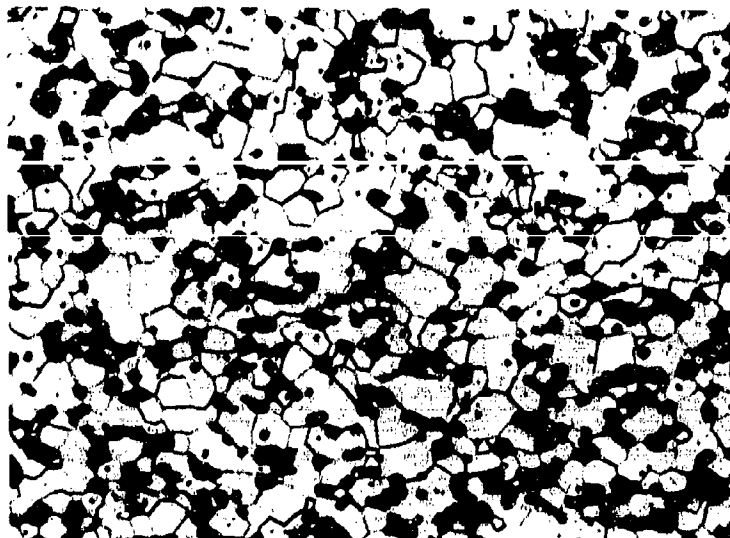
ManLabs Plate No. 5258
Etched   500X

V07F R26L
5.53 g/cc
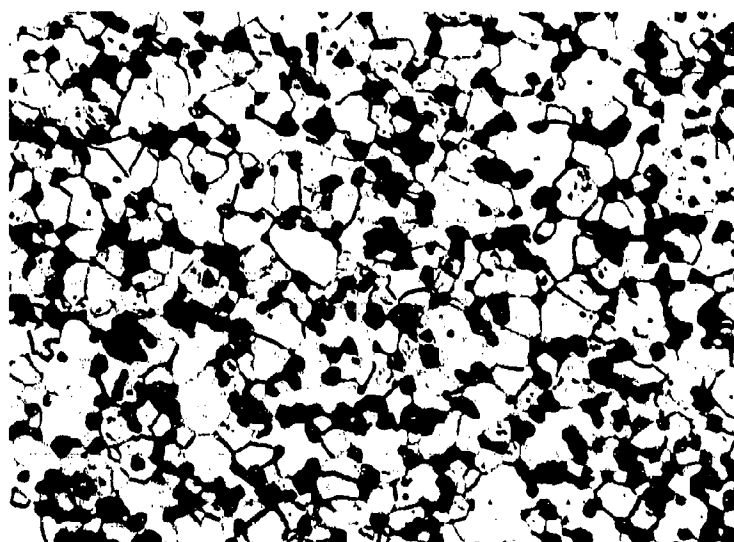
ManLabs Plate No. 5691
Etched   500X

V07F R31L
5.53 g/cc

Figure 13.   Phase Three Structures for Fully Dense
             Material V.

64
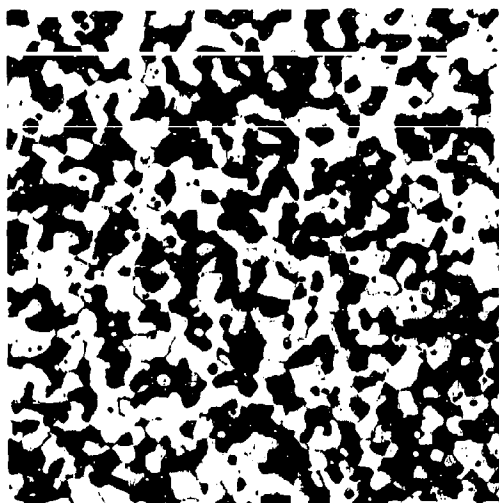
Avco Plate No. 5273
Etched   500X
       V07F D0845K
          4.83 g/cc
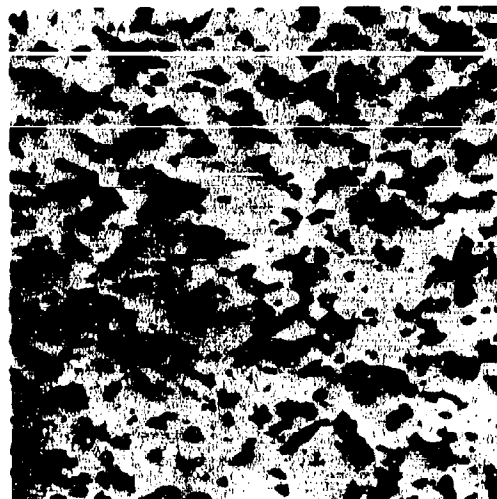
ManLabs Plate No. 5265
As Polished   500X
       V07F D0849K
          4.95 g/cc
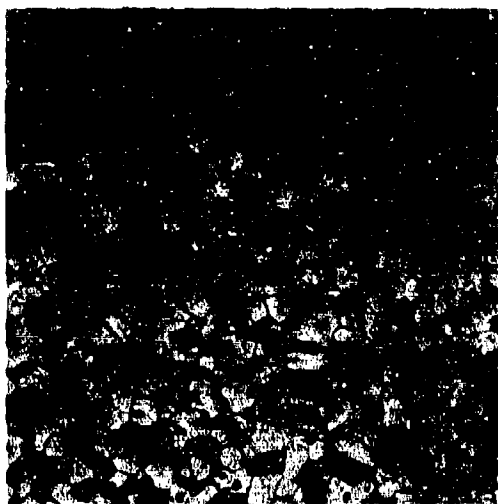
Avco Plate No. 4876-12
Etched   500X
       V07F D0850K
          4.94 g/cc
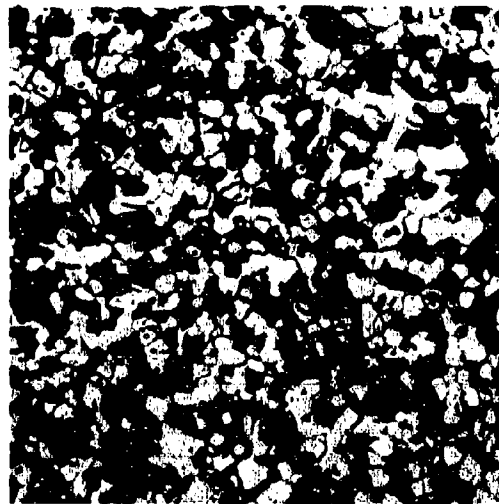
ManLabs Plate No. 5702
Etched   500X
       V07F D0851K
          4.79 g/cc

Figure 14.   Phase Two Structures for Ninety Percent Dense
             Material V.

65
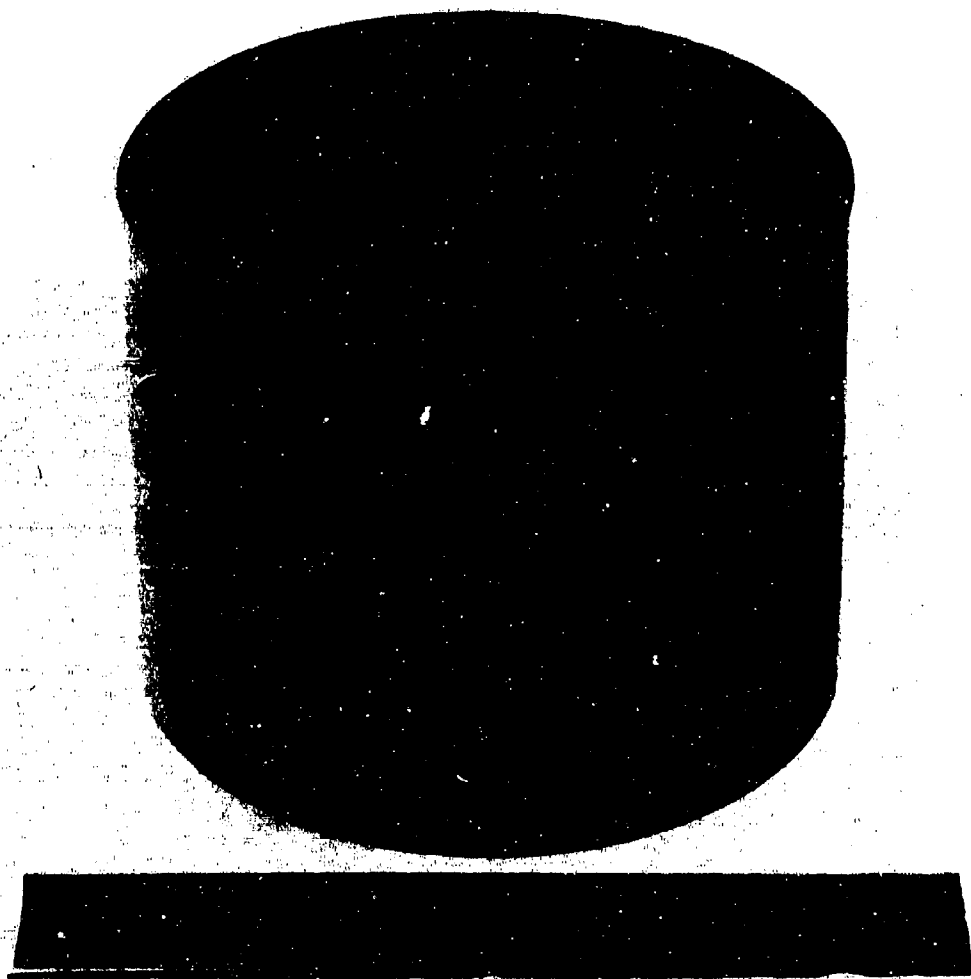
Figure 15. Photograph of Hot Pressed Cylinder, Billet V07F Q2409H.
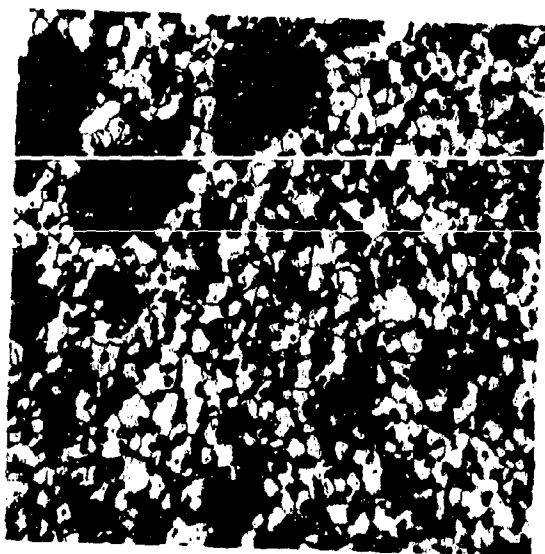
Avco Plate No. 4751-C
Etched
                                 500X
        VIII07F D0760K
          4.66 g/cc
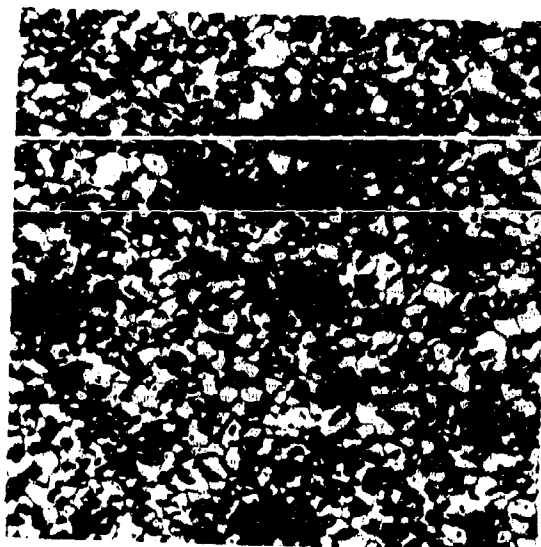
ManLabs Plate No. 5291
Etched
                                 500X
        VIII07F D0767K
          4.65 g/cc
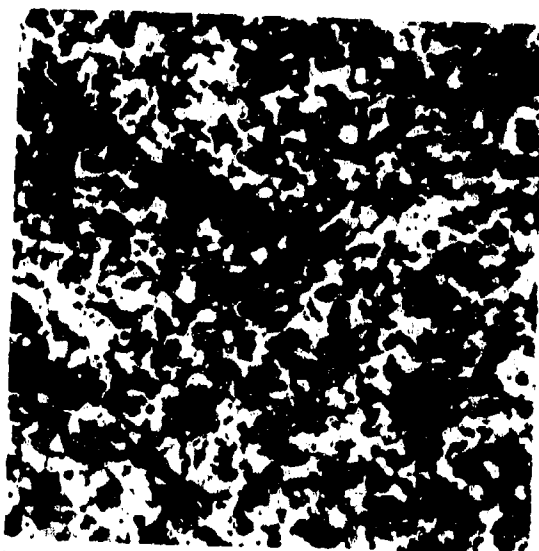
ManLabs Plate No. 5704
As Polished
                                 500X
        VIII07F D0768K
          4.63 g/cc
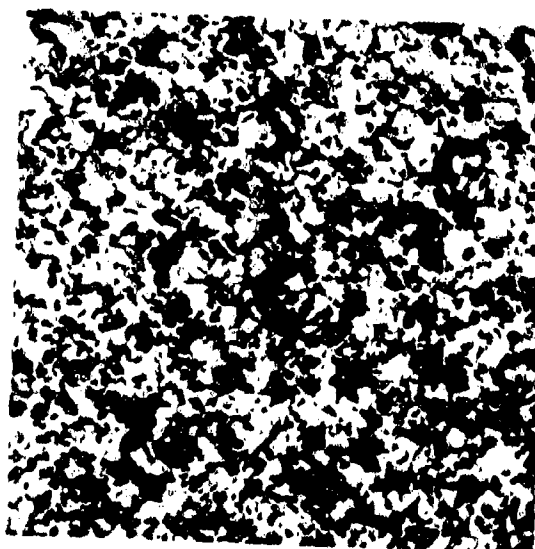
ManLabs Plate No. 5703
As Polished
                                 500X
        VIII07F D0975K
          4.58 g/cc

Figure 16. Phase Two Structures for Fully Dense Material
VIII.
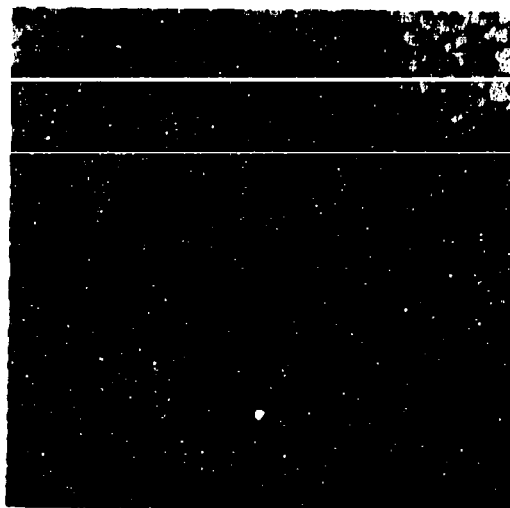
Avco Plate No. 4876-1
Etched   500X
    VIII(18,10)07F D0919K
       5.26 g/cc
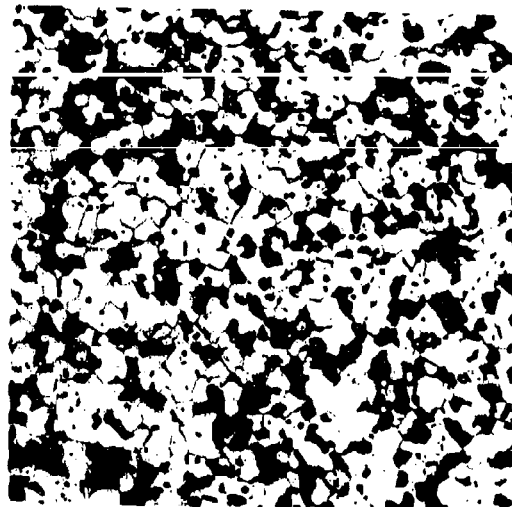
ManLabs Plate No. 5442
Etched   500X
    VIII(18,10)07F D0917K
       5.14 g/cc
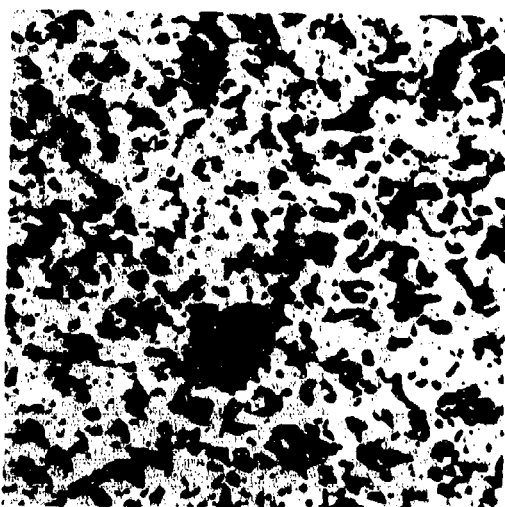
ManLabs Plate No. 5695
Etched   500X
    VIII(18,10)07F D0920K
       5.25 g/cc
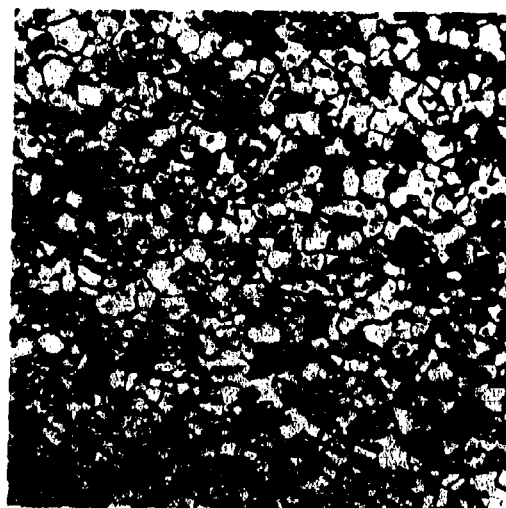
ManLabs Plate No. 5716
Etched   500X
    VIII(18,10)07F D0904K
       5.28 g/cc

Figure 17.   Phase Two Structures for Fully Dense Material
VIII(18,10).

68
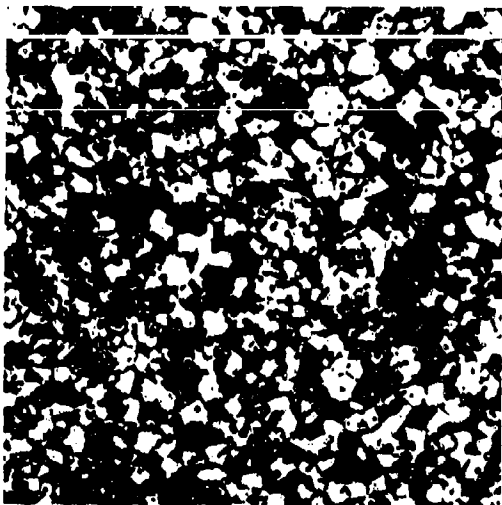
ManLabs Plate No. 5355
As Polished   500X
VIII07F Q 2321L
4.19 g/cc
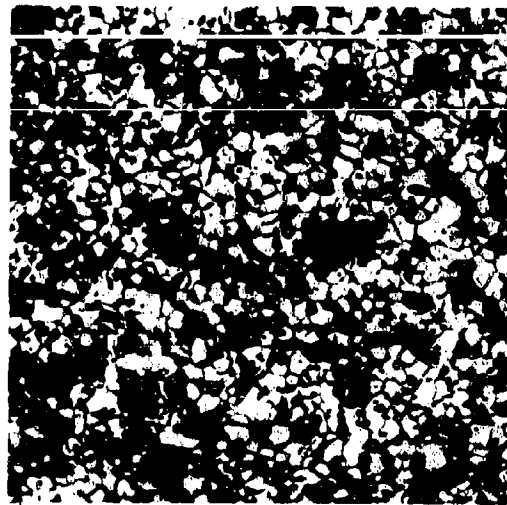
ManLabs Plate No. 5344
As Polished   500X
VIII(18,10)07F R33L
5.16 g/cc
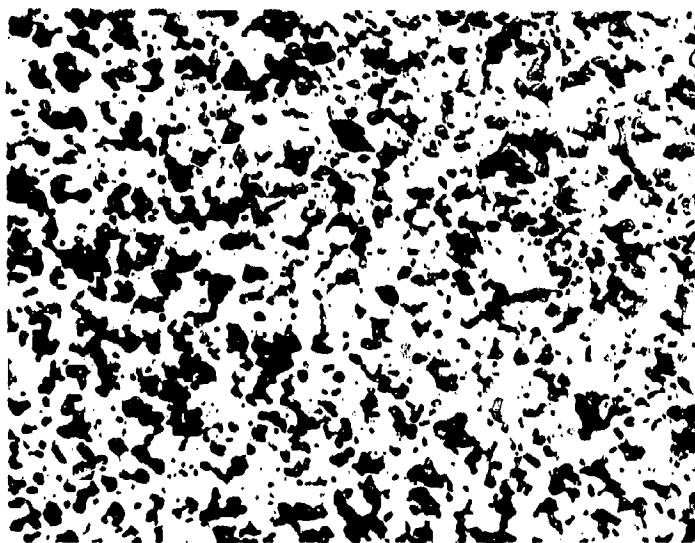
ManLabs Plate No. 5466
As Polished   500X
VIII(18,10)07F R40L
5.21 g/cc

Figure 18.   Phase Three Structures of Material VIII and
Material VIII(18,10).
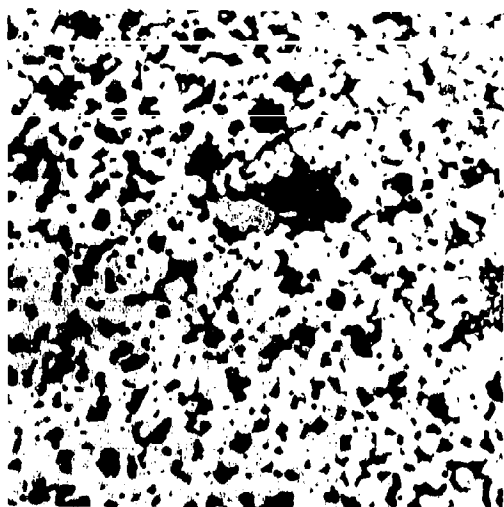
Avco Plate No. 4600-N
As Polished   500X
        X07F   D0634
Pressing Temperature, 1700°C
        5.28 g/cc
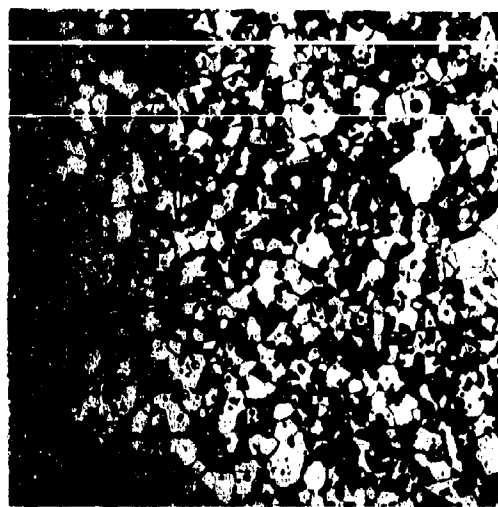
Avco Plate No. 4539-W
Etched   500X
        X07F   D0597
Pressing Temperature, 1800°C
        5. 28 g/cc
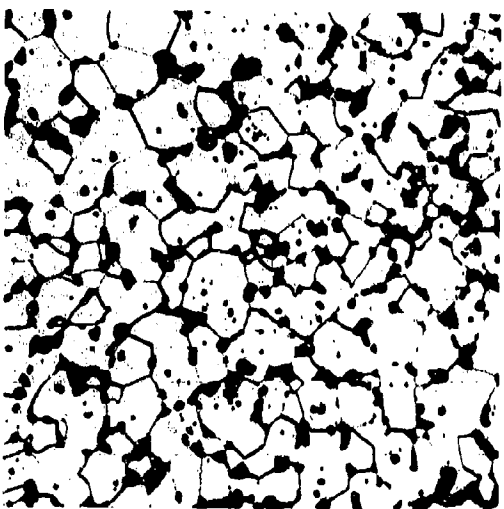
Avco Plate No. 4539U
Etched   500X
        X07F   D0596
Pressing Temperature, 1900°C
        5.53 g/cc

Avco Plate No. 4600-Q
Etched   500X
        X07F   D0635
Pressing Temperature, 2000°C
        5.81 g/cc

Figure 19.   Material X Structures of Billets Hot Pressed at 1700°, 1800°,
               1900° and 2000°C.

70

Etched   500X
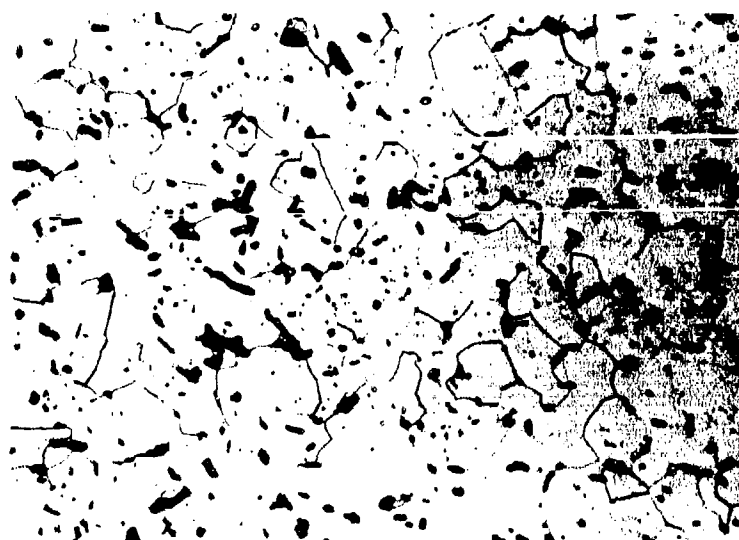
XII(5)07F D0668
5.82 g/cc

Avco
Plate No.
4647D
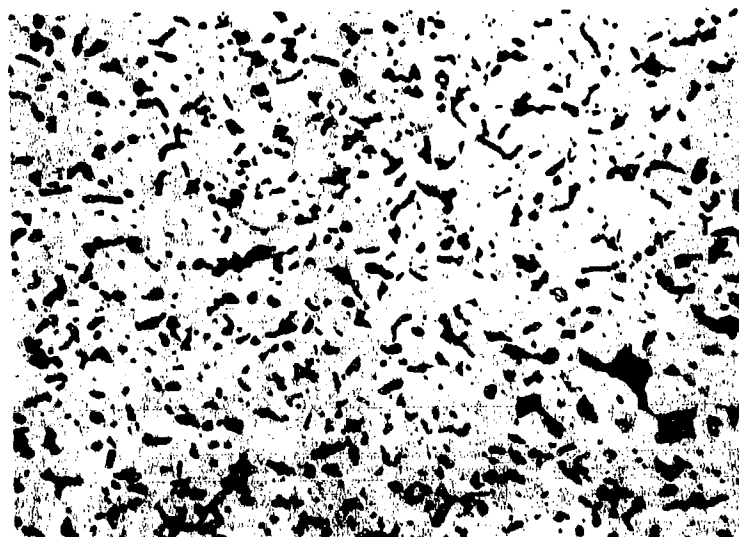
As Polished   500X

XII(10)07F D0667
5.64 g/cc

Avco
Plate No.
4647A

Figure 20. Microstructural Features of Material XII(5)
and Material XII(10) Fabricated with Poco
Graphite.

71

Avco Plate No. 4775-F
Etched   500X
    XII(20)07F D0805K
     5.43 g/cc
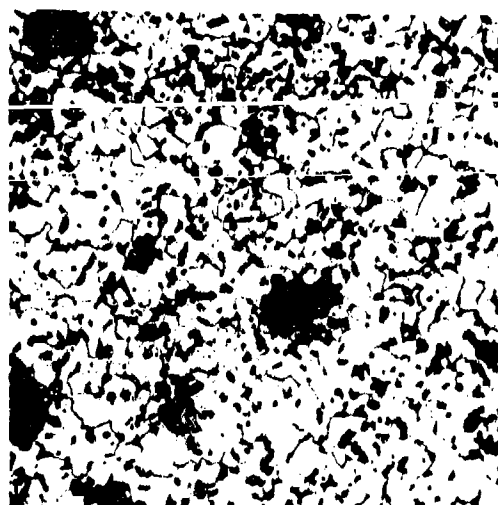
ManLabs Plate No. 5281
Etched   500X
    XII(20)07F D0809K
     5.36 g/cc
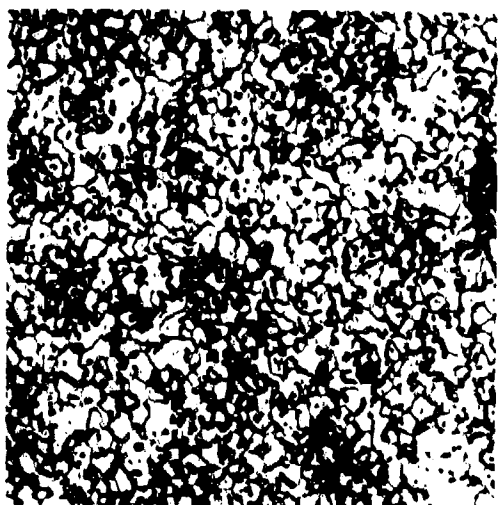
ManLabs Plate No. 5277
Etched   500X
    XII(20)07F D0810K
     5.36 g/cc
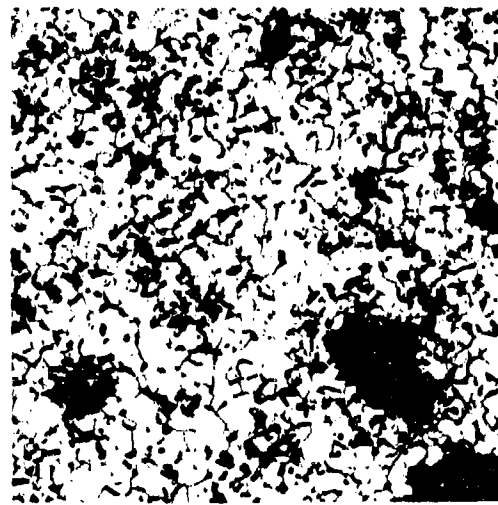
ManLabs Plate No. 5446
Etched   500X
    XII(20)07F D0812K
     5.37 g/cc

Figure 21. Phase Two Structures for Fully Dense Material
XII(20).

72
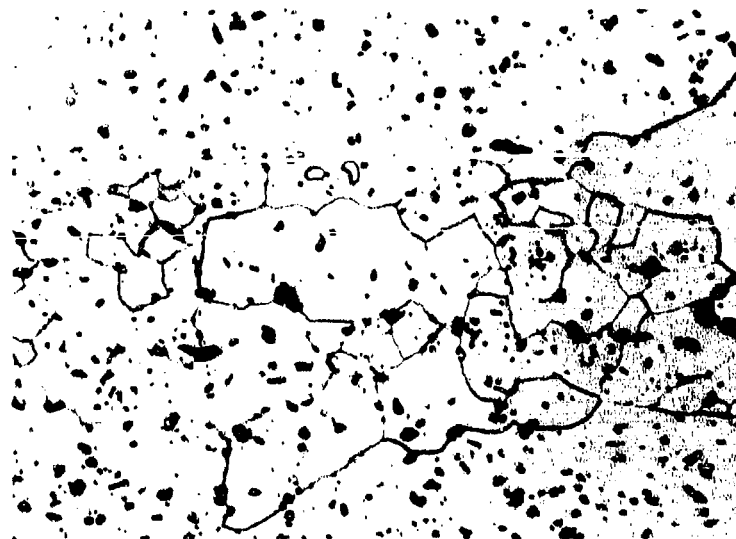
Avco Plate
No. 4600T

Etched   500X

XII(5)07F D0638
5.89 g/cc

Figure 22. Morphology of Large Grains Produced in Material
XII Grain Growth Anomaly.

ManLabs
Plate No.
5682

Etched   500X

XI'(20)07F R56L
5.45 g/cc

Figure 23. Phase Three Structure of Fully Dense Material
XII(20).

73
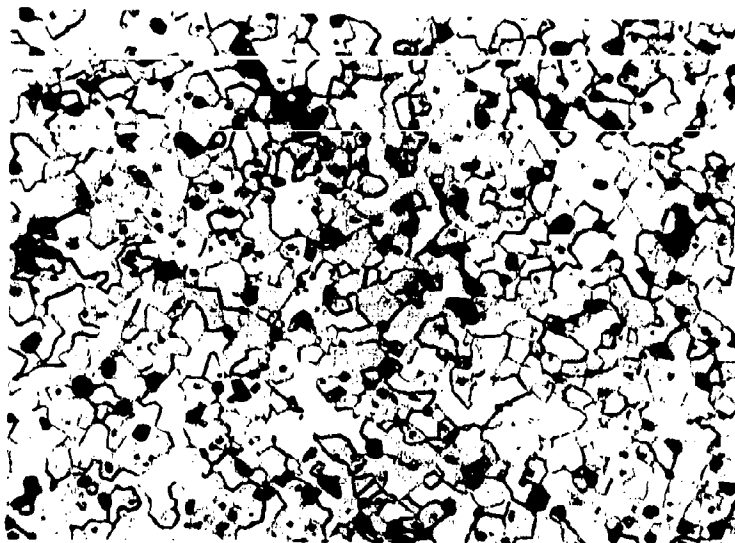
ManLabs Plate No. 1-7349

Etched   500X

II06B D0672

Figure 24. Representative Microstructure of Material II06B.
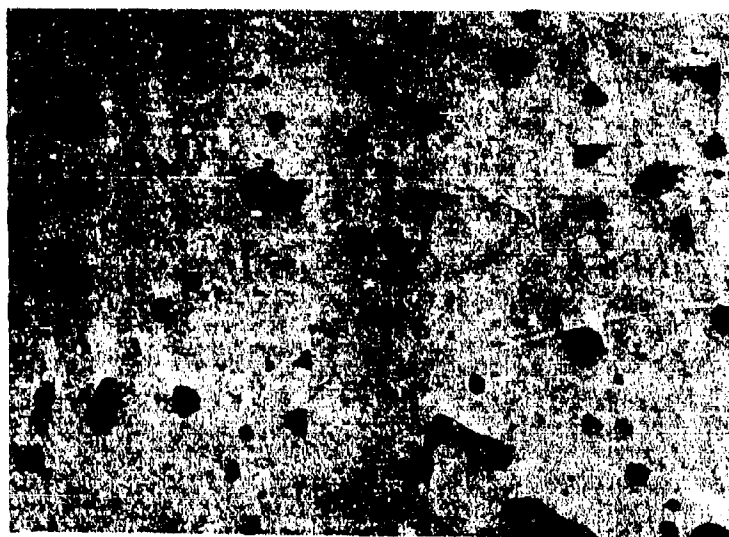
Avco Plate No. 4751-J

As Polished   500X

II09F D0784

Figure 25. Representative Microstructure of Material II09F.

74
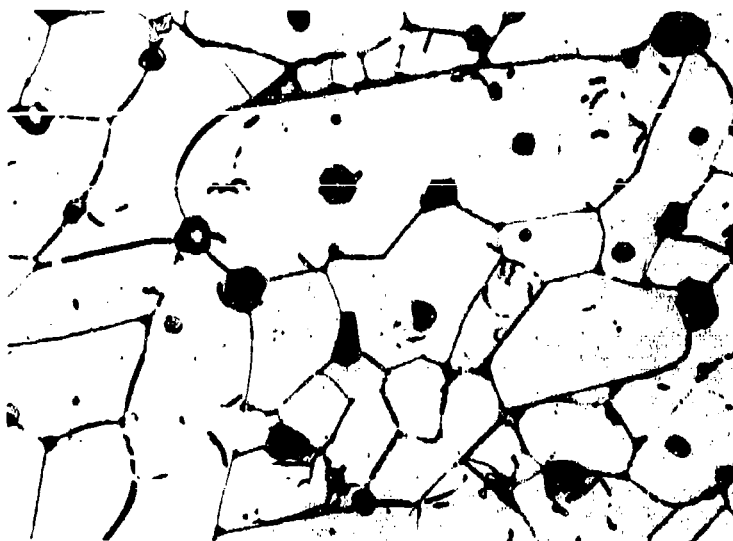
Avco Plate No. 4846A
Etched   500X
                    II09F D0898

Figure 26. Representative Microstructure of Coarse
            Grained Material II09F.

Avco Plate No. 4678-D
As Polished   500X
                    II10 D0726

Figure 27. Representative Microstructure of Material
            II10.

75
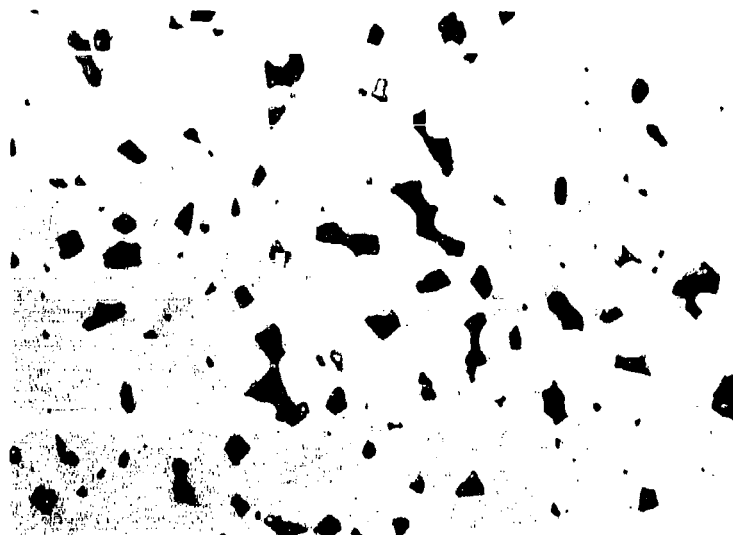
ManLabs Plate No. 5310
As Polished

Figure 28. Microstructural Features of Hot Pressed Five
Volume Percent SiC and II06B HfB$_2$, III(5)06B
D0915.

ManLabs Plate No. 5312
As Polished

Figure 29. Microstructural Features of Hot Pressed Five
Volume Percent SiC and II10 HfB$_2$, III(5)1D
D0918.

76
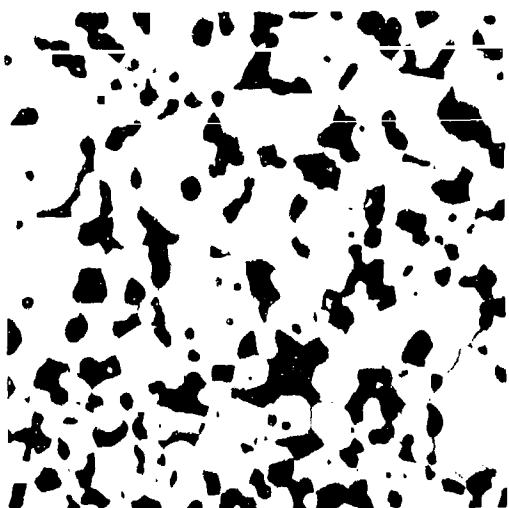
Avco Plate No. 4861-2
As Polished   500X
    III10 D0941K
     9.21 g/cc
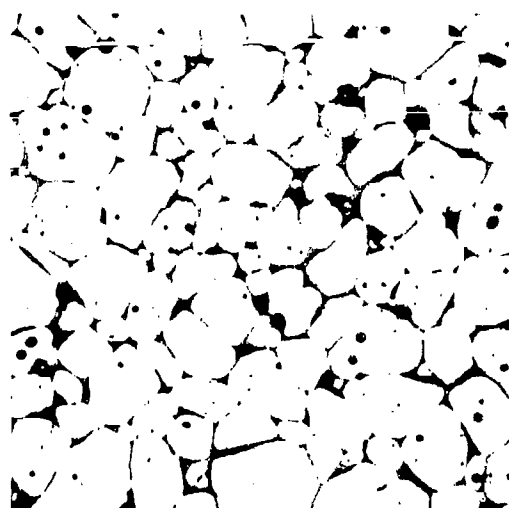
ManLabs Plate No. 5431
As Polished   500X
    III10 D0943K
     9.21 g/cc
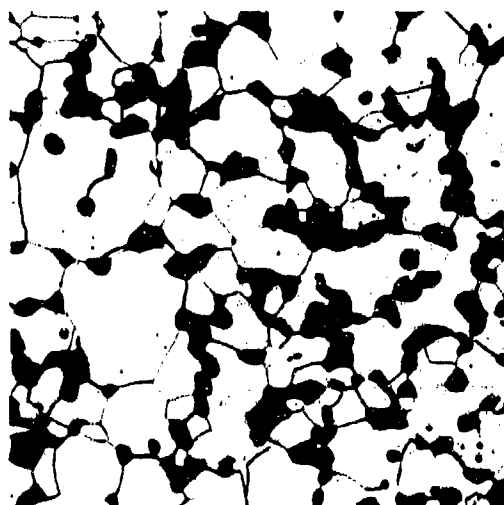
ManLabs Plate No. 1-9847
Etched   500X
    III10 D0944K
     9.21 g/cc

Figure 30. Phase Two Structures for Dense Material III10.
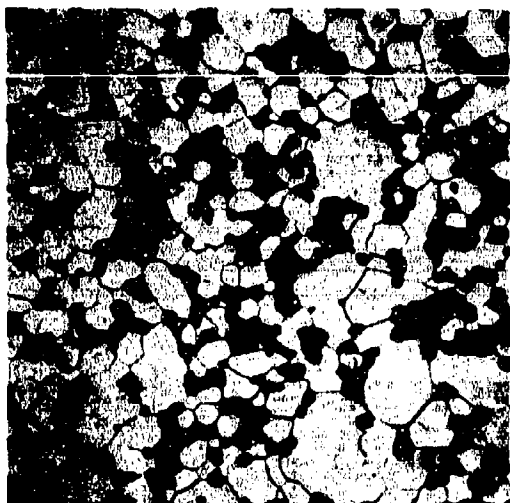
Avco Plate No. 4876-7
Etched   500X
          IV09F D0808K
          8.42 g/cc
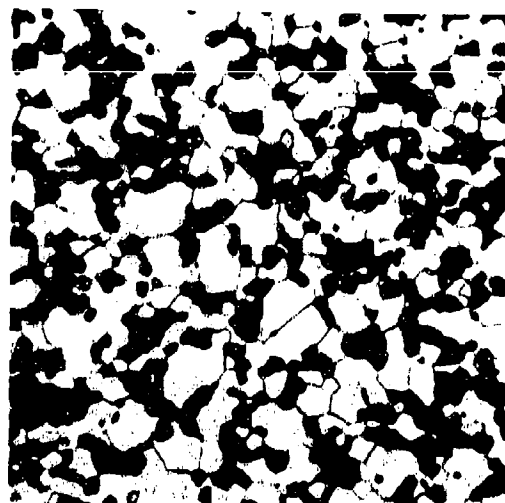
ManLabs Plate No. 5289
Etched   500X
          IV09F D0804K
          8.38 g/cc
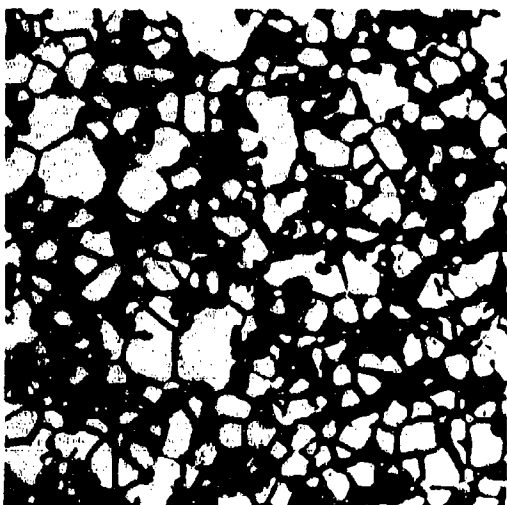
ManLabs Plate No. 5283
Etched   500X
          IV09F D0807K
          8.26 g/cc
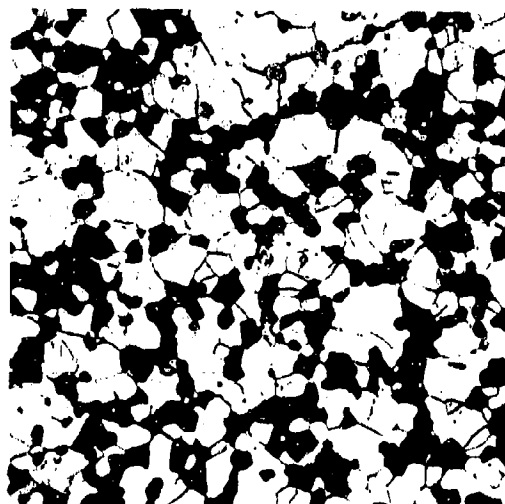
ManLabs Plate No. 5375
Etched   500X
          IV09F D0811K
          8.39 g/cc

Figure 31. Phase Two Structures for Dense Material IV09F.
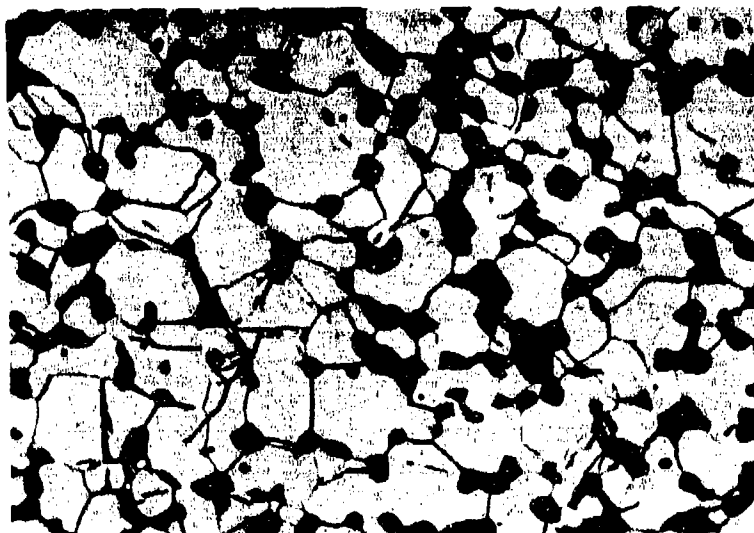
ManLabs Plate No. 5712
Etched   500X

Figure 32. Microstructural Features of Phase Three Billet
            III 10R52L.

79
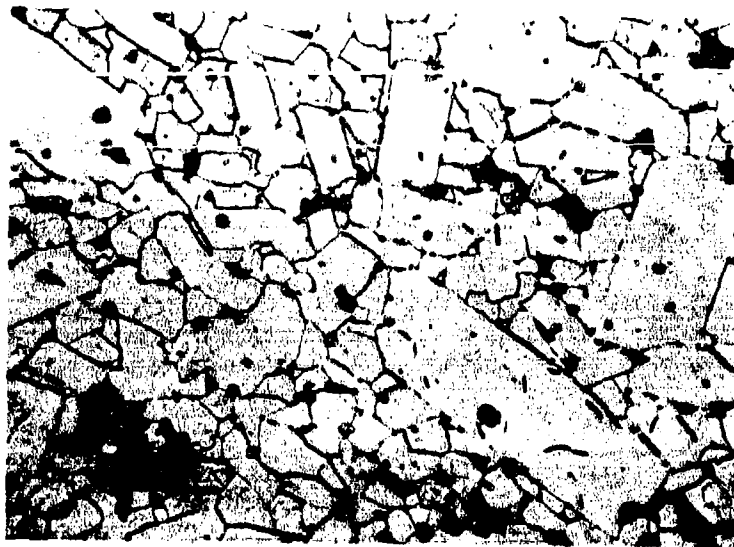
As-polished   Avco Plate No.
4727-I

500X

Figure 33. Microstructural Features of Material IX09F
D0745 Fabricated at 1900°C.
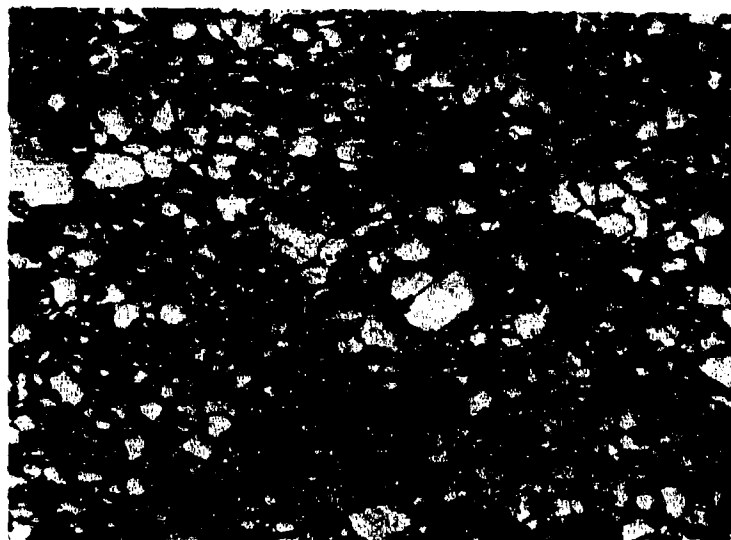
Etched   Avco Plate No.
4725-O

500X

Figure 34. Microstructural Features of Material XIV09F
D0751.
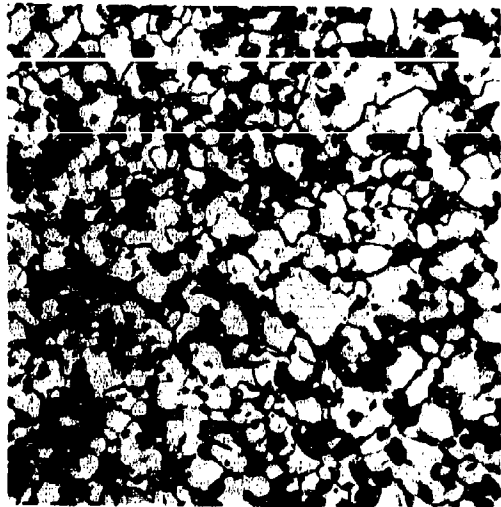
Avco Plate No. 4965A
Etched   500X
        XIV09F D1036K
          8.67 g/cc
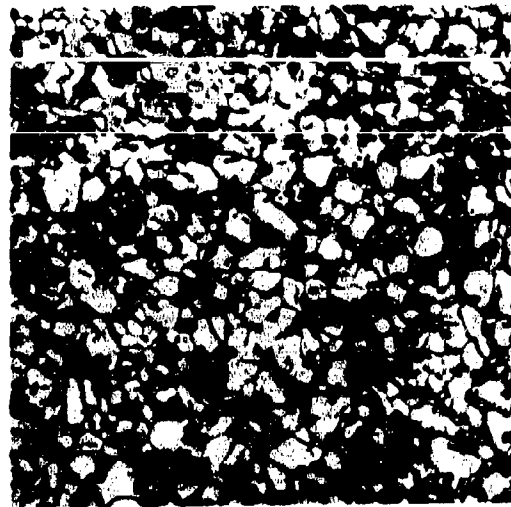
ManLabs Plate No. 5710
Etched   500X
        XIV09F D1033K
          8.56 g/cc
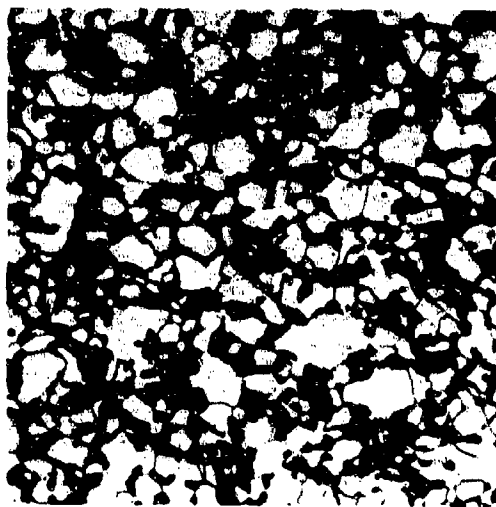
ManLabs Plate No. 2-0036
Etched   500X
        XIV09F D1037K
          8.55 g/cc

Figure 35.   Phase Two Structures of Fully Dense Material
              XIV(18, 10).

81
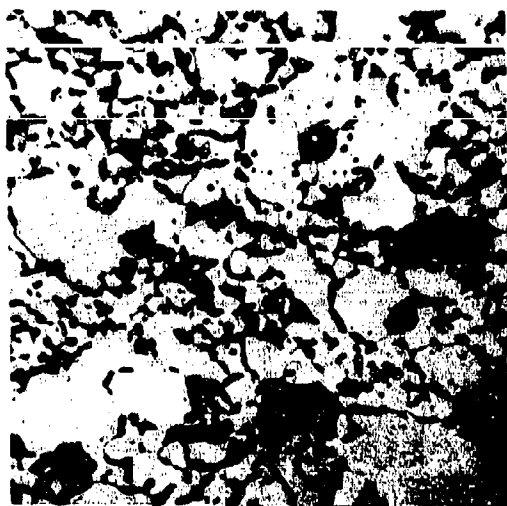
Avco Plate No. 4965
Etched   500X
     XV(20)10 D1031K
      8.95 g/cc

ManLabs Plate No. 5708
Etched   500X
     XV(20)10 D1027K
      8.84 g/cc
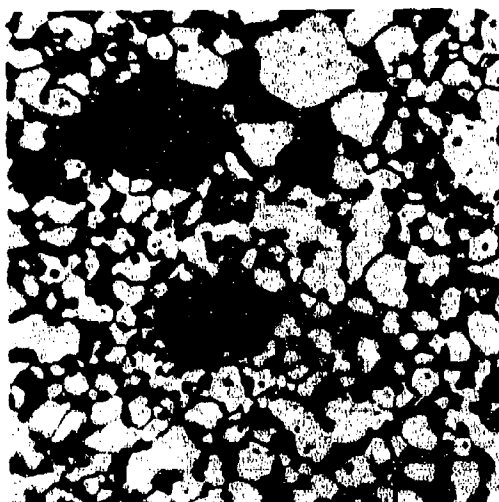
ManLabs Plate No. 5582
Etched   500X
     XV(20)10 D1054K
      8.72 g/cc

Figure 36.   Phase Two Structures of Fully Dense Material XV(20).

82
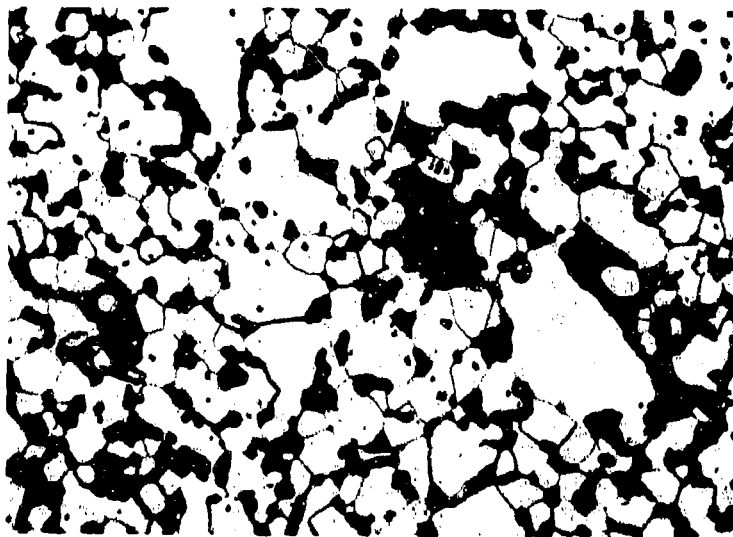
ManLabs Plate No. 5714
Etched   500X
      XV(20)10 R62L,   8.93 g/cc

Figure 37.   Phase Three Structure of Fully Dense Material
            XV(20).

Position Across Billet
Material VD2A DO614
89% Dense Structure
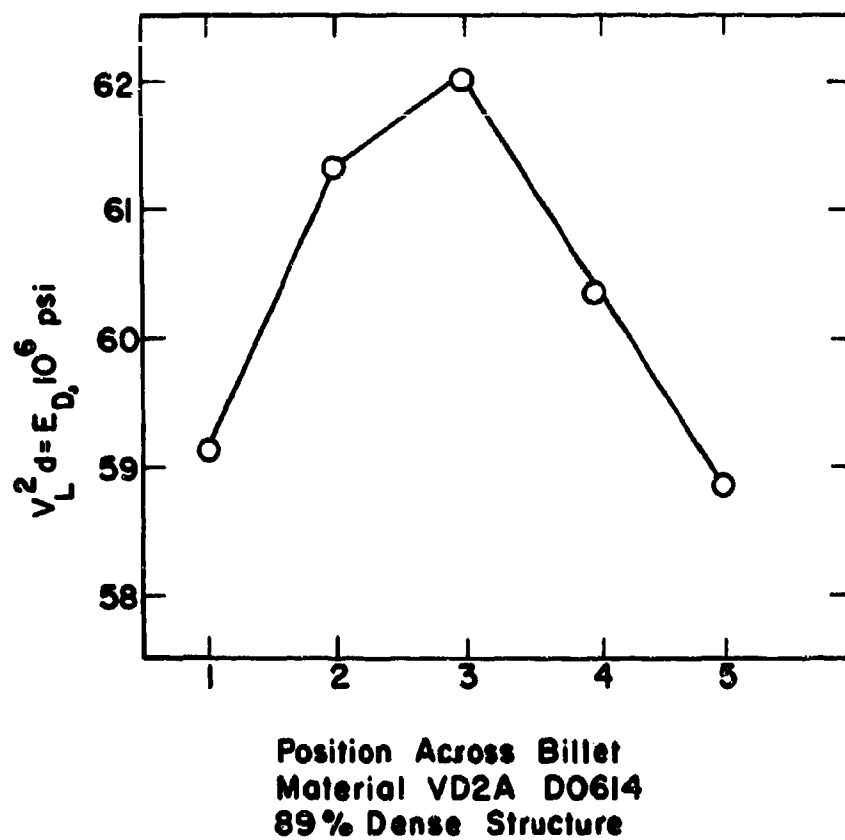
Figure 38. Modulus Variation in Material V Structure
Obtained Nondestructively by Ultrasonic
Velocity Measurements.

84
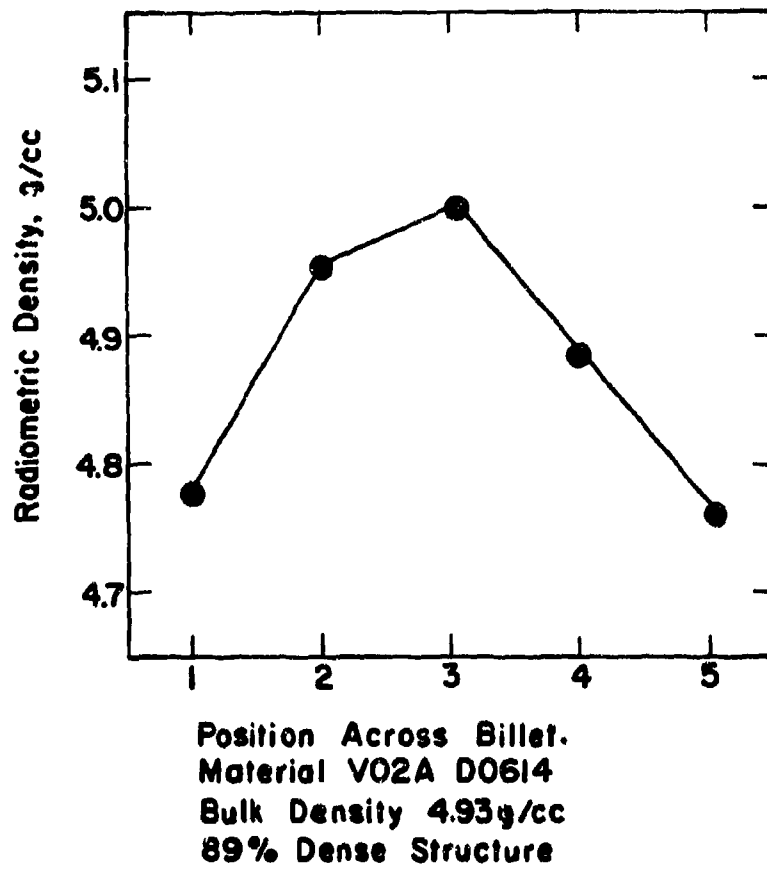
Figure 39. Density Variation in Material V Structure Obtained Nondestructively by Gamma Radiometry.
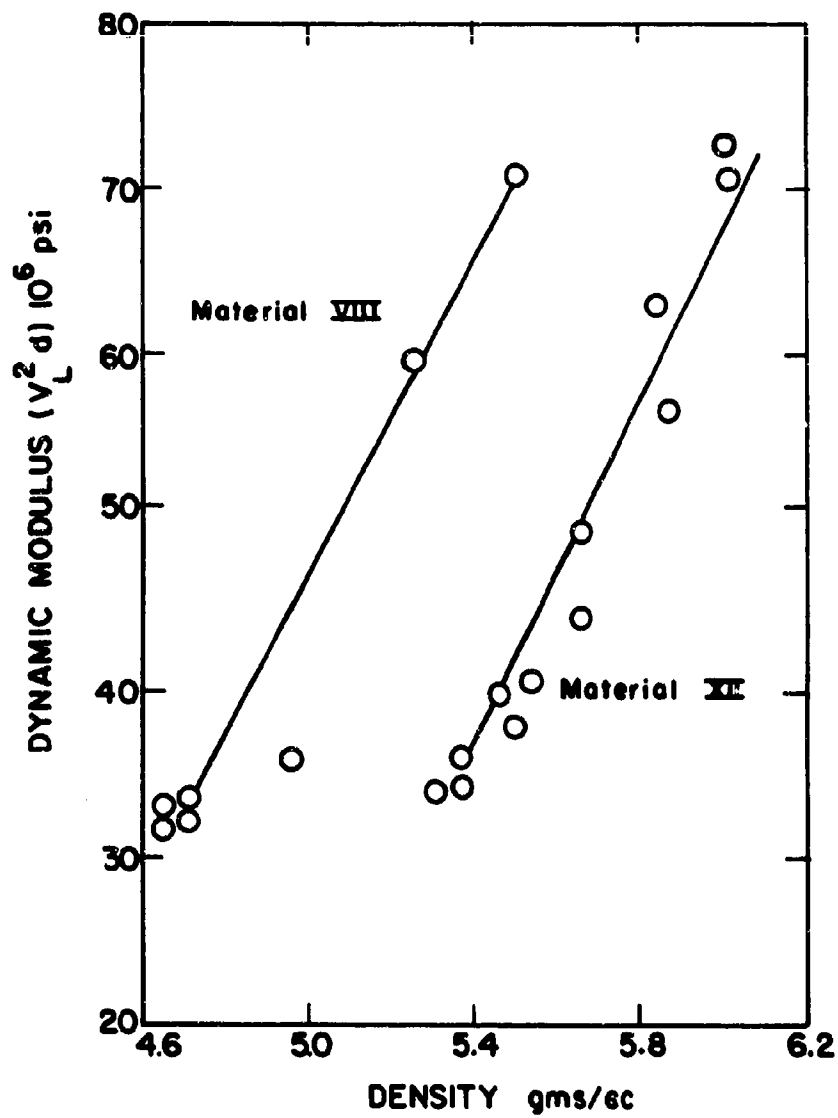
Figure 40. Variation of Dynamic Modulus for Compositional
Variations of Material VIII and XII.

0°

TOP VIEW

EDGE VIEW
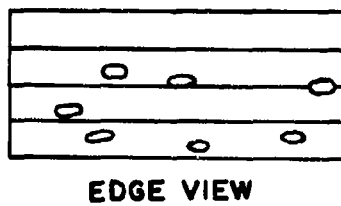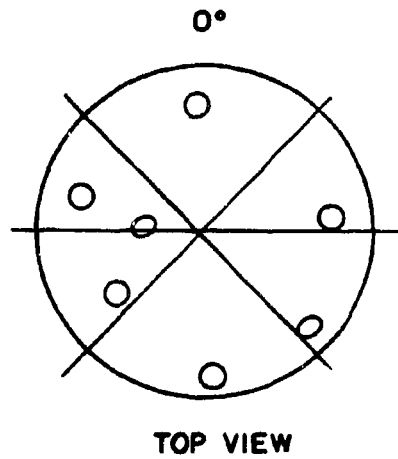
78-3853

Figure 41. Ultrasonic Pulse Echo Indications Noted on Map
of Diboride Billet.
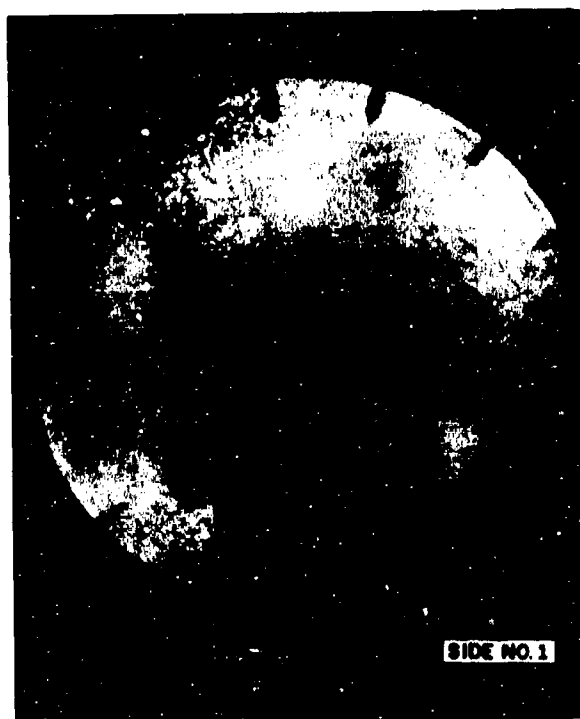
78-3850

Figure 42. Cracks and Porosity Detected By Dye
Penetrant Technique.
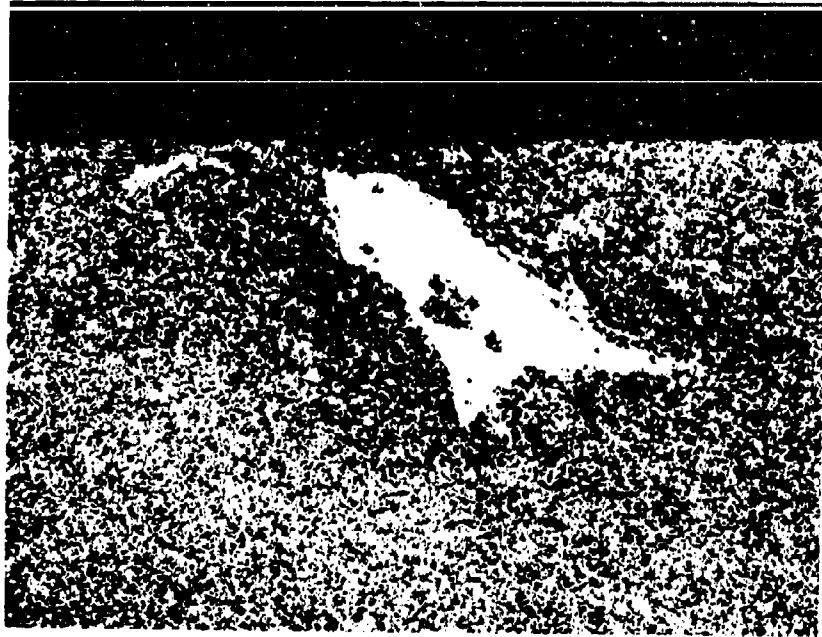
Figure 43. High Density Inclusion in ZrB_2 + SiC Billet Detected By Radiography.
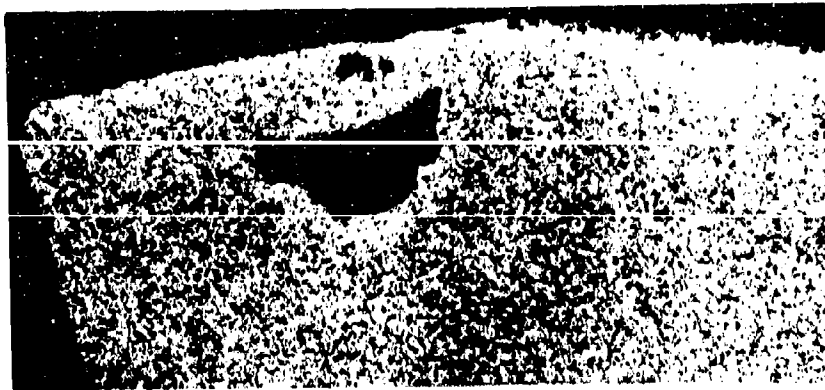
Figure 44. Typical Defect Site Found By Ultrasonic
Pulse Echo Technique.

	2	3	4	5
	R33L	Top		
6	5.425	5.387 — 5.387	5.425	5.462
7	5.362	5.337 — 5.318	5.312	5.400
8	5.287	5.274 — 5.130	5.218	5.356
9	5.362	5.256 — 5.251	5.293	5.349
10	5.349	5.343 — 5.312	5.368	5.331
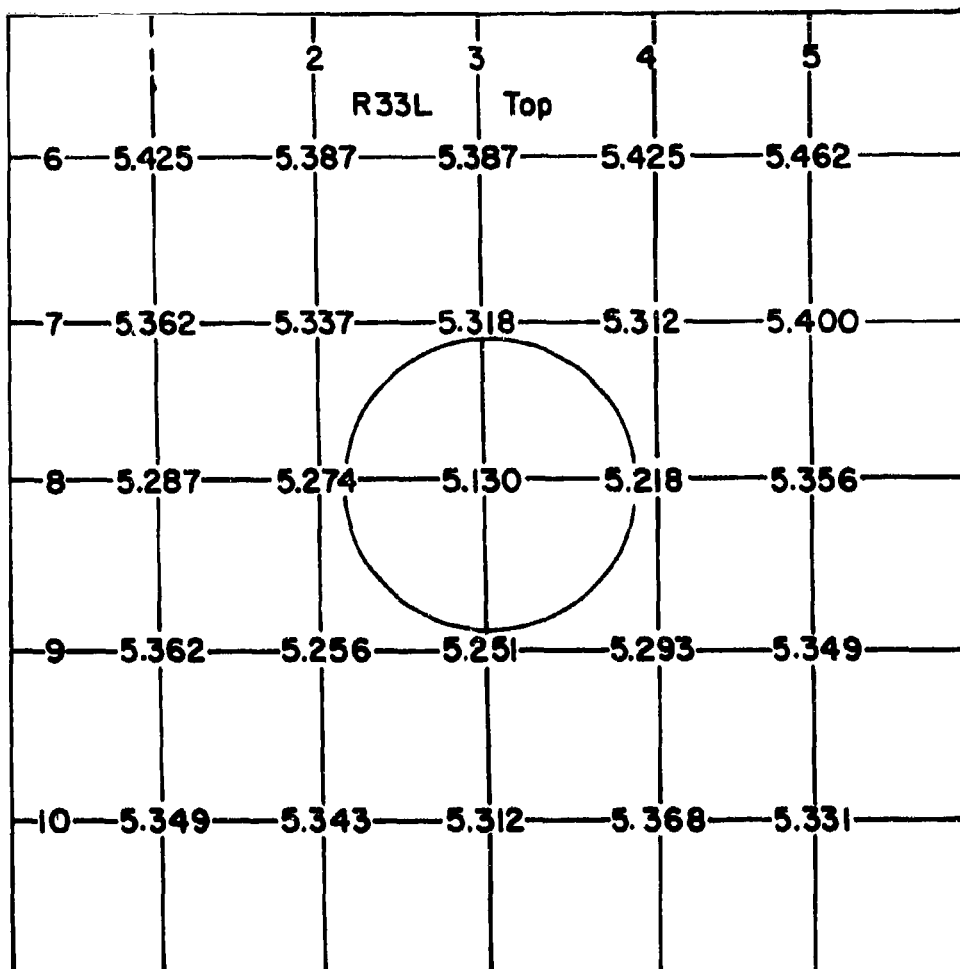
NOTE: Excessive Material Variability

Figure 45. Radiometric Density Profile of Top of VIII(18,10)07F R33L.

91
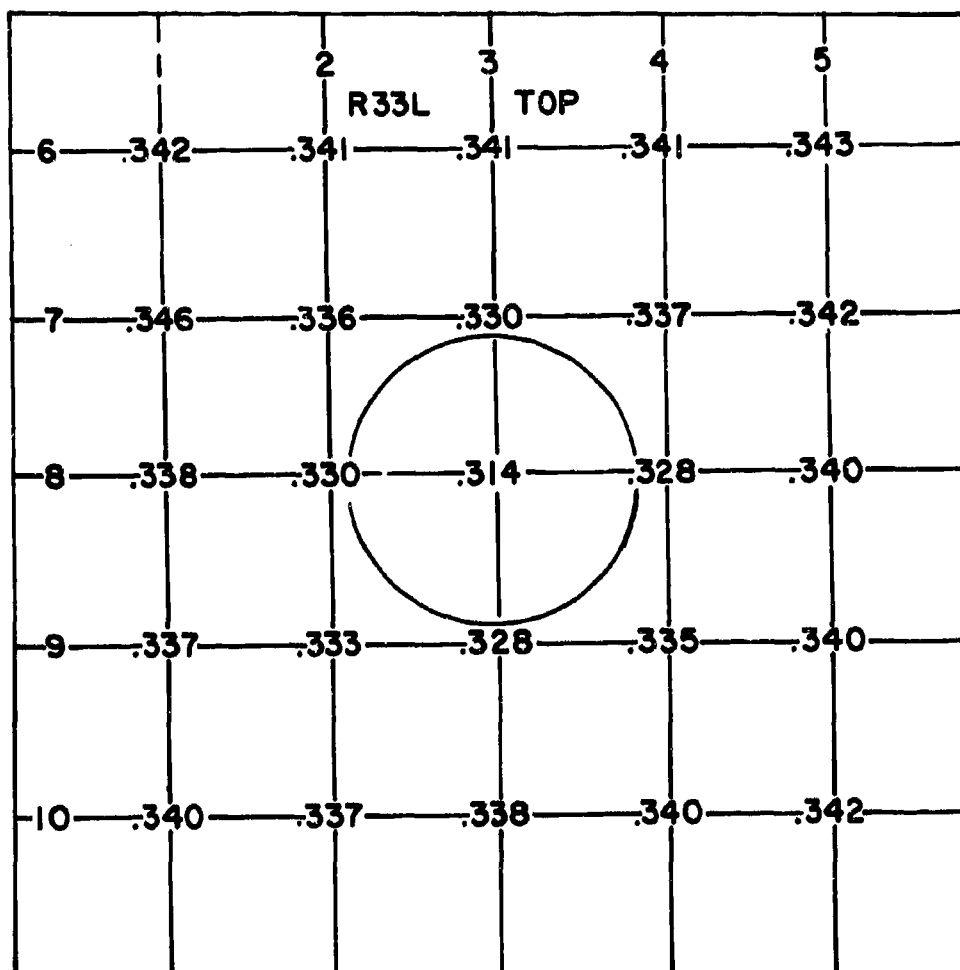
Velocity

NOTE: Excessive Material Variability

Figure 46. Ultrasonic Velocity Profile of Top of VIII(18,10)07F R33L.

92
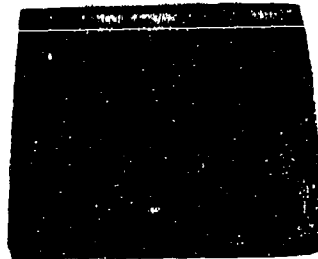
ManLabs Plate No. 5706   Macrograph

Figure 47. Top Surface of Attempted Pyrolytic Deposit of ZrB_2.

As Polished   100X
ManLabs Plate No. 5654

Figure 48. Microstructure of ZrB_2+B Eutectic Obtained in Attempted
            Pyrolytic Deposit of ZrB_2.

93

ManLabs Plate No. 5705   Macrophotograph

Figure 49. Top Surface of Attempted Pyrolytic Deposit of ZrB_2+SiC.
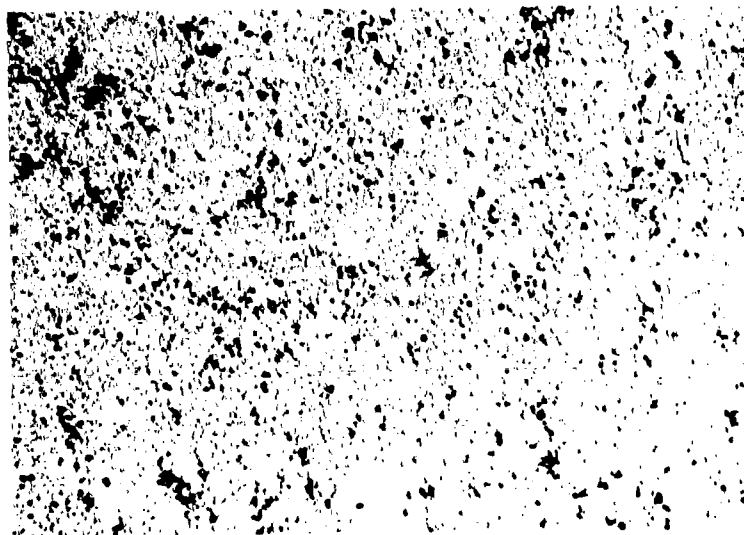
As Polished   100X
ManLabs Plate No. 5653

Figure 50. Light Micrograph of ZrB_2+B_4C Obtained from Attempted
            Pyrolytic Deposit of ZrB_2+SiC.

94

Replicated Surface
ManLabs Plate No. 4056   10,000X
Note: Smooth B_4C Grains in ZrB_2 Matrix

Figure 51. Electron Micrograph of Structure of ZrB_2+B_4C Obtained
from Attempted Pyrolytic Deposition of ZrB_2+SiC.

95

Avco Plate
No. 4782

As Polished   500X

Figure 52. Microstructural Features of Sintered I05A(Zr_1)B20.

96
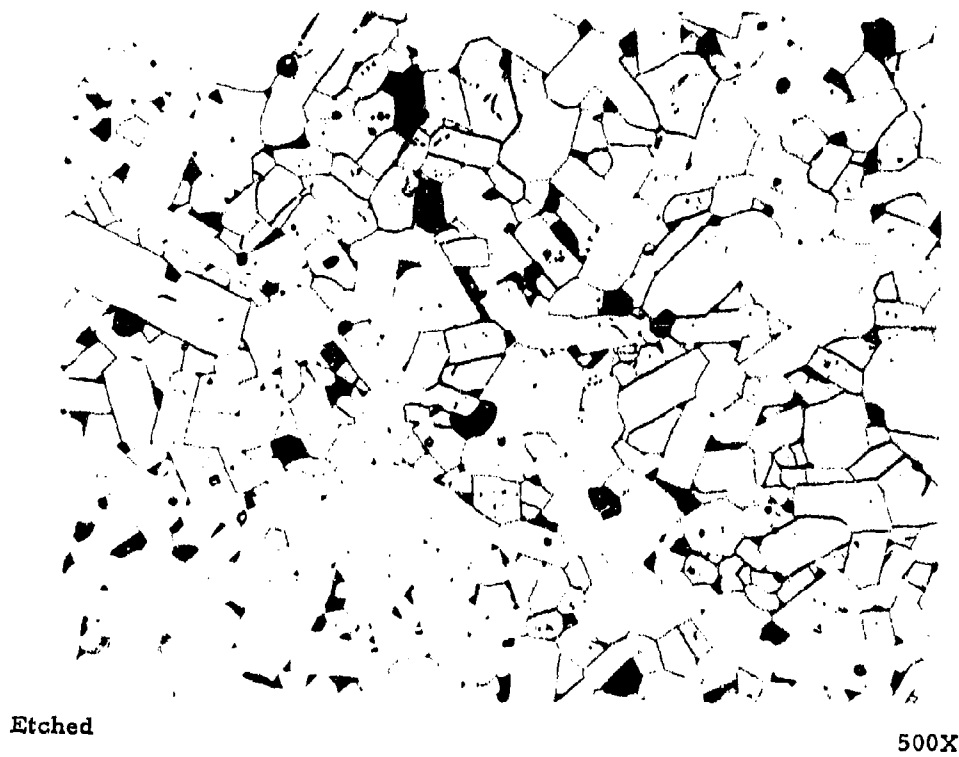
Avco Plate
No. 4812-5

Etched   500X

Figure 53. Microstructural Features of Sintered I05A(Zr₂)B27.

97
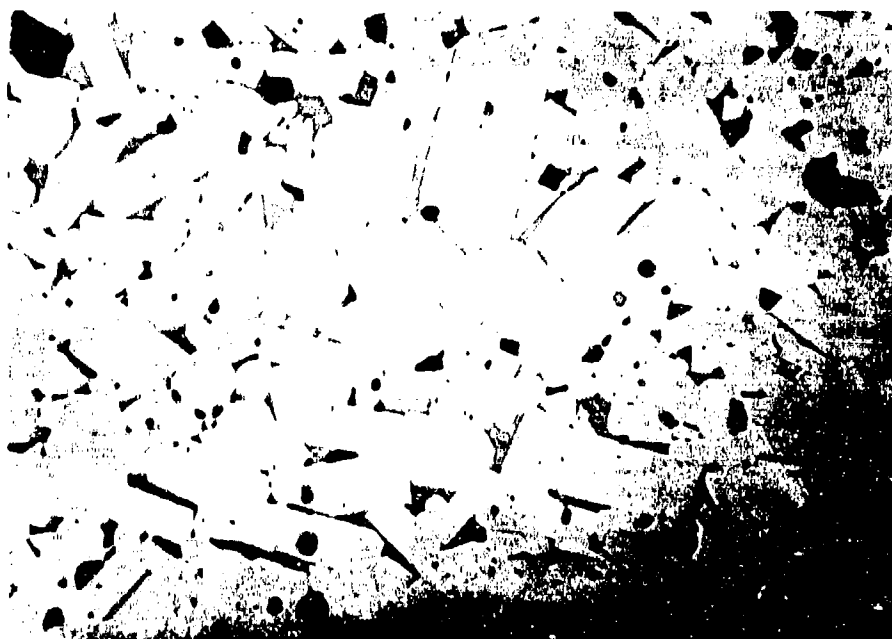
As Polished   500X

Figure 54. Microstructural Features of Sintered I05A(Zr$_3$)B46.
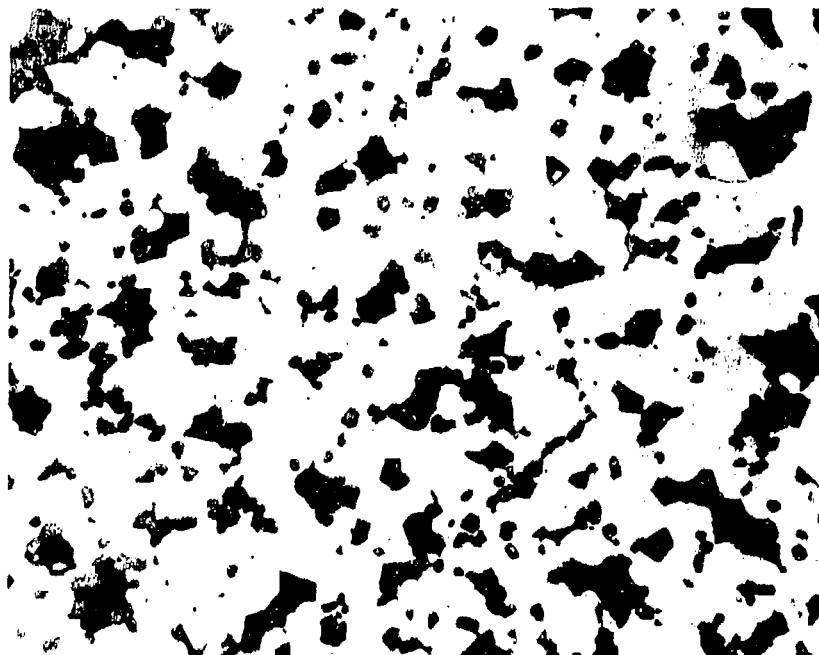
Avco Plate No.
3699

As Polished   500X

Figure 55. Microstructural Features of Sintered V05A(Zr_1)B35.
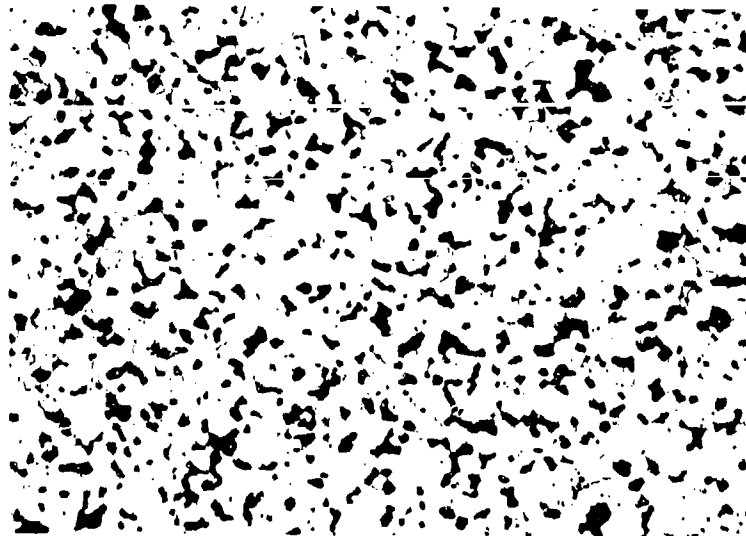
Battelle
Plate No.
OD 907

As Polished   500X
Fabrication Conditions: 1650°C, 36,000 psi, 2 hours
Density: 5.3 g/cc

Figure 56. Microstructural Features of Isostatically Hot Pressed
            I03A.
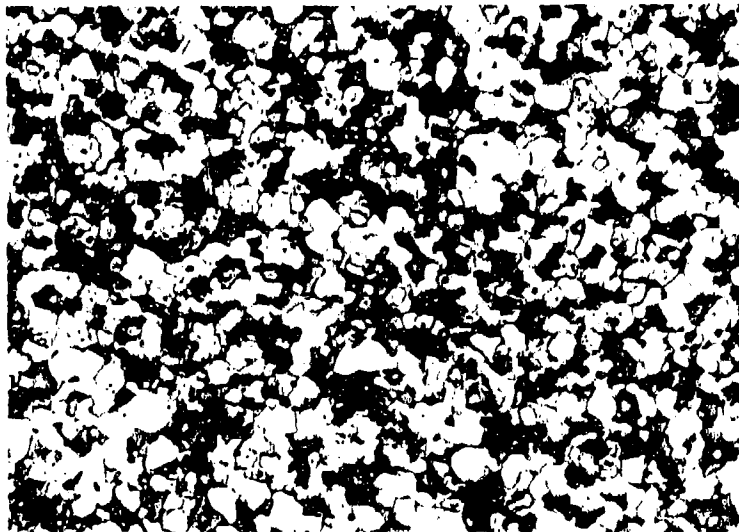
ManLabs
Plate No.
5337

Etched   500X
Fabrication Conditions: 1650°C, 36,000 psi, 2 hours
Mixing Procedure: Liquid Slurry
Density: 5.5 g/cc

Figure 57. Microstructural Features of Isostatically Hot Pressed
            V03A Composition Prepared with Liquid Slurry Mixing
            Procedure.

100
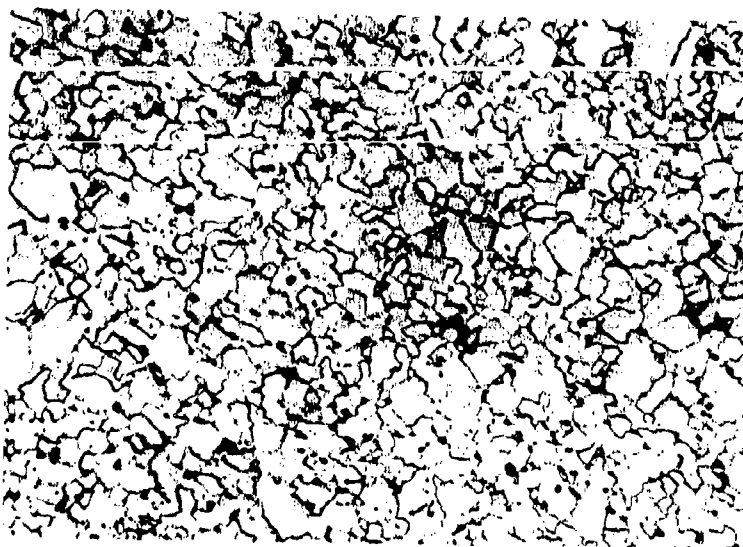
Etched   500X
ManLabs Plate No. 5623
Billet Density 10.48 g/cc; Powder Density 10.39 g/cc

Figure 58.   Microstructural Features of Isostatically Hot
Pressed Material II09F.
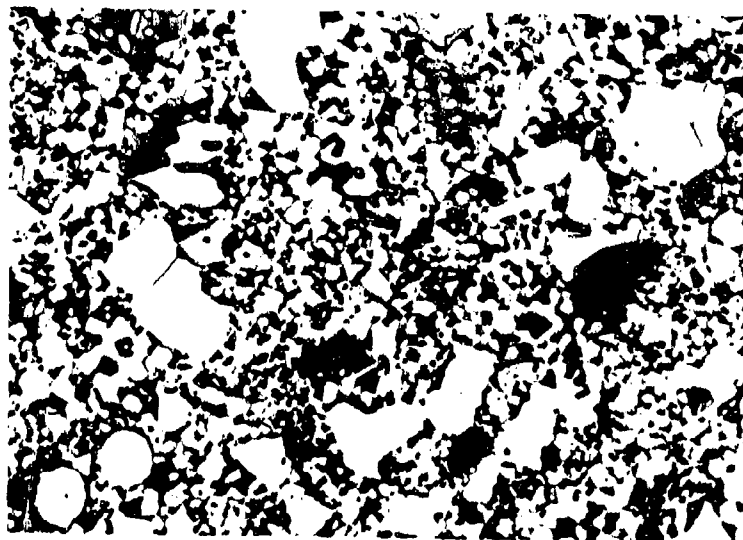
Etched   500X
ManLabs Plate No. 5627
Billet Density 9.12 g/cc; Powder Density 10.32 g/cc

Figure 59.   Microstructural Features of Isostatically Hot
Pressed Material II10.

101
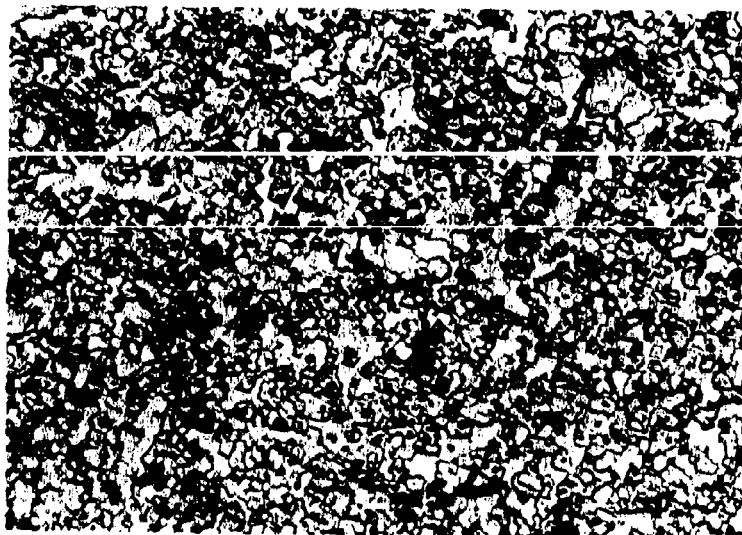
Etched   500X
ManLabs Plate No. 5619
Billet Density 10.92 g/cc; Powder Density 10.79 g/cc

Figure 60. Microstructural Features of Isostatically Hot
Pressed Material II06B.
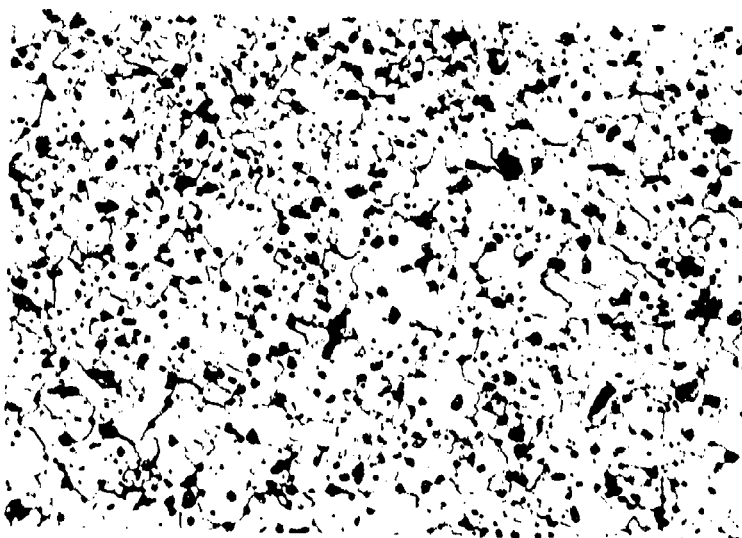
Etched   500X
ManLabs Plate No. 5617
Billet Density 5.95 g/cc; Powder Sensity 5.96 g/cc

Figure 61. Microstructural Features of Isostatically Hot
Pressed Material I07F.

102
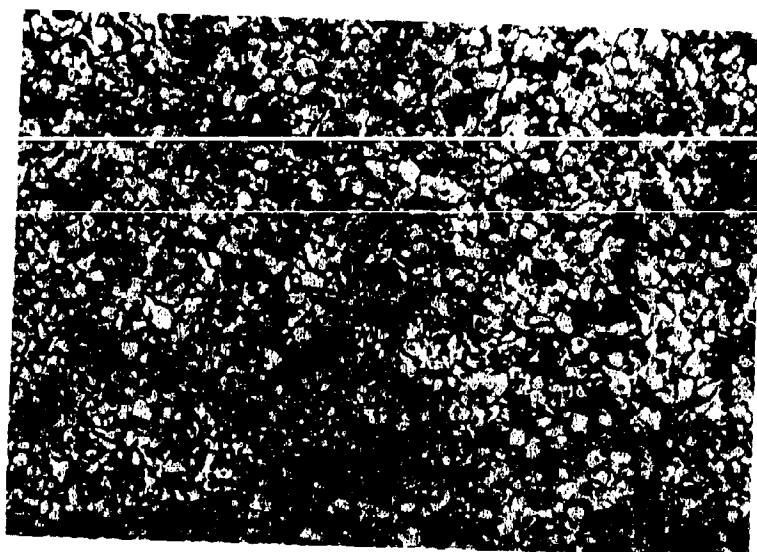
Etched   500X
ManLabs Plate No. 5628
Billet Density 5.62 g/cc; Powder Mixture Density 5.82 g/cc

Figure 62. Microstructural Features of Isostatically Hot
          Pressed Material V(5)07F.
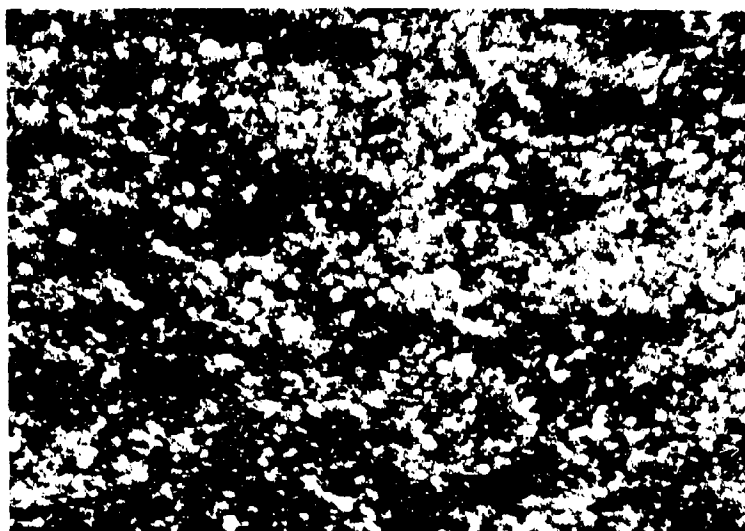
As Polished   500X
ManLabs Plate No. 5636
Billet Density 3.84 g/cc; Powder Mixture Density 4.45 g/cc

Figure 63. Microstructural Features of Isostatically Hot
          Pressed Material VIII(14,30)02A.

103
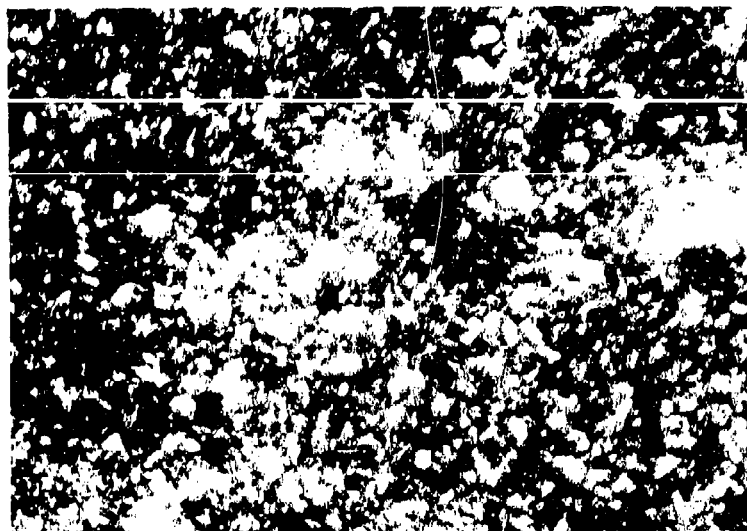
As Polished   500X
ManLabs Plate No. 5638
Billet Density 4.91 g/cc; Powder Mixture Density 5.21 g/cc

Figure 64.   Microstructural Features of Isostatically Hot
             Pressed Material XII(20)02A.
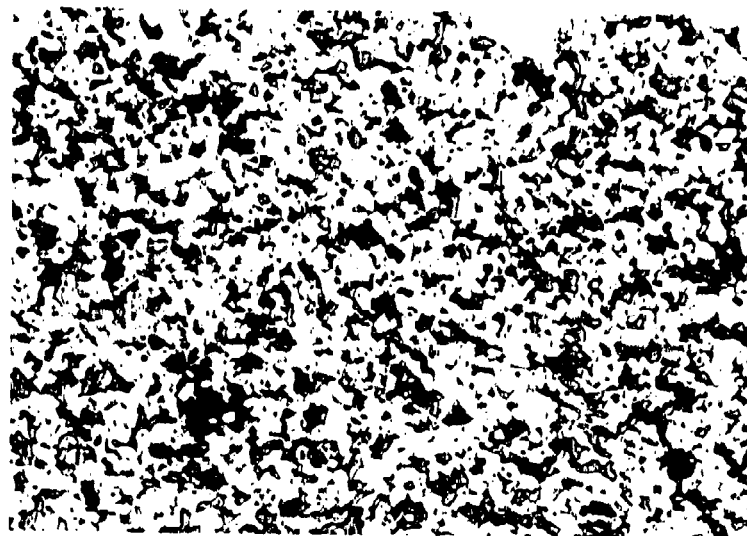
As Polished   500X
ManLabs Plate No. 5632
Billet Density 5.02 g/cc; Powder Mixture Density 5.10 g/cc

Figure 65.   Microstructural Features of Isostatically Hot
             Pressed Material VIII(18,10)02A.

104
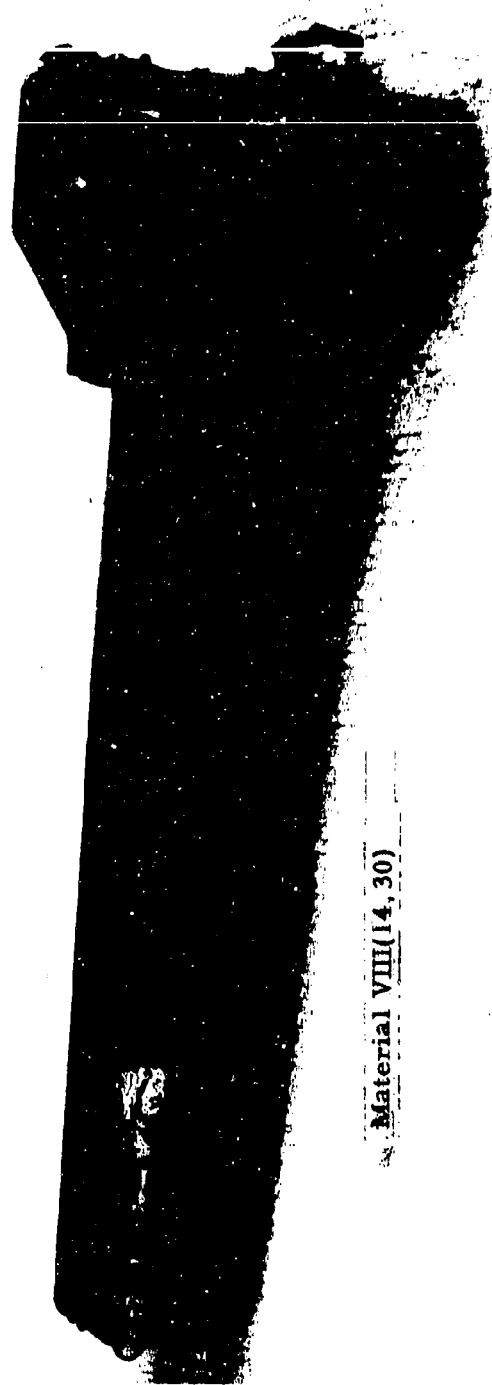
Material VIII(14, 30)

Figure 66. Arc Cast ZrB_2+SiC+C Composite Prepared at Battelle Memorial Institute.

105
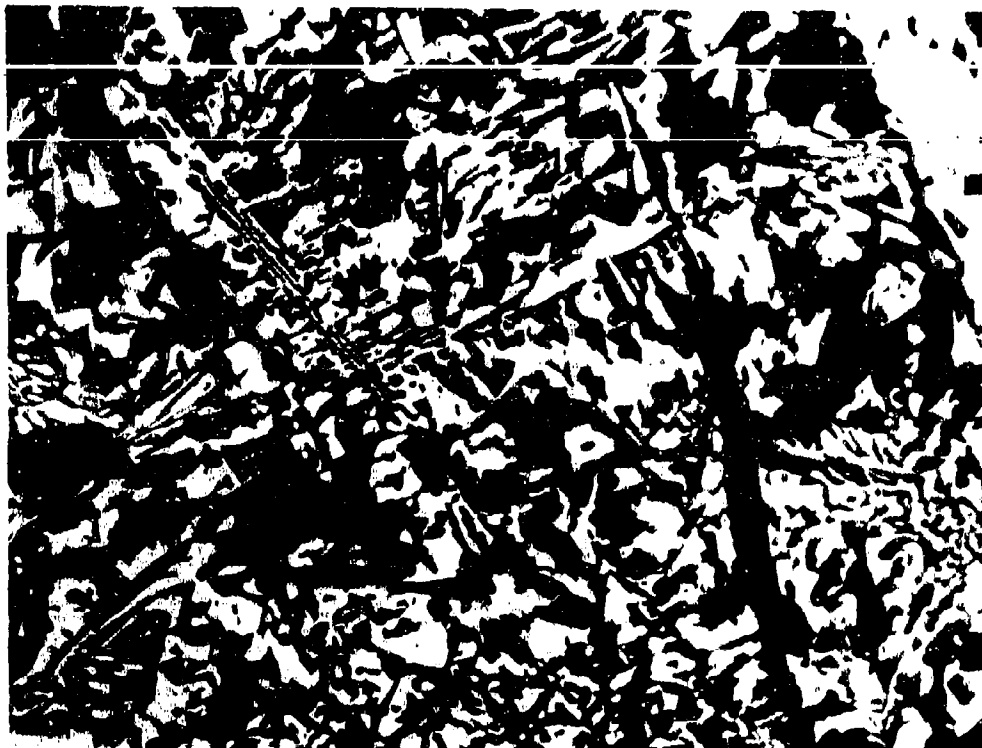
As Polished   500X

Figure 67. Microstructural Features of Arc Cast Zr$_2$+SiC+C Fabricated
            at Battelle.

106
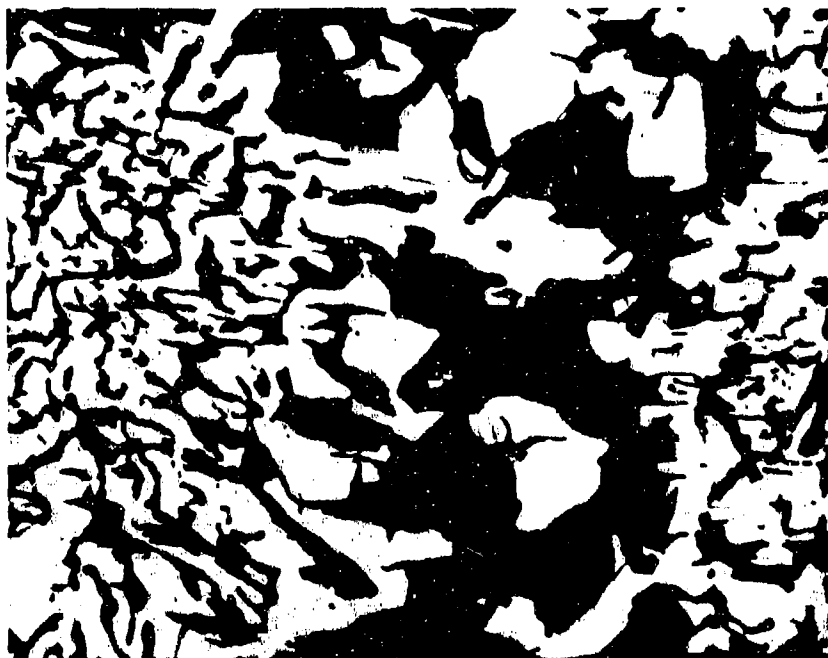
As Polished   500X

Figure 68. Microstructure of Molten Material Extruded from Hot Forging of
Billet I05A D0650K.

107

Figure 69. Deformation Vs. Time for the Hot Forging of Material V07 D0716K.

The figure shows a graph with axes "Piston Movement, Inches" and "Time, Minutes", with legend entries.

△ Specimen No. I Failed
O Specimen No.2 Successfully Forged

Y-axis: Piston Movement, Inches (0.2, 0.4, 0.6)
X-axis: Time, Minutes (0, 20, 40, 60, 80)

Caption: Figure 69. Deformation Vs. Time for the Hot Forging of Material V07 D0716K.

Figure 69.   Deformation Vs. Time for the Hot Forging of Material V07 D0716K.

108
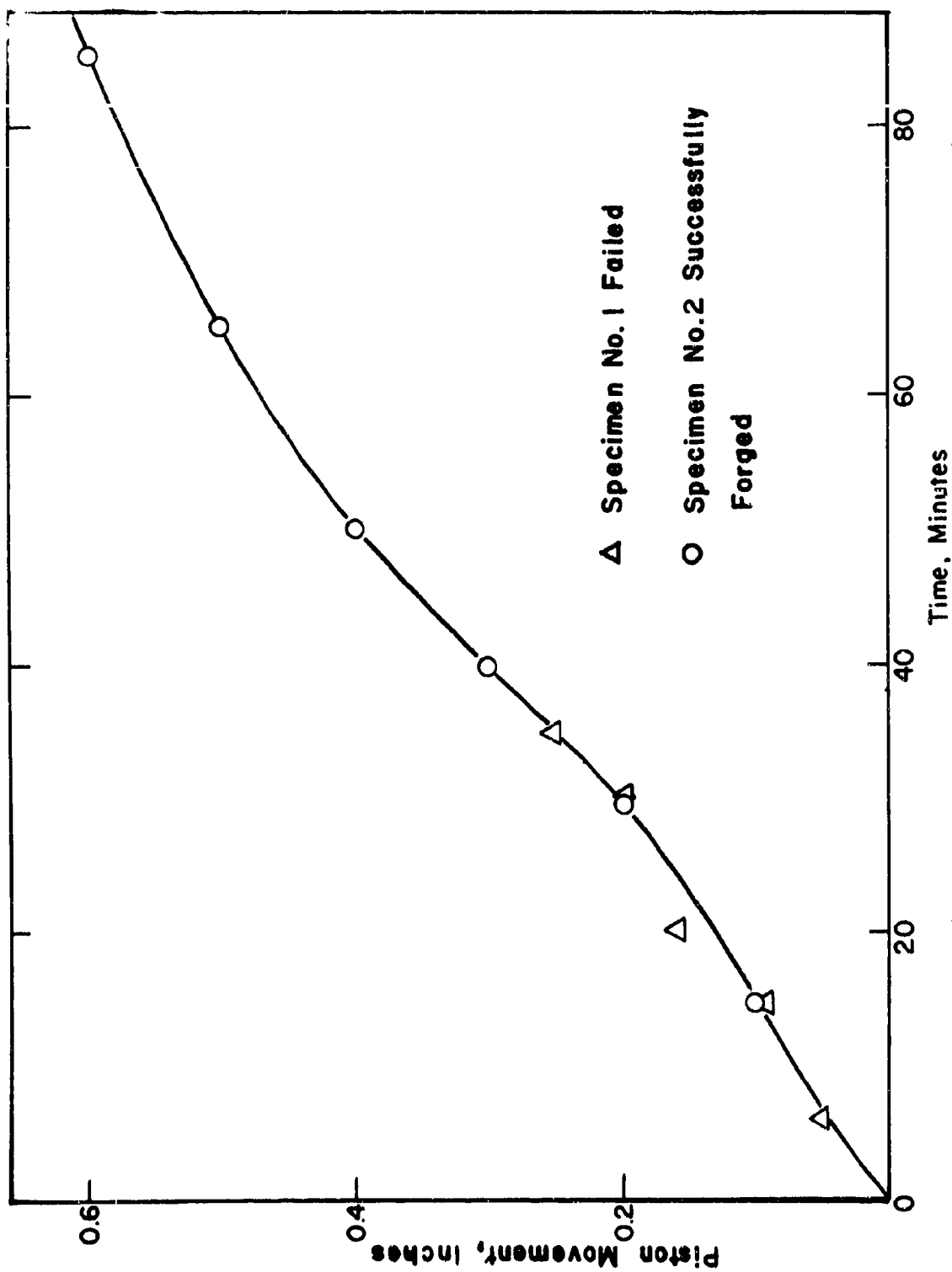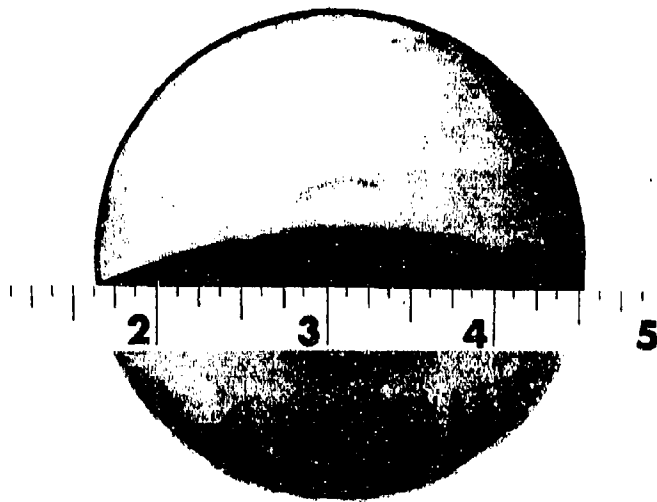
Figure 70. Photograph of Forged Disc of Billet V07 D0761K.
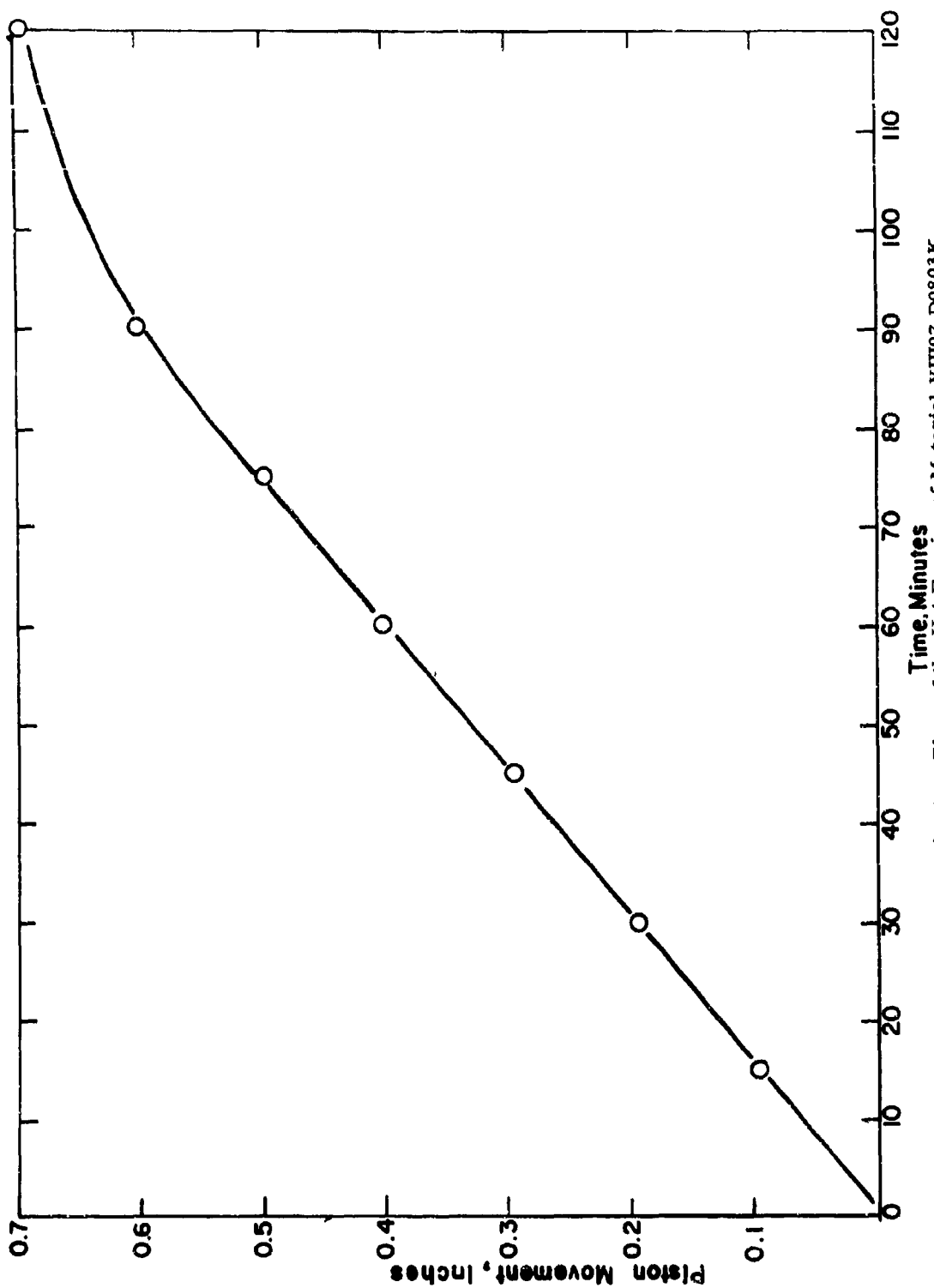
Figure 71. Deformation Vs. Time of the Hot Forging of Material VIII07 D0803K.
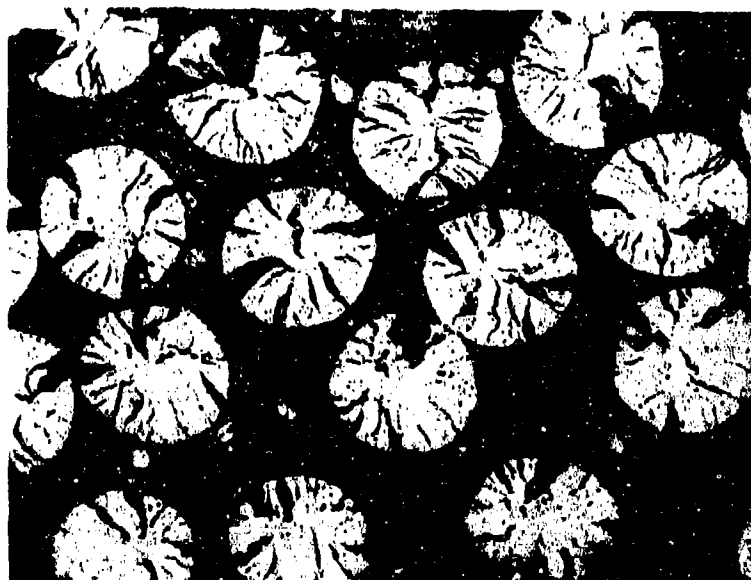
Avco Plate
No. 4492

As Polished   500X

Figure 72. Cross Section of Tungsten Filament
            Material II Composite.
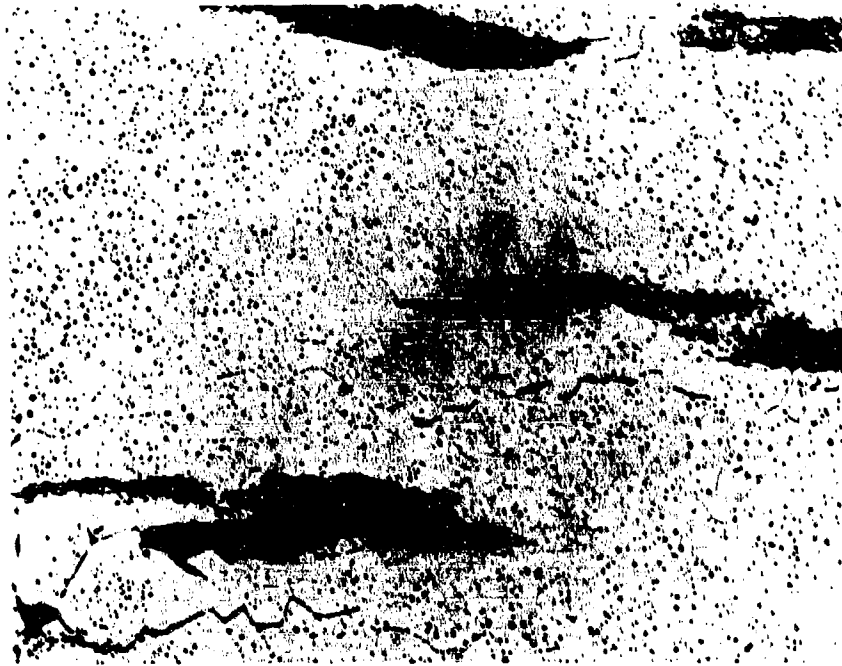
Avco Plate No.
4678-A

As Polished   100X

Figure 73.   Representative Microstructure of ZrB_2 Reinforced
             with Thornel 25 Carbon Fiber, Billet XIIf(5) D0644.

Ta

Mo

Nb

Ta

Mo

Ta

Mo

ZrB_2

ZrB_2

ZrB_2

$ZrB_2 + SiC$

$ZrB_2 + SiC$

$ZrB_2 + SiC + C$

$ZrB_2 + SiC + C$

Figure 74. Welds Between ZrB_2 Compositions and
Various Materials.

113

TABLE 1

DIBORIDE MATERIAL IDENTIFICATION: PHASE CONSTITUTION
AND BASE COMPOSITION

Diboride Material	Designation	Remarks and Rationale for Specific Additives
I	ZrB_2	Zirconium diboride, no additive
II	HfB_2	Hafnium diboride, no additive
III	HfB_2+SiC	Hafnium diboride with twenty volume percent silicon carbide to enhance oxidation resistance
IV	HfB_2+SiC	Hafnium diboride with thirty volume percent silicon carbide to enhance oxidation resistance
V	ZrB_2+SiC	Zirconium diboride with twenty volume percent silicon carbide to enhance oxidation resistance
VI	$HfB_2+Hf-Ta$	Hafnium diboride with four volume percent hafnium tantalum alloy to provide an oxidation resistant metallic binder phase and enhance strength properties
VII	HfB_2+SiC	Boron rich hafnium diboride with silicon carbide additive to enhance oxidation resistance
VIII	$ZrB_2+SiC+C$	Zirconium diboride with fourteen volume percent silicon carbide, thirty volume percent carbon to enhance thermal stress resistance and maintain improved oxidation resistance relative to ZrB_2
IX	HfB_2+HfSi	Hafnium diboride with twenty volume percent hafnium silicide to enhance oxidation resistance
X	ZrB_2+SiB_6	Zirconium diboride with twenty volume percent silicon hexaboride to enhance oxidation resistance
XI	ZrB_2+Cr	Zirconium diboride with eight volume percent chromium to enhance mechanical strength properties
XII	ZrB_2+C	Zirconium diboride with fifty volume percent carbon to enhance thermal stress resistance
XIII	ZrB_2+W	Zirconium diboride with tungsten to enhance mechanical properties
XIV	$HfB_2+SiC+C$	Hafnium analogue of VIII
XV	HfB_2+C	Hafnium analogue of XII

TABLE 2

IDENTIFICATION OF COMPOSITIONAL VARIATIONS
IN DIBORIDE MATERIALS

Diboride Material	Base Composition volume percent
III	80 HfB_2 20 SiC
III(5)	95 HfB_2 5 SiC
XV	50 HfB_2 50 C
XV(20)	80 HfB_2 20 C
V	80 ZrB_2 20 SiC
V(10)	90 ZrB_2 10 SiC
VIII	56 ZrB_2 14 SiC 30 C
VIII(18, 10)	72 ZrB_2 18 SiC 10 C
X	80 ZrB_2 20 SiB_6
X(10)	90 ZrB_2 10 SiB_6
XII	50 ZrB_2 50 C
XII(20)	80 ZrB_2 20 C
XIIf(5)	95 ZrB_2 5 C filament

TABLE 3

CHARACTERIZATION OF ZIRCONIUM DIBORIDE POWDER, I02

Supplier: U. S. Borax Research Corporation

Quantity: I02 (1 pound sample) - I02A (94 pound lot)

1. **Qualitative Analysis**
   (weight per cent, w/o)

Ti, Cr, Fe	0.1 - 1.0
V	0.01 - 0.1

2. **Quantitative Analysis (w/o)**

Zr	79.6
Ti	0.02
Cr	0.10
Fe	0.08
B	18.3
C	0.38
O (AA)	0.70
Total	99.18

3. **Atomic Ratio**

   Over-all $_{**}$B/Zr$_*$ = 1.93
   Corrected** B/Zr* = 2.06

4. **X-ray Phase Identification**

   ZrB_2
   ZrO_2 (impurity)
   ZrC (impurity)

5. a) Powder Density(Measured)

   6.03 g/cc

   b) Powder Density(Calculated)

   6.06 g/cc

6. **Particle Size Distribution**

Range (μ)	w/o
0-5	4.0
5-10	23.4
10-20	64.5
20-40	7.6
>40	0.5

7. **Phase Assay (volume per cent)**

	ZrB_x	ZrO_2	ZrC
Calculated from Composition	94.0	3.0	3.0

**Atomic ratio corrected for metal assumed to be present as metal dioxide and metal monocrabide and diboride as ZrB_x where x = B/Zr*

116

TABLE 4

CHARACTERIZATION OF ZIRCONIUM DIBORIDE POWDER. 103

Supplier: U. S. Borax Research Corporation

Quantity: I03 (1 pound sample) - I03A (100 pound lot)

1. Qualitative Analysis
    (weight per cent, w/o)

    Ca, Fe   0.01 - 0.1

2. Quantitative Analysis (w/o)

    Zr   79.8
    B   17.7
    C   0.03
    O (AA)   1.15

    Total   98.68

3. Atomic Ratio

    Over-all B/Zr = 1.87
    Corrected ** B/Zr^* = 1.96

4. X-ray Phase Identification

    ZrB_2

    ZrO_2 (impurity)

5.a) Powder Density(Measured)

      6.04 g/cc

  b) Powder Density(Calculated)

      6.10 g/cc

6. Particle Size Distribution

Range (μ)	w/o
0-5	7.5
5-10	37.9
10-20	48.9
20-40	5.5
>40	0.2

7. Phase Assay (volume per cent)

	ZrB_x	ZrO_2	ZrC
Calculated from Composition	94.9	4.9	0.2

**Atomic ratio corrected for metal assumed to be present as metal dioxide
  and metal monocarbide and diboride as ZrB_x where x = B/Zr^*.

117

TABLE 5

CHARACTERIZATION OF ZIRCONIUM DIBORIDE POWDER, I05A

Supplier: Shieldalloy Corporation (H. C. Starck Berlin)

Quantity: 100 pounds[1]

1. Qualitative Analysis (weight per cent, w/o)

Ti, Fe, Co   0.01-0.1

2. Quantitative Analysis (w/o)

Zr	79.3
B	18.65
C	0.02
O (AA)	0.15
Total	98.12

3. Atomic Ratio

Over-all $B/Zr_x = 1.98$
Corrected[**] $B/Zr^* = 2.00$

4. X-ray Phase Identification

ZrB_2

5.a) Powder Density(Measured)

5.97 g/cc

b) Powder Density(Calculated)

6.10 g/cc

6. Particle Size Distribution

Range (μ)	w/o
0-5	7.7
5-10	26.6
10-20	44.7
20-40	17.8
>40	1.1

7. Phase Assay (volume per cent)

	ZrB_x	ZrO_2	ZrC
Calculated from Composition	99.2	0.65	0.15

[1] The original five pound sample designated I05 was found unsatisfactory for this program as it contained significant amounts of ZrO_2 and ZrC. The I05A was obtained by reprocessing the I05.

[**] Atomic ratio corrected for metal assumed to be present as metal dioxide and metal monocarbide and diboride as ZrB_x where x = B/Zr^*.

TABLE 6

CHARACTERIZATION OF ZIRCONIUM DIBORIDE POWDER, 107

Supplier: U. S. Borax Research Corporation

Quantity: 400 pounds[1]

1. Qualitative Analysis
    (weight per cent, w/o)

    Fe, Ca, Ti   0.01 - 0.1

2. Quantitative Analysis (w/o)

	A	B	C	Ave.
Zr	78.5	78.6	78.4	78.5
Ti	-	-	1.30	1.30
B	19.1	18.4	18.2	18.6
C	0.22	0.31	0.25	0.26
O (AA)	1.11	1.12	1.12	1.12
O (VF)	-	(1.15)	-	-
Total	98.93[+]	98.43[+]	99.27	99.78

3. Atomic Ratio

    Over-all[**] $B/Zr_* = 1.94$
    Corrected[**] $B/Zr^* = 2.07$

4. X-ray Phase Identification

    ZrB_2

    ZrO_2 (impurity)

5.a) Powder Density (Measured)

    5.96 g/cc

b) Powder Density (Calculated)

    6.00 g/cc

6. Particle Size Distribution

Range (μ)	w/o
0-5	7.9
5-10	33.8
10-20	52.1
20-40	5.0
>40	1.2

7. Phase Assay (volume per cent)

    Calculated from Composition

ZrB_x	ZrO_2	ZrC
93.3	4.7	2.0

[1] The four hundred pound lot was blended then shipped in three separated
containers designated A, B and C.

[**] Atomic ratio corrected for metal assumed to be present as metal dioxide
and metal monocarbide and diboride as ZrB_x where $x = B/Zr^*$.

[+] Titanium not analysed.

119

TABLE 7

CHARACTERIZATION OF ZIRCONIUM DIBORIDE POWDER, 108^{**}

Supplier: U. S. Borax Research Corporation

Quantity: 100 pound lot

1. Qualitative Analysis
   (weight percent, w/o)
   Ti 0.3-3.0
   Fe 0.03-0.30
   Si 0.01-0.10

2. Quantitative Analysis (w/o)
   Zr   74.62
   B   18.66
   Ti   0.55
   Si   0.27
   Fe   0.15
   C   1.12
   O   1.87
   B_2O_3 0.71, 0.55
   Residue* 2.72
   _____
   Total   99.96
   (-B_2O_3)

3. Atomic Ratio
   Overall B/Zr = 1.93
   Corrected*   = 2.03

4. X-ray Phase Identification
   ZrB_2
   ZrO_2

5. Powder Density
   - Not Measured

6. Particle Size Distribution
   - Not Determined

7. Phase Assay
   - Not Determined

*Corrected for boron in B_2O_3 and zirconium in redue.
**This powder lot was not employed for hot pressing nor for other fabrication techniques.

120

TABLE 8

CHARACTERIZATION OF HAFNIUM DIBORIDE POWDER, II05 AND II05A

Supplier: Wah Chang Corporation

Quantity: II05 (20 pound sample) - II05A (80 pound lot)

1. Qualitative Analysis
    (weight per cent, w/o)

    | Zr | 1 - 10 |
    | Si | 0.1 - 1.0 |
    | Al | 0.01- 0.1 |

4. X-ray Phase Identification

    HfB_2

    HfC (impurity)

2. Quantitative Analysis (w/o)

	II05	II05A	Ave.
Hf+Zr	89.7	89.4	89.55
Zr	(1.15)	-	(1.15)
B	10.4	10.5	10.45
C	0.21	0.12	0.16
O (IGF)	0.07	0.11	0.09
Total	100.38	100.13	100.25

5,a) Powder Density(Measured)

      10.69 g/cc

   b) Powder Density(Calculated)

      11.11 g/cc

3. Atomic Ratio

    Over-all** B/Hf = 1.902
    Corrected** B/Hf* = 2.03

6. Particle Size Distribution

Range (μ)	w/o
0-5	7.7
5-10	29.7
10-20	32.2
20-40	30.1
>40	0.3

7. Phase Assay (volume per cent)

	Hf(Zr)B$_x$	HfO$_2$	HfC
Calculated from Composition	97.1	0.7	2.2

**Atomic ratio corrected for metal assumed to be present as metal dioxide
and metal monocrabide and diboride as Hf(Zr)B$_x$ where x = B/Hf*.

121

TABLE 9

CHARACTERIZATION OF HAFNIUM DIBORIDE POWDER 1106

Supplier: Shieldalloy Corporation (H. C. Starck, Berlin)

Quantity: 1106A - 2 Pounds, 1106B - 43 Pounds

1. Qualitative Analysis
    (weight per cent, w/o)

    Ti   0.1 - 1.0
    Zr   0.01 - 0.1

2. Quantitative Analysis (w/o)

    Hf+Zr   89.03
    Zr   (0.89)[+]
    Ti   0.31
    B   10.49
    C   0.04
    O (AA)   ^.55
                ─────
    Total   100.42

3. Atomic Ratio B/Me[*]

    Over-all [**]1.90
    Corrected 2.0

4. X-ray Phase Identification

    HfB_2
    HfO_2 impurity
    HfC   trace impurity

5.a) Powder Density(Measured)

      11.15 g/cc

  b) Powder Density(Calculated)

      10.98

6. Particle Size Distribution

Range (μ)	w/o
0-5	22.2
5-10	54.0
10-20	20.6
20-40	2.5
>40	0.8

7. Phase Assay (volume per cent)
    - Calculated from Composition

MeB_2	HfO_2	HfC
95.35	4.1	0.55

    MeB_2 = 1.2 TiB_2 and 98.8 $Hf(Zr)B_x$

8. Impurity Assay (volume per cent)
    - Metallographic Analysis of High
    Pressure Hot Pressed Sample

    8.3%

[**]Over-all atomic ratio corrected for hafnium assumed to be present as metal
dioxide and metal monocarbide and diboride as $Hf(Zr)B_x$ where x = B/Me[*].

[+] Based on 1% Zr in Hf.

122

TABLE 10

CHARACTERIZATION OF HAFNIUM DIBORIDE POWDER 1109

Supplier: The Carborundum Corporation

Quantity: 100 Pounds

1. Qualitative Analysis
    (weight per cent, w/o)

Ti,Zr	1.0 - 10
Fe	0.1 - 1.0
S	0.01 - 0.

2. Quantitative Analysis (w/o)

Hf+Zr	87.05
Ti	1.10
Zr	(0.87)
Fe	0.35
B	11.13
C	0.11
O (AA)	0.11
Total	99.85

3. Atomic Ratio B/Me^*

Over-all	1.97
Corrected[**]	2.05

4. X-ray Phase Identification

HfB_2
HfO_2 (tetragonal) impurity
HfC impurity

5.a) Powder Density(Measured)

10.5 g.cc As Received

b) Powder Density(Calculated)

10.81 g/cc

6. Particle Size Distribution

a) As Received

Range (μ)	w/o
0-5	5.8
5-10	12.0
10-20	19.5
20-40	16.3
>40	46.4

b) Fluid Energy Milled

Range (μ)	w/o
0-5	24.8
5-10	43.6
10-20	25.0
20-40	3.7
>40	2.8

7. Phase Assay (volume per cent)
    - Calculated from Composition

MeB_2	HfO_2	HfC	FeB
97.7	0.8	1.5	0.6

MeB_2 = 4.2 TiB_2 and 95.8 $Hf(Zr)B_x$

8. Impurity Assay (volume per cent) - Metallographic
    Analysis of High Pressure Hot Pressed Sample

    6.8%

[**]Over-all atomic ratio corrected for hafnium assumed to be present as metal
dioxide and metal monocarbide and diboride as $Hf(Zr)B_x$ where x = B/Me^*.

123

TABLE 11

CHARACTERIZATION OF HAFNIUM DIBORIDE POWDER II10

Supplier: Wah Chang Corporation

Quantity: II 10-3 Pounds, II 10A-97 Pounds

1. Qualitative Analysis
    (weight per cent, w/o)

B	1-10
Zr	0.1-1.0
Fe	0.01-0.1

2. Quantitative Analysis (w/o)

Hf+Zr	87.86 [***]
Zr	(0.88)
B	10.77
C	0.32
O (AA)	0.41
Total	99.36

3. Atomic Ratio

    Over-all [**] B/Hf = 2.00
    Corrected [**] B/Hf^* = 1.97

4. X-ray Phase Identification

    HfB_2, HfO_2

5.a) Powder Density(Measured)

    10.32 g/cc

  b) Powder Density(Calculated)

    10.20 g/cc

6. Particle Size Distribution

Range (μ)	w/o
0-5	9.4
5-10	23.8
10-20	32.8
20-40	31.2
>40	2.7

7. Phase Assay (volume per cent)
    - Calculated from Composition

$Hf(Zr)B_x$	HfO_2	B_4C	Graphite
87.2	2.8	8.9	1.1

8. Impurity Assay (volume per cent)
    - Metallographic Analysis of High
    Pressure Hot Pressed Sample

    10.5 v/o

[**] Atomic ratio corrected for metal and carbon assumed to be present as
metal dioxide and boron carbide, respectively and diboride as $Hf(Zr)B_x$
where x = B/Hf^*.

[***] Based upon 1% Zr in Hf.

TABLE 12

REVISED POWDER SPECIFICATION FOR ZrB_2 AND HfB_2 FOR HOT PRESSING WITH SiC AND/OR* C

The chemistry specifications for diboride powder used for the fabrication of ManLabs' diboride base materials are:

	ZrB_2 Weight Percent	HfB_2 Weight Percent
Hf	0.0-3.0	88.0-89.5 (Hf+Zr)
Zr	79.5-80.5(Hf+Zr)	0.0-2.0
B	18.0-19.0	10.0-10.5
C	< 0.50	< 0.50
O	< 1.00	< 0.50
Ti	< 0.10	< 0.10
Fe	< 0.05	< 0.05
Other Metals	< 0.10	< 0.10
N	< 0.05	< 0.05
H	< 0.05	< 0.05
Atomic Ratio: B/Hf+Zr	< 2.0	< 2.0

Limitations imposed by present powder production technology, oxide availability and cost factors of ZrB_2 and HfB_2 for hot pressing purposes results in the presence of 0.5 to 1.5 percent nonmetallic impurities - principally oxygen and carbon. The above overall chemical composition has been established to insure that these impurities are present as metal oxides, metal carbides, or as metal oxy-carbides. All metallic impurities are kept below 0.1 percent.

Diboride powder particle size specification is -325 mesh or finer. Fluid energy milling can be employed to break up particulate aggregates.

Diboride powder fabricated by hot pressing without additives shall be free of metallographically identifiable phases such as B_4C which occur at grain boundaries in hot pressed structures of 85 to 100% relative density.

*See Table 13 for SiC and C specifications.

TABLE 13

Powder Specifications for Ceramic Additives

Silicon Carbide Powder

Carborundum, Grade 1000 RA
Particle Size: 3 to 8 microns
Representative Analyses:
    Qualitative Spectroscopic Analysis:
        Si > 10%; Ti, 0.1 to 1%, V, 0.01 to 0.1%; all other
        metallic impurities less than 0.01%
    Quantitative Chemical Analysis:
        Si, 69.8%; C, 29.5%
    X-ray Phase Identification:
        Si C

Carbon Powder

Cabot, Regal Carbon, Grade 330R
Particle Size: 25 millimicrons
Manufacturer's Assay: 99+% Carbon; 1% Volatiles
Physical State: Amorphous

TABLE 14

POLISHING AND ETCHING PROCEDURES FOR DIBORIDE MATERIALS

Mounting Method A: Cold mount with steel ball bearings in mount to present abrasive wear; 1/2 hour cure (ManLabs)

Mounting Method B: Hot mount with diallyl phthalate, FS-6; press at elevated temperature (Avco)

Grinding Procedures for Cold and Hot Mounted Samples:

Cold Mount (ManLabs)	Hot Mount (Avco)
1. Remove excess mount on belt sander	1. 100% surface sample on coarse diamond disc
2. 100% surface sample on 170μ diamond disc	2. 100% surface sample on 170μ diamond disc
3. 100% surface sample on 45μ diamond disc	3. 100% surface sample on 45μ diamond disc
4. 100% surface sample by lapping with 30μ diamond paste on a glass plate	4. 100% surface sample on 15μ diamond disc
5. Automatic polish on Pellon cloth with 0.3μ Al_2O_3 slurry 1/2 to 3 hours	5. Automatic polish on Pellon cloth with 0.3μ Al_2O_3 slurry 1/2 to 3 hours
6. If necessary, polish on blue cashmere cloth with 0.06μ $Al_2O_3+Cr_2O_3$ distilled water slurry	

Etching Solutions:

ManLabs	Avco
15cc glycerine	30cc glycerine
5cc nitric acid	10cc nitric acid
5cc hydrochloric acid	5cc hydrochloric acid
3cc hydrofluoric acid	1-5cc hydrofluoric acid
Application: Immersion for 2 minutes	Application: Swab

TABLE 15

EFFECTIVE NDT TECHNIQUES FOR DIBORIDE BILLETS

Effective NDT Technique	Variable Detected or Monitored	Effect on Properties
Radiography	Cracks, porosity, inclusions	Lower ultimate strength, Changes in modulus
Dye Penetrant	Cracks, porosity, (open to surface)	Degradation of mechanical properties and modulus
Ultrasonic Pulse-Echo	Internal cracks, inclusions, voids	Not established yet
Thermoelectric	Chemistry (impurities content in HfB_2)	Decrease in fabricability with increased impurity, Affects crack incidence in billets of HfB_2
Ultrasonic Velocity	Changes in velocity or density	Changes in dynamic modulus - correlates with tensile modulus
Radiometric Gaging	Changes in density (radiation transmitted), chemistry	Changes in modulus
Eddy Current	Chemistry, structure, electrical conductivity, density	Not established yet

128

TABLE 16

POWDER DENSITIES AND MAXIMUM BILLET DENSITIES FOR MATERIALS

Material Designation	Air Pycnometric Powder Density or Calculated (c) Density gm/cm^3	Maximum Density Based on Hot Pressing gm/cm^3
I02A	6.03 + 0.02	*
I03A	6.04 ∓ 0.01	*
I04	6.00 ∓ 0.02	*
I05	6.33 ∓ 0.02	*
I05A	6.15 ∓ 0.02	*
I06	5.96 ∓ 0.02	6.03
I07	5.96 ∓ 0.02	*
II05	10.69 ∓ 0.04	*
II06	11.15 ∓ 0.04	11.17
II06B	10.79 ∓ 0.03	10.95
II07	10.25 ∓ 0.04	*
II08A	7.57 ∓ 0.03	*
II09	10.39 ∓ 0.04	*
II10	10.32 ∓ 0.09	*
III05	9.20 (c)	9.50
III09	8.98 (c)	9.23
III10	8.91 (c)	9.34
IV05	8.45 (c)	8.62
IV09	8.24 (c)	8.42
V02A	5.47 (c)	5.54
V03A	5.47 (c)	*
V05A	5.58 (c)	5.64
V07	5.42 (c)	5.56
VI05	10.89 + 0.02	10.97
VIII02A Regal	4.37 (c)	4.50
VIII07 Regal	4.32 (c)	4.99
VIII(18,10)07 Regal	5.05 (c)	5.26
VIII07 Poco	4.44 (c)	*
IX09	10.09 (c)	10.75
X07	5.24 (c)	5.81
XII02A Poco	4.11 (c)	*
XII05A Regal	3.98 (c)	*
XII07 Poco	4.07 (c)	*
XII07 Regal	3.88 (c)	*
XIV06B Regal	7.03 (c)	7.68
XIV09 Regal	6.81 (c)	7.58
XIV(18,10)09 Regal	8.12 (c)	8.67
XV06B Regal	6.30 (c)	*
XV(20)06B Regal	8.99 (c)	9.98
XV(20)10 Regal	8.62 (c)	*
SiC	3.23 + 0.02	-
Graphite Poco	2.18	-
Carbon Regal	1.80	-
HfSi$_2$	9.12 + 0.05	-
III06B	9.28 (c)	9.65
XII(20)07 Regal	5.21	5.43

*Maximum billet density did not exceed powder density for powders marked with an asterisk.

129

TABLE 17

MATERIAL I HOT PRESSING CONDITIONS AND RESULTS

Designation	Temp. °C	Pressure psi	Time min.	Density gm/cc	Grain Intercept μ	Furnace No.
I02A D0613	2060	4000	60	5.45	21.1	2
I03 D0619K*	2000	2500	140	6.02	18	2
I02A D0645V	1900	4000	220	5.58		2
I02A D0649V	2100	4000	150	cracked		3
I02A D0650K	2080	2500	120	5.92	32.0	2
I02A D0651V	2100	4000	150	cracked		3
I03A D0656	1900	4000	58	5.16		3
I03A D0657	2100	4000	60	5.92		2
I02A D0670V	1950	4000	215	5.53		2
I02A D0673V	1900	4000	180	5.56		2
I07F D0700K*	2000	2500	230	5.91	27.0	1
I07F D0701K*	2000	2500	260	5.93	56.3	1
I07 D0801	2050	4000	127	5.83		2
I05A D0818*	2200	4000	60	6.07		2
I05A D0819*	2200	4000	60	6.04		1
I05A D0820*	2100	4000	60	6.08		3
I05A D0821*	2050	4000	60	5.99		2
I05A D0842*	1850	4000	60	5.27		2
I05A D0848*	1900	4000	60	5.25		
I07F D0905K*	1860	2500	215	5.40		3
I07F D0936K*	1800	2500	110	5.21		1
I07F D0937K	1800	2500	90	5.24		3
I07F D0938K	2040	2500	195			3
I07F D0940K*	1800	2500	90	5.03	8.2	2
I07F D0950K	2100	2500	225	5.74		3
I07F R37L	2080	3000	75	5.32		-
I07F R38L	2100	3000	128	5.46	27.8	-
I07F D0974K	2000	2500	300	5.65		2
I05 R44L	2050	3000	200	6.14	28.5	-
I07F D1020K	2000	2500	250	5.78		1

*Underscored billets were employed for Phase Two property measurements.
Billets marked with an asterisk (but not underscored) were employed for
special NDT measurements (4).

130

TABLE 18

METALLOGRAPHIC PHASE ANALYSES FOR MATERIAL I

Material Designation	Density g/cc	ZrB2 v/o	Impurity v/o	Void v/o	Porosity[*] v/o
I07F D0628	5.98	94.4	5.6	0	0.5
I07F D0700K	5.91	88.2	6.1	5.7	1.0
I07F D0940K	5.03	79.2	4.4	15.5	1.5

*Porosity based on billet density and powder density, Table 16.

TABLE 19

ELECTRON PROBE MICROANALYSIS OF I05 D0450

X-Ray Intensity (Counts in 50 sec.)

Phase	B	O	C*	C (Corr.)**
White (matrix)	6664	(244)	1320	0
Orange	848	91	1688	248
Dark Grey[+]	238	2896	-	-
ZrC	118	(15)	2595	1145
ZrO_2[+]	-	5773	-	-

Parenthetical numbers represent minus values.

[*]Values obtained by extrapolating 10, 20, 30 and 40 second data to time zero.

[**]Normalized to white phase = 0 to correct for ZrM_α line interference.

[+]Light blue fluorescence observed under electron bombardment.

TABLE 20

MATERIAL V, HOT PRESSING CONDITIONS AND RESULTS

Material Designation	Temp. °C	Pressure psi	Time min.	Density gm/cc	Grain Intercept μ	Furnace No.
V07F D0580K*	2100	2500	55	5.56	7.0	2
V(10)07F D0661K	2100	2500 (1000 cold)	72	5.84		3
V(10)07F D0662K	2100	2500 (1000 cold)	77	5.83		2
V(10)07F D0663K	2100	2500 (1000 cold)	60	5.85		2
V(10)07F D0671K	2050	4000 (1000 cold)	95		10.1	2
V07Q 2315L	2050	2500	240	5.38		
V07F D0703K*	2100	2500	90	5.51	9.7	3
V07F D0704K	2080	2500	68	5.50		1
V07F D0705K	2080	2500	60	5.49		3
V07F D0706K*	2080	2500	57	5.50	8.6	1
V07F D0714K	2150	2500	25 + 15	cracked		2
V07F D0714K	2150	2500	55	5.50		2
V07F D0716K	2150	2500	37	5.47	8.5	2
V07F D0717K	2150	2500	32	5.51		2
V07F D0719K	2150	2500	107	5.52		2
V(10)07F D0720K	2100	2500 (1000 cold)	90	5.82	9.9	2
V(10)07F D0721K	2100	2500	108	5.80	13.0	2
V07F R26L*	2020	3000	135	5.53		2
V(10)07F D0788	1900	4000	250	5.91	7.5	3
V(5)07F D0795K	2060	2500	110	5.77	10.5	3
V(10)07F D0796K	2060	2500	129	5.69		3
V(5)05A D0828	2050	4000	185	6.05		2
V(10)05A D0829	2050	4000	202	5.96		3
V(15)05A D0830	2050	4000	65	5.74		1

TABLE 20 (CONT)

MATERIAL V, HOT PRESSING CONDITIONS AND RESULTS

Material Designation	Temp. °C	Pressure psi	Time min.	Density gm/cc	Grain Intercept μ	Furnace No.
V05A D0831	2050	4000	153	5.64		3
V(50)05A D0832	2050	4000	97	4.75		2
V(50)07F D0840	2140	4000	125	cracked		2
V(50)07F D0843	2100	4000	50	cracked 4.62	3.7	1
V07F D0844K	2080	2500	60	5.53	4.2	3
V07F D0845K*	1900	2500	95	4.83		2
V07F D0846K	1900	2500	90	5.20		2
V07F D0847K	1880	2500	88	5.26		2
V07F D0849K*	1880	2500	47	4.95	5.9	1
V07F D0850K	1880	2500	56			2
Repressed, 850K*	1880	2500	30	4.94	5.1	2
V07F D0851K*	1880	2500	34	4.79		
V07F D0900K	2100	2500	207	5.52		1
V07F D0901K	2100	2500	130	5.57		1
V07F D0902K*	2100	2500	90	5.52	9.0	2
V07F D0946K	2060	2500	173	5.52		3
V07F R31L*	2040	3000	90	5.53		
V07F D0955K	2100	2500	77	5.56		2
V07F Q2409H	2060	2500	82	5.16		

*Underscored billets with terminal identification letter "K" were employed for Phase Two property measurements, with letter "L", for simple structural elements in Phase Three (11).

134

TABLE 21

METALLOGRAPHIC PHASE ANALYSES FOR MATERIAL V

Material Designation	ZrB_2 v/o	SiC v/o	Impurity Phase v/o	Void v/o
V02A D0370	79.8	20.2		
V02A D0372	75.4	24.6		
V02A D0387	79.0	18.9		2.1
V02AF D0393	71.0	22.8		6.2
V02AF D0394	79.1	20.9		
V02A D0396	79.7	20.3		
V03A D0478	74.8	21.0	4.2	
V03A D0480	71.8	21.6		6.6
V07 D0480K	80.5	18.3	1.2	
V02A D0612	81.0	19.0		
V02A D0614	68.8	20.8		10.4
V02A D0618	77.1	22.9		
V07F D0703K	80.4	19.6		
V(10)07F D0788	89.9	8.6	1.5	
V(5)07F D0795K	92.5	2.0		5.5
V(5)05A D0828*	93.2	4.7	1.3	0.8
V(10)05A D0829*	90.7	9.1	---	0.2
V(15)05A D0830*	83.9	12.0	4.0	---
V05A D0831*	79.9	19.9	0.2	---
V(50)05A D0832*	49.1	49.0	---	1.9
V(50)07F D0840	47.5	49.8		2.7
V(50)07F D0843	52.1	47.9		
V07F D0850K	75.0	13.0		12.0
V07F R26L Core No. 1 Slice No. 3	84.4	14.2	1.0	0.0

TABLE 22

MICROSTRUCTURE STUDY OF SPECIAL MATERIALS USED FOR MATERIAL V ANALYSIS

Billet No.	Powder Mixture Composition	X-ray Phase Identification Before	X-ray Phase Identification After	Microhardness, KHN* Accepted Kg/mm^2	Microhardness, KHN* Measured Kg/mm^2	Color	Result of Etching with HNO$_3$+HF	Result of Etching with HNO$_3$	Result of Etching with H$_2$SO$_4$
D0622	20v/o ZrB$_2$ 80v/o SiC	ZrB$_2$ SiC	ZrB$_2$ SiC						
D0628	20v/o ZrC 80v/o SiC	ZrC SiC	ZrC SiC						
D0624	20v/o ZrO$_2$ 80v/o SiC	ZrO$_2$ SiC	ZrSi$_2$ ZrC SiC	950 (50g) 1030 (100g) 3000 (100g) 1875 (100g)	967 (25g) 1231 (25g) 2241 (25g)	white gray dk. gray	etched etched	no attack etched no attack	no attack etched no attack
D0625	20v/o ZrB$_2$ 20v/o ZrC 60v/o SiC	ZrB$_2$ ZrC SiC	ZrB$_2$ ZrC SiC						
D0626	20v/o ZrB$_2$ 20v/o ZrO$_2$ 60 v/o SiC	ZrB$_2$ ZrO$_2$ SiC	ZrB$_2$ ZrSi$_2$ ZrC SiC	2250K (100g) 1128K (25g) 950 (50g) 1030 (100g) 3000 (100g) 1875 (100g)	1128 (25g) 833 (25g) 1321 (25g) 1723 (25g)	white white gray dk. gray	etched no attack no attack etched	etched no attack no attack no attack	etched no attack etched no attack
D0627	20v/o ZrC 20v/o ZrO$_2$ 60v/o SiC	ZrC ZrO$_2$ SiC	ZrC ZrSi$_2$ SiC						

* Load values shown in parentheses.

136

TABLE 23

ANOMALOUS GRAIN GROWTH IN MATERIAL V BILLETS

Material Designation	Observation
V(10)02 D0532	Isolated large grains
V(5)02 D0531	Large grains
V(10)07 D0664K	Isolated large grains
V(10)07 D0671K	Large grains
V(10)07 D0720K	Isolated large grains
V(10)07 D0721K	Large grains
V(10)07 D0661K	Large grains
V(10)07 D0663K	Large grains
V07 D0715	Small grains
V(10)07 D0788	Small grains
V(10)07 D0796K	Small grains
V(5)05A D0828	Small grains
V(10)05A D0829	Small grains

TABLE 24

MATERIAL VIII, HOT PRESSING CONDITIONS AND RESULTS

Material Designation	Temp. °C	Pressure psi	Time min.	Density gm/cc	Grain Intercept μ	Furnace No.
VIII07F D0621K	2060	2500	155	4.47		1
VIII07F Q2301L	2000	2500	140	4.27		-
VIII07F Q2317L	2050	2500	245	4.41		-
VIII07F Q2318L	2050	2500	240			-
VIII07F Q2321L	2030	2500	285	4.19		-
VIII07F D0722K	2140	2500	220	4.38		2
VIII07F Q2343N	2020	3000	170	3.63		-
VIII07F D0723K	2160	2500	173	4.52		3
VIII07F D0724K	2120	2500	180	4.30		2
VIII07F D0725K	2120	2500	160	4.34		3
VIII07F Q2345N	2100	2500	150			-
		+3000	75	4.20		
VIII07F D0760K*	2160	2500	325	4.66	2.5	3
VIII07F D0761K*	2160	2500	368	4.64		3
VIII07F D0767K*	2160	2500	278	4.65		3
VIII07F D0768K*	2160	2500	260	4.63		2
VIII(19)(5)07F D0771	2100	4000	100	5.47	3.9	2
VIII(18,10)07F D0772	2100	4000	108	5.27	2.6	3
VIII07F D0797 MTFF	2000	4000	165	4.51		1
VIII07F D0803K	2160	2500	208	4.99		1
VIII07F Q2374K	2020	2500	190	4.48		-
VIII(17,15)07F D0858	2050	4000	127	5.16		2
VIII(19,5)07F D0860	2100	4000	67	5.41		1
VIII(18,10)07F D0861	2100	4000	83	5.29		-

TABLE 24 (CONT)

MATERIAL VIII, HOT PRESSING CONDITIONS AND RESULTS

Material Designation	Temp. °C	Pressure psi	Time min.	Density gm/cc	Grain Intercept μ	Furnace No.
VIII07F D0893K	2160	2500	190	4.52		2
VIII07F D0896K	2160	2500	220	4.51		1
VIII07F D0897K	2160	2500	300	4.52		2
VIII(18,10)07F D0904K*	2160	2500	130	5.28		1
VIII07F Q2400L	2140	2500	100	delaminated		-
VIII07F R27L	2160	2500	85	delaminated		-
VIII(18,10)07F D0916K	2160	2500	75	5.24	5.7	2
VIII(18,10)07F D0917K*	2160	2500	90	5.14		3
VIII(18,10)07F D0919K*	2160	2500	90	5.26	6.4	3
VIII(18,10)07F D0920K*	2160	2500	90	5.25		2
VIII(18,10)07F D0922K	2160	2500	87	5.25		2
VIII07F D0956K	2160	2500	257	4.56		3
VIII(18,10)07F R33L	2040	3000	145	5.16	6.0	-
VIII(18,10)07F R35L	2040	3000	105	5.21		-
VIII07F D0965K	2160	2500	227	4.39		1
VIII07F D0967K	2160	2500	165	4.42		1
VIII(18,10)07F R40L*	2045	3000	145	5.21	4.0	-
VIII(18,10)07F D0973K	2160	2500	257	4.59		2
VIII07F D0975K*	2160	2500	265	4.58		1
VIII07F D0976K	2160	2500	270	4.63		2

*Underscored billets with terminal identification letter "K" were employed for Phase Two property measurements, with letter "L", for simple structural elements in Phase Three (11).

METALLOGRAPHIC PHASE ANALYSES OF MATERIAL VIII

Material Designation	ZrB_2 v/o	SiC v/o	Graphite v/o	Void v/o
VIII07 D0760K	63.1	17.8	19.1	---
VIII(19,5)07 D0771	74.7	20.0	3.7	1.6
VIII(18,10)07 D0772	72.5	14.7	9.4	3.4
VIII(18,10)07 D0919K	75.5	20.7	3.8	0.0
VIII(18,10)07F R33L Slice No. 1 Core No. 3	76.8	16.5	5.7	1.0

TABLE 26

MATERIAL X, HOT PRESSING CONDITIONS AND RESULTS

Material Designation	Temp.	Pressure	Time	Density	Grain Intercept	Furnace No.
	$^{\circ}$C	psi	min.	gm/cc	μ	
X07F D0596	1900	4000	40	5.53	12	1
X07F D0597	1800	4000	50	5.28	4	1
X07F D0634	1700	4000	195	5.28	4.8	1
X07F D0635	2000	4000	140	5.81	15.0	3
X(5)07F D0792	2000	4000	147	6.01		3
X(10)07F D0793	2000	4000	95	5.8		1
X(15)07F D0794	2000	4000	133	5.75		2

TABLE 27

METALLOGRAPHIC PHASE ANALYSES OF MATERIAL X

Material Designation	Pressing Temp.	ZrB_2	SiB_6	Void
	$^{\circ}$C	v/o	v/o	v/o
X07F D0634	1700	80.3	14.0	5.7
X07F D0597	1800	59.6	20.4	20.0
X07F D0596	1900	83.6	13.2	3.2
X07F D0635	2000	86.5	11.6	1.9

141

TABLE 28

MATERIAL XII, HOT PRESSING CONDITIONS AND RESULTS

Material Designation	Temp. °C	Pressure psi	Time min.	Density gm/cc	Grain Intercept μ	Furnace No.
XII(5)07F D0665 Poco	1900	4000 (2000 cold)	120	5.85		3
XII(10)07F D0667 Poco	2050	4000 (2000 cold)	202	5.64	5.8	3
XII(5)07F D0668 Poco	2050	4000 (2000 cold)	200	5.82	13.8	1
XII(20)07F D0805K*2080		2500	207	5.43		3
XII(20)07F D0809K*2080		2500	145	5.36	8.5	1
XII(20)07F D0810K*2080		2500	115	5.36	7.2	3
XII(20)07F D0812K*2080		2500	132	5.12		3
XII(10)05A D0834	2080	4000	87	5.84		2
XII(5)05A D0835	2080	4000	157	6.06		3
XII(15)05A D0837	2080	4000	88	5.71		2
XII(20)05A D0838	2080	4000	155	5.52		3
XII05A D0839		4000	203	3.68		2
XII(20)07F D0889K	2080	2500	124	5.42		2
XII(20)07F D0891K	2080	2500	175	5.37		1
XII(20)07F D0892K	2080	2500	175	5.38		2
XII(20)07F R56L*	2080	3000	200	5.45		-

*Underscored billets with terminal identification letter "K" were employed for Phase Two property measurements with letter "L", for simple structural elements in Phase Three (11).

TABLE 29

ANOMALOUS GRAIN GROWTH IN MATERIAL XII

Material Designation	Observation
XIIf(5)03A D0572 Thornel	Large grains
XII(5)07F D0638 Regal	Large grains
XII(5)07F D0602 Poco	Large grains
XII(10)07F D0601 Poco	Large grains
XII(10)07F D0639 Poco	Large grains
XII(5)07F D0668 Poco	Large grains
XII(10)07F D0667 Poco	Small grains
XII(5)07F D0615 Thornel	Small grains
XII(15)07F D0641 Regal	Small grains
XII(10)05A D0834 Regal	Small grains
XII(5)05A D0835 Regal	Small grains
XII(15)05A D0837 Regal	Small grains

143

TABLE 30

MATERIAL II, HOT PRESSING CONDITIONS AND RESULTS

Material Designation	Temp. °C	Pressure psi	Time min.	Density gm/cc	Grain Intercept μ	Furnace No.
II06B D0740K	2180	2500	280	10.95*	13.4	3
II06B D0742K	2200	2500	165	10.92*	14.2	3
II06B D0743K	2180	2500	290	10.88*	15.5	2
II06B D0744K	1900	2500	270	6.91	See D0790	3
II06B D0758K	2180	2500	320	10.82*		2
II06B D0790K**	2180	2500	440	10.84*		2
II09F D0697	2200	4000	150	10.04	60.2	3
II09F D0713	2150	4000	185	10.09		2
II09F D0750	2080	4000	232	10.12	14.4	3
II09F D0774K	2160	2500	260	9.89	10.0	2
II09F D0784	2160	4000	155	10.33	25.9	1
II09F D0898	2200	4000	207	10.13	24.2	1
II09F D0909K	2200	2500	252	10.18		2
II09F D0911K	2200	2500	201	10.16		3
		3000	107			
II09F D0913K	2220	3000	330	10.17		3
II10 D0726	2150	4000	142	10.12	18	3
II10 D0823K	2150	2500	217	9.96	65.1	2
II10 D0899	2200	4000	207	10.34	95.4	3
II10 D0914K	2200	3000	225	10.13		2
II10 D0923K	2240	3000	300			3
II10 D0933K	2200	3000	200	10.32		3
II10 D0934K	2200	3000	200	10.11	79.0	2

*Billets showed surface cracks.

**D0790K repressed D0744K.

TABLE 31

METALLOGRAPHIC PHASE ANALYSES FOR MATERIAL II

Material Designation	HfB_2 v/o	2nd Phase v/o	Void v/o
II06A D0672	93.0	7.0	0
II10 D0726	91.0	4	5
II06B D0740K	94.6	5.1	0.3
II06B D0742K	93.5	6.0	0.5
II06B D0743K	95.7	4.2	0.1
II09 D0750F	93.0	1.7	5.3
II09 D0784F	93.0	5.0	2.0
II10A D0823K	83.7	7.4	8.9
II10 D0899	88.3	6.2	5.3
II10 D0934	91.7	3.9	4.4

TABLE 32

MATERIAL III AND IV, HOT PRESSING CONDITIONS AND RESULTS

Material Designation	Temp. °C	Pressure psi	Time min.	Density gm/cc	Grain Intercept μ	Furnace No.
III(50)05 D0593	2050	4000	120	6.79	5.1	3
III09F D0727K	2150	2500	180	9.04		3
III09F D0741	2150	4000	110	9.13	7.2	2
III(5)06B D0778K	2160	2500	203	10.61	12.7	2
III(10)09F D0786	2160	4000	103	9.81	12.1	2
III(40)09F D0824	2150	4000	67	7.71	7.1	2
III10A D0825	2150	4000	96	9.34	8.9	3
III(50)09F D0841	2200	4000	195	6.94	7.8	2
III09F D0852K	2140	2500	210	9.24		1
III09F D0854K	2100	2500	142	9.23	8.7	2
III10 D0903	2050	4000	33	die broke		2
III10 D0906K	2150	2500	88	9.30		1
III10 D0907K	2150	2500	107	9.33		2
III10 D0908K	2150	2500	108	9.20		1
III(5)06B D0915	2200	4000	243	----		1
III(5)10 D0918	2200	4000	253	----		1
III10 D0941K*	2000	2500	75	9.21	13	1
III10 D0943K*	2200	2500	60	9.21		1
III10 D0944K*	2200	2500	90	9.21		3
III10 D0945K	2200	2500	66	9.02		1
III10 D0948K	2140	2500	broke	8.90		3
III09F D0951K	2180	2500	172	9.17		1
III06B D0961K	2200	2500	102	9.52		1
III06B D0962K	2200	2500	90	9.52		1
III06B D0966K	2200	2500	92	9.65 cracked		1
III(5)09F D1011	2100	4000	180	9.61		1
III10 R52L	2200	3000	90	9.03		-
III(5)09F D1034K	2130	2500	105	9.02		1

TABLE 32 (CONT)

MATERIAL III AND IV, HOT PRESSING CONDITIONS AND RESULTS

Material Designation	Temp.	Pressure	Time	Density	Grain Intercept	Furnace No.
	°C	psi	min.	gm/cc	μ	
III(5)09F D1059K*	2160	2500	125	9.49		3
III(5)09F D1035K	2130	2500	75	8.99		3
III(5)09F D1061K**	2160	2500	127	9.44		1
IV09 D0804FK*	2150	2500	250	8.38		1
IV09 D0807FK*	2150	2500	160	8.26		3
IV09 D0808FK*	2150	2500	203	8.42	8.5	3
IV09 D0811FK*	2150	2500	115	8.39		3

*Underscored billets with terminal identification letter "K" were employed for Phase Two property measurements.

**III(5)09F D1059K and III(5)09F D1061K were repressed from D1034K and D1035K, respectively.

TABLE 33

METALLOGRAPHIC PHASE ANALYSES FOR MATERIAL III AND IV

Material Designation	HfB$_2$ v/o	SiC v/o	Other v/o	Void v/o
III09 D0741	75.5	22.6	1.5	0.4
III(5)06B D0778	90.4	3.8	3.2	2.6
III(10)09F D0786	85.5	11.8	2.7	0
III(40)09F D0824	50.5	44.3	1.8	3.4
III10 D0825	82.5	16.9	0	0.6
III(50)09F D0841	48.6	49.0	0.6	1.8
III09F D0854K	81.3	18.3	---	0.5
III10 D0941K	84	13	0	3
IV09F D0808K	68.3	30.3	1.3	0.1

TABLE 34

MATERIAL IX HOT PRESSING CONDITIONS AND RESULTS

Material Designation	Temp. $^\circ C$	Pressure psi	Time min.	Density gm/cc	Grain Intercept μ	Furnace No.
IX09F D0745	1900	4000	110	10.75		3
IX09F D0749	2000	4000	85	10.75		3
IX(11)10 D0947	1950	4000	240	*		3

*Billet broken in several pieces.

TABLE 35

METALLOGRAPHIC PHASE ANALYSES OF MATERIAL IX

Material Designation	HfB_2 v/o	$HfSi_2$ v/o	2nd Phase v/o	Void v/o
IX09F D0745	89.1	6.0	3.9	1.0
IX09F D0749	91.6	4.3	2.9	1.2

TABLE 36

MATERIAL XIV, HOT PRESSING CONDITIONS AND RESULTS

Material Designation	Temp. °C	Pressure psi	Time min.	Density gm/cc	Grain Intercept μ	Furnace No.
XIV09F D0751	2080	4000	250	7.21	3.6	3
XIV09F D0752	2080	4000	215	7.10	3.3	3
XIV09F Q2375K	2120	2400	195	7.58		-
XIV09F D0869	2100	4000	215	7.13		1
XIV06B D0874	2140	4000	135	7.68		1
XIV(18,10)09F D1033K*	2080	2500	125	8.56		1
XIV(18,10)09F D1036K*	2080	2500	140	8.67	7.6	3
XIV(18,10)09F D1037K*	2080	2500	120	8.55		1
XIV(18,10)09F R68L	2080	3000	120	8.54		

*Underscored billets with terminal identification letter "K" were employed for Phase Two property measurements.

TABLE 37

METALLOGRAPHIC PHASE ANALYSIS OF MATERIAL XIV

Material Designation	HfB_2 v/o	SiC v/o	Graphite v/o
XIV(18,10)09F D1036K	74.5	23.2	2.2

150

TABLE 38

MATERIAL XV, HOT PRESSING CONDITIONS AND RESULTS

Material Designation	Temp. °C	Pressure psi	Time min.	Density gm/cc	Grain Intercept μ	Furnace No.
XV(20)06B D0813	2160	4000	55	9.13		-
XV(20)06B D0876	2160	4000	65	9.98		2
XV(20)06B D0886	2160	4000	125	9.74		2
XV(5)09F D0921	2200	4000	330			1
XV(5)10 D0924	2220	4000	255			1
XV(5)06B D0929	2220	4000	157			3
XV(20)10 D1027K*	2080	2500	210	8.84		1
XV(20)10 D1031K*	2080	2500	200	8.95	7.9	3
XV(20)10 D1054K*	2080	2500	200	8.72		1
XV(20)10 R62L*	2080	3000	120	8.93		-

*Underscored billets with terminal identification letter "K" were employed for Phase Two property measurements; with letter "L" for simple structural elements in Phase Three (11).

TABLE 39

METALLOGRAPHIC PHASE ANALYSIS OF MATERIAL XV

Material Designation	HfB_2 v/o	Graphite v/o	Impurity v/o
XV(20)10 D1031K	83.5	10.9	5.5

151

TABLE 40

COMPARISON OF NDT DYNAMIC MODULUS AND
MECHANICAL TEST TENSILE MODULUS

Material Designation	Dynamic Modulus $V_L^2 D = E_D$ $(10^6$ psi)	Elastic Modulus Reported by Mechanical Testing (9)
I	68.7	72.0, 75.7
II	67.11	73.0
III(10)	76.4	70.1
III		77.5
IV	76.2	73.6, 74.2
V(5)	68.3	
V(10)	71.25	69.8
V	79.4	76.0
V(50)	76.8	72.0
VIII	36.0	33.9
VIII(19,5)	71.5	70.9
XII(15)	49.3	50.0

TABLE 41

HOT PRESSINGS OF VARIOUS DIBORIDE COMPOSITIONS
SHOWING DEGREE OF PROCESS CONTROL

Material Designation	Temp. °C	Pressure psi	Time min	Density gm/cc	Relative Density %	Furnace No.
I02A D0283	2050	6000	60	5.87	97.4	
I02A D0304*	2070	6000	60	5.83	96.6	
I02A D0305	2075	6000	60	5.99	99.3	
I02A D0289	2050	6000	30	5.80	96.2	
I02A D0290	2050	8000	30	5.85	96.9	
I03A D0311	1800	6000	120	5.54	92.0	
I03A D0314	1800	6000	120	6.00	99.5	
I03A D0324	1800	6000	30	5.56	92.1	1A
I03A D0328	1800	6000	25	5.37	89.1	1A
I03A D0330	1900	4000	90	5.98	99.3	1A
I03A D0339	1900	4000	100	5.52	91.5	1B
III05 D0400	2000	4000	110	8.86	93.3	1B
III05 D0444	2000	4000	100	8.52	89.9	1B
III05 D0385	2050	4000	75	9.25	98.6	2B
III05 D0386	2050	4000	60	9.26	98.6	3B
V02A D0395	1900	4000	115	5.22	94.5	3B
V02A D0397	1900	4000	110	5.28	95.1	1B
V02A D0392	2000	4000	45	5.21	94.5	1B
V02A D0393	2000	4000	35	5.40	97.6	2B
V02A D0394	2000	4000	50	5.47	98.8	3B

*Ball milled powder.

153

TABLE 42

EFFECT OF PRESSURE ON HOT PRESSING MATERIAL II AT 2200°C

Material Designation	Pressure psi	Time min	Density gm/cc	Density %	Furnace No.
II05 D0316	6000	120	10.62	99.5	3B
II05 D0348	6000	200	10.58	99.0	2B
II05 D0351	4000	200	10.53	98.6	2B
II05 D0353	4000	140	10.52	98.6	2B
II05 D0355 a and b	4000	120	10.46	97.9	1B
II05 D0437	2500	110	9.93	93.0	2B

TABLE 43

BILLET DENSITIES OF MATERIAL I03A HOT PRESSED
AT 2000°C, 4000 PSI FOR 75 MINUTES

Billet Number	Furnace	Relative Density %
D0360	1A	97.6
D0367	1A	97.0
D0359	2A	98.5
D0368	2A	94.1
D0366	3A	98.1
D0369	3A	99.5
Average		97.1
Standard Deviation		1.7
Maximum Deviation		5.4

TABLE 44

PLASMA SPRAYING RESULTS FOR ZrB_2 POWDER

Substrate	Qualitative Remarks
II05 D0435	Porous, sections fractured easily
303 Stainless Steel	Porous, flaky
V02A D0611	0.050 inch thick, porous
I07 D0555	0.035 inch thick, adherent, relatively dense
I07 D0555	0.040 inch thick, adherent, relatively dense

TABLE 45

PLASMA SPRAYING RESULTS FOR HfB_2-BASE POWDERS

Powder	Substrate	Thickness	Qualitative Remarks
II06B	I03A D0656	0.020 inches	Adherent
II06B	I03A D0657	0.021 inches	Adherent
II06B	II05 D0425	0.010 inches	Porous
II06B	II05 D0435	0.040 inches	Adherent
III05A	I07 D0555	0.020 inches	Adherent
III05A	I02A D0304	0.010 inches	Adherent
III05A	Ta	0.020 inches	Very adherent
II06B	Ta	0.100 inches	Porous
II06B	TZM (2 samples)	0.065 inches	Adherent
III05A	TZM (2 samples)	0.020 inches	Very adherent, relatively dense
III05A	TZM (2 samples)	0.010 inches	Very adherent, relatively dense

155

TABLE 46

SINTERING EXPERIMENTS AND RESULTS

Material Designation*	Cold Press. Pressure	Temp. °C	Time min	Density gm/cc	Shrinkage %	Laminations
I05A Zr$_1$ B13	10	1800	120	2.84	0.0	Internal
I05A Zr$_1$ B14	15	1800	120			Internal
I05A Zr$_1$ B15	15	1650	60		0.1	Internal
I05A Zr$_1$ B16	40	1700	60	4.81	0.6	No
I05A Zr$_1$ B17	40	1700	240	5.01		No
VI05 B18	10	2000	60	6.39	0.0	
I03A B19	20	2200	240	2.98	2.1	No
I05A Zr$_1$ B20	70	1700 2200	60 240	6.00		No
I05A Zr$_1$ B21	40	1700 2200	60 240	5.98	10.8	
II06 B22	40	2200	240	7.00	1.8	No
VI05 B23	40	2200	240	7.59	0.7	No
VI05 F24	10	2200	240	8.54	7.7	No
II06 B25	40	2400	240			
I05A Zr$_1$ B26**	40	2200	240	5.95	9.7	2 on edge
I05A Zr$_2$ B27**	40	1700 2200	60 240	6.00	10.4	No
I05A Zr$_2$ B28	70	2200	240	6.02	10.4	Yes
V05A Zr$_1$ B29	40	1700 2200	60 240	4.86	10.7	No
V05A Zr$_1$ B30	70	1700	60	4.86	8.7	No
I05A Zr+B$_4$C+ HfSi$_2$ B31	20	2000	180	3.86	2.3	No
I05A Zr+B$_4$C+ HfSi$_2$ B32	40	2000	180	3.91	5.4	Yes
I05A Zr+B$_4$C+ HfSi$_2$ B33	70	2000	180	4.08	4.5	No
V05A Zr$_1$ B34	50	1700 2000	60 240	5.68		Yes
V05A Zr$_1$ B35	70	1700 2000	60 240	5.37	11.7	No

TABLE 46(CONT)

SINTERING EXPERIMENTS AND RESULTS

Material Designation	Cold Press. Pressure	Temp. °C	Time min	Density gm/cc	Shrinkage %	Laminations
I05A Zr$_2$ B36	40	1700 2000	60 240	5.68	2.2	No
VI05A B37	20	2300	240	6.87	(8.1% wt. loss)	Edge
VI05A B38	30	2300	240	7.42		Yes
V05A Zr$_1$ B39**	40	1700 2000	60 240	5.19	(3.3% wt. loss)	No
I05A Zr$_2$ B40**	40	1700 2200	60 240	5.61	8.0 (1.5% wt. loss)	Yes
I03A B41**	40	2200	240	3.43	0	None
II10 Hf$_2$ B42	40	2190	180	6.13		
II10 Hf$_2$ B43	40	2190	180	6.13		
I05A Zr$_3$ B44	40	2200	240	5.34	13.6	None
I05A Zr$_3$ B45	40	2200	240	5.37	14.0	None
I05A Zr$_3$ B46	70	2280	240	5.68	14.0	Yes
V05A Zr$_2$ B47	40	2000	245	5.14	11.0	None
I05A Zr$_2$ B48**	30 ISO	2200	240	5.91	17.3	Yes (one central)

*Samples 1/2 inch diameter by 1/4 inch high except those with ** which are 1 inch diameter by 1 inch high; the parenthetical additives are (Hf$_2$), 8.0 wt. % Hf addition; (Zr$_1$), 14.2 wt. % Zr addition; (Zr$_2$), 8.0 wt. % Zr addition; and (Zr$_3$), 4.0 wt. % Zr addition.

TABLE 47

QUANTITATIVE METALLOGRAPHY AND PHASE IDENTIFICATION
OF I05A (Zr$_1$)B20

Concentration Volume Per Cent	Tentative Identification*
88.8	ZrB$_2$
5.0	ZrB
4.1	ZrO$_2$
0.5	Zr
1.6	Pores

*Partially based on X-ray results of I05A(Zr$_1$)B17.

TABLE 48

BEND STRENGTH OF SINTERED MATERIAL I VS. TEMPERATURE

10^{3}psi at

	23°C	800°C	1400°C	1800°C
I05A(Zr$_1$)B26	38.2	32.6	11.7	5.1
	35.5	39.9	13.7	4.1
	42.5		16.1	5.0

158

TABLE 49

MECHANICAL PROPERTIES OF ISOSTATICALLY HOT PRESSED V03A[*]

Bend Strength, 10^3 psi at

23°C	800°C	1400°C	1800°C
	26.0	22.6 NB	35.0 B
	27.2	22.6 NB	34.0 B
	22.6		

Elastic Modulus at 23°C, 74.5 x 10^6 psi

[*]See Reference (9) for details of mechanical property measurements; the letters NB and B employed with the bend strength values at 1400° and 1800°C refer to the absence and the presence of gross plastic bending in the test specimens, respectively.

TABLE 50

HOT ISOSTATIC PRESSING CONDITIONS AND BILLET DENSITIES

Fabrication Conditions

Billet Size: 1/2 inch diameter by 2 inches long
Temperature: 1700°C
Time: 2 hours
Pressure: 36,000 psi

Billet and Powder Densities

Material	(Density, g/cc)			
	Max. Obs. Conv. Hot Pressed	Powder or Calc. Mixture	Obs.	Isostatic
II09F	10.33	10.39	8.96	10.48
II10	10.32	10.32	8.92	9.12
II06B	10.84	10.79	10.92	10.93
I07F	5.93	5.96	5.95	5.94
V(5)07F	5.77	5.82	5.62	5.64
VIII(18,10)02A	5.29[*]	5.10[*]	4.99	5.02
VIII(14,30)02A	4.46[*]	4.45[*]	3.80	3.84
XII(20)02A	5.43[*]	5.21[*]	4.91	4.22

[*]Based on I07F powder density = 5.96 g/cc ; I02A powder density = 6.03 g/cc.

159

TABLE 51

BEND STRENGTH[*] OF HOT FORGED MATERIAL V AND VIII

Material Designation Density, Grain Size	Bend Strength, 10^3 psi at	
	$23°C$	$1400°C$
V07F D0716	44.6	16.7
100%, 8.5μ	57.1	15.2
VIII07F D0803K	50.7	36.7
100%, 4μ	44.8	46.0

*See Reference (9) for details of mechanical testing.

TABLE 52

BEND STRENGTH[*] OF THORNEL FIBER REINFORCED DIBORIDE MATERIAL

Material Designation Density, Grain Size	Bend Strength 10^3 psi at			
	$23°C$	$800°C$	$1400°C$	$1800°C$
XIIf(5) D0572	31.3*	41.4*	29.7* NB	21.7* NB
Thornel	34.6*	39.3*	15.1* NB	23.9* NB
100%, 5μ	32.9	34.3*	22.4 NB	16.4* NB

*See Reference (9) for details of mechanical property measurements.

TABLE 53

SUMMARY OF WELDING BEHAVIOR OF ZIRCONIUM DIBORIDE COMPOSITIONS[*]

Material	Weld Character	Modulus of Rupture $(10^3$ psi)
ZrB_2-Ta	Dense, pore-free	16-31
ZrB_2-Mo	Many fine pores with an occasional large pore.	19-30
ZrB_2-Nb	Dense, pore-free	19
ZrB_2+SiC-Ta	Many fine pores at weld-diboride interface	16
ZrB_2+SiC-Mo	Few pores at weld-diboride interface	24-31
ZrB_2+SiC+C-Ta	Few pores. Poor penetration. Cracked during handling	-
ZrB_2+SiC+C-Mo	Many pores. Poor penetration. Cracked during handling	-
ZrB_2-POCO Graphite	Many pores. Cracked during cooling	-
ZrB_2-Graph-i-tite G	Few fine pores	1.8
ZrB_2-321 Stainless Steel	Pore-free. Cracked during handling	-

[*]ZrB_2 designations: I03A D0619K and I07 D0801
ZrB_2 + SiC designations: V07 D0580K and V03A D0659
ZrB_2 + SiC + C designation: VIII02 D0592

No differences in welding behavior were observed for different designations of the same composition.

APPENDIX I

BILLET DESIGNATION SYSTEM

All billets prepared in this program are designated by a series of letters and numbers to identify the powders and their relative amounts and the hot pressing billet. The designation system requires:

(1)   a roman numeral to identify the base composition, Table 2, or a roman numeral followed by a parenthetically enclosed number or set of numbers to identify a compositional variation of the base composition, Table 3.

(2)   an arabic number to identify a particular lot of the base powder, or an arabic number followed by the letter "F" to indicate a fluid energy milled base powder lot.

(3)   a combination of a letter, and an arabic number or a letter, an arabic number and a letter to identify the billet pressing.

This is illustrated in the following examples:

(a)   I07F D0701K designates Material I, ZrB_2; the 07 powder lot fluid energy milled, billet pressing D0701K where the D identifies the 75 ton Dake press and the K the billet size of 3 inch diameter by 1 inch high.

(b)   V(5)05A D0829 designates Material V, ZrB_2 with 20 volume percent SiC in the base composition but modified in this billet to 5 volume percent as shown by "(5)" and billet pressing D0829 where the omission of a terminal letter indicates a billet size of 2 inch diameter by 0.7 inch high.

The letters for pressing or furnace identification include:

S,   a 20 ton Dake Press;
D,   a 75 ton Dake Press;
Q,   a 125 ton press;
C,   hot pressed at Carborundum;
B,   vacuum furnace for sintering;
R,   a 400 ton Rogers Press.

The letters for billet size identification include:

K,   3 inch diameter by 1 inch high;
N,   5 inch diameter by 1 to 2 inch high;
M,   6 inch diameter by 1 to 2 inch high;
L,   5.75 inch square by 1 to 2 inch high;
H,   hollow cylindrical billet.

162

OXYGEN ANALYSES OF DIBORIDE POWDERS AND PRESSINGS

Powders	Inert Gas[+] Fusion Analysis (w/o)	Activation Analysis[+] (w/o) Corrected for Boron	Uncorrected
I02	0.78	0.70	1.05, 0.96[*]
I03	1.30	1.15	1.49
I05	----	1.54	0.57*, 0.42*
I07	1.15	1.12	1.31
II05	0.10	----	0.27*
II06B	0.56	0.55	0.85, 0.76*
II09	0.18	0.11	0.42
II10	----	0.41	0.74

Pressings

	Inert Gas Fusion Analysis (w/o)	Corrected for Boron	Uncorrected
I02 D0282	0.72	----	----
I02 D0327	----	----	0.43*
I03 D0310	----	----	1.26*
I05 D0450	----	0.97	1.47
V02 D0372	0.39	----	----
V02 D0398	----	----	0.39*
V07 D0716K	----	0.05	0.50
XII(20)07 D0805K	----	0.02	0.28
XII(35)07 D0604	----	0.04	0.46
II05 D0315	0.11	----	----
II05 D0482B	----	----	0.16*, 0.25*
II05 D0380	----	----	0.15*
II06A D0672	----	0.40	0.71
II06B D0740K	----	0.30	0.62
II09 D0713	----	0.01	0.34
II09 D0784	----	ND	0.28
II10 D0726	----	ND	0.27
III05 D0408	0.10	----	----
III09 D0741	----	ND	0.25

+Inert gas fusion and activation analyses were performed at M. I. T., Material Science Department, and Gulf-General Atomics, San Diego, respectively.

*Earlier measurements; values corrected for boron are not available.

APPENDIX III

BILLET CHARACTERIZATION

		I05 D0450	I07 D0700F	V07 D0580K	V07 D0716K	V07 D26L
A.	**Chemical Analysis**					
	1. Zr(w/o)	80.44	77.15	70.94	66.52	
	Fe		0.36[+]	0.29	0.31[+]	
	B	17.06	18.97	*	17.22	
	C	0.94	0.37	3.59	3.76	
	O	0.97	*	0.22	0.05	
	Si	-----	-----	8.41	8.57	
	Ti	*	0.89	0.58	1.12	
	Total	99.41	98.65		97.62	
	2. B/Me Atom Ratio					
	Overall	1.788			2.113	
	Corrected	2.039			2.145	
	3. Phase Assay (v/o)					
	MeB_2	88.33			77.84	
	MeO_2	4.12			0.19	
	MeC	7.55			21.23	
	SiC	-----			21.23	
	B_4C	-----			-----	
	C	-----			-----	
B.	**Metallography**					
	1. Density (g/cc)					
	Bulk	6.11	5.91	5.56	5.47	
	Calc. (powder)	6.33	5.96	5.42	5.42	
	Calc. (assay)	6.09			5.40	
	2. Lineal Analysis (v/o)			80.5	69.2	
	MeB_2			1.2	1.3	
	Impurity			18.3	29.5	
	SiC			----	----	
	Void					
C.	**X-ray Diffraction**					
	Phases Detected	ZrB_2 ZrC ZrO_2	ZrB_2	ZrB_2 SiC	ZrB_2 SiC	

*Not measured.
[+]Calculated from diboride powder impurities

164

BILLET CHARACTERIZATION

		VIII(18,10)107 D0904K	XII(20)07 D0805K (Regal)	XII(35)07 D0604 (Poco)
A.	**Chemical Analysis**			
1.	Zr (w/o)	65.60	73.25	66.57
	Fe	ND	0.34[+]	0.31[+]
	B	15.58	17.76	16.22
	C	4.83	6.28	16.29
	O	*	ND	0.04
	Si	9.30	-----	-----
	Total	(95.31)	97.63	99.45
2.	B/Me Atom Ratio			
	Overall		2.028	
	Corrected		2.147	
3.	Phase Assay (v/o)			
	MeB_2		79.01	58.26
	MeO_2		-----	0.12
	MeC		3.36[++]	2.89[++]
	SiC		-----	-----
	B_4C		-----	-----
	C		17.44[++]	38.73
B.	**Metallography**			
1.	Density (g/cc)		5.43	4.61
	Bulk		4.89	4.64
	Calc. (powder)		5.30	4.39
	Calc. (assay)			
2.	Lineal Analysis (v/o)			
	MeB_2			
	Impurity			
	SiC			
	Void			
C.	**X-ray Diffraction**			
	Phases Detected			

*Not Measured.
[+]Calculated from diboride powder impurities.
[++]Assumes 0.50 w/o C is combined.

BILLET CHARACTERIZATION

		II06B D0740K	II09 D0784F	II10 D0726
A.	**Chemical Analysis**			
	1. Hf (w/o)	87.07	85.49	88.26
	Zr	-----	0.86	-----
	Ti	0.30	1.11	-----
	Fe	-----	0.35	-----
	B	11.09	11.59	10.95
	C	0.09	0.08	0.24
	O	0.30	ND	ND
	Si	-----	-----	-----
	Total	98.85	99.48	99.45
	2. B/Me Atom Ratio			
	Overall	2.075	2.069	2.047
	Corrected	2.150	2.115	1.885
	3. Phase Assay (v/o)			
	MeB_2	96.46	98.91	83.27
	MeO_2	2.27	-----	-----
	MeC	1.26	1.09	-----
	SiC	-----	-----	-----
	B_4C	-----	-----	16.73
	C			
B.	**Metallography**			
	1. Density (g/cc)			
	Bulk	10.95	10.33	10.12
	Calc. (powder)	10.79	10.39	10.32
	Calc. (assay)	11.03	10.77	9.81
	2. Lineal Analysis (v/o)			
	MeB_2	94.6	93.0	91.0
	Impurity	5.1	5.0	4.0
	SiC	----	----	----
	Void	0.3	2.0	5.0
C.	**X-ray Diffraction**			
	Phases Detected	HfB_2 HfO_2 HfC	HfB_2 HfC	HfB_2

BILLET CHARACTERIZATION

			III09 D0741F	III10 D0943
A.	Chemical Analysis			
	1.	Hf (w/o)	79.25	78.84
		Zr	0.80	-----
		Ti	1.02	-----
		Fe	0.33	0.08
		B	10.84	9.88
		C	2.13	2.05
		O	ND	-----
		Si	4.97	4.85
	Total		99.34	95.70
	2.	B/Me Atom Ratio		
		Overall	2.088	2.061
		Corrected	2.108	2.082
	3.	Phase Assay (v/o)	79.50	80.13
		MeB_2	-----	-----
		MeO_2	0.06	-----
		MeC	20.44	19.87
		SiC	-----	-----
		B_4C		
		C		
B.	Metallography			
	1.	Density (g/cc)	9.13	
		Bulk	8.98	
		Calc. (powder)	9.22	9.58
		Calc. (assay)		
	2.	Lineal Analysis (v/o)	75.5	
		MeB_2	1.5	
		Impurity	22.6	
		SiC	0.4	
		Void		
C.	X-ray Diffraction			
	Phases Detected		HfB_2 HfC SiC	

APPENDIX IV
NONDESTRUCTIVE TEST DATA
TABLE IV-1
BILLET TEST DATA

Billet	Radiography	Dye Penetrant
V02A D0612	Exhibits minute voids. One 1/2" diam. area inclused all except the larger	Appears to have foreign material embedded on surface
I02A D0613	Exhibits a flim density blemish and one delam. - like crack, 1/4" long	No defects noted, except "flake" indication on one surface
V02A D0614	Appears uniform and homogeneous	Porous: bleeds on both surfaces
XII(5)07 D0615 Thorn	Multiple cracking in lower central areas. Top surface has higher density that gets wider next to the edges	Severe cracks, both surfaces
V07 D0616	Two small LD areas that should be avoided if bend test specimens are to be machined	No defects noted
I07F D0628	No defects noted	No defects noted
XII07 D0629K Regal	Has an approx. 3/8" layer of HD adjacent to the top surface. The lower portion has relatively uniform appearance	Too porous for any penetrant indications that would be meaningful
XII07 D0630K Regal	There are several short LD lines parallel to the original billet faces, randomly scattered throughout the specimen	Too porous for any penetrant indications that would be meaningful
X07 D0634	Exhibits a LD biscuit-like core w/HD surrounding on 4 sides plus a slightly higher density are in the center	Crack 1/4" from edge runs full length of one face and 1/8" down the opposite
X07 D0635	Top face has an 1/16" wide HD layer: this widens to approx. 1/4" along edges	Appears to have 3 fine cracks on 3 surfaces
XII(5)07 D0638 Regal	No defects noted	No defects noted

LD = low density
HD = high density

168

TABLE IV-1 (CONT)

BILLET TEST DATA

Billet	Radiographic Test	Dye Penetrant
I02AV D0645	Has LD core extending to 1/4-1/2" of edge	Top surface has two 1/8" diam. areas of "slight bleeding"
I02AV D0649	Appears to have hair-like crack from 11 o'clock toward center. Exhibit irregular density-porous center	1/2" diam. area porous. Top and crack 1/8" from edge, then 5/8" along periphery. Bottom short R cracks
I03A D0656	1/8" edge is LD, otherwise billet appears uniform and homogeneous	Too porous to present any defect (identification).
I03A D0657	1/8" around periphery is LD, otherwise billet appears uniform and homogeneous	No defects noted
V03A D0658	No defects noted	Top has approx. 1" diam. porous center. No other defect noted.
V03A D0659	There were no defects noted other than LD caused by chipping around the edges.	Appears to have short radial cracks around periphery, no over 1/8" long.
V(10)07 D0661K	Uniform and homogeneous	Top surface exhibited one "pinpoint" cavity, while the bottom has about 8. No cracking noted.
V(10)07 D0662	Uniform and homogeneous	Top Surface: No defects noted. Bottom surface has four very small cavities: no other defects
V(10)07 D0663	Uniform and homogeneous	No defects were noted
V(10)07 D0664	Uniform and homogeneous	Top and bottom surfaces exhibited grain-like cracking covering 80% of the surface
XII(5)07 D0665 Poco	Uniform and homogeneous	No defects were noted

LD = low density
HD = high density

TABLE IV-1 (CONT)

BILLET TEST DATA

Billet	Radiographic Test	Dye Penetrant
XII(10)07 D0667 Poco	Defects restricted to edges where there was loss of mat'l	No defects were noted
XII(5)07 D0668 Poco	No defects noted on bottom	Circumferential cracking 1/8" from edge. No defects were noted on the top surface.
V(10)07 D0671K	HD inclusion along the edge st 4 o'clock	Slight color appeared in top center and bottom exhibited tiny cavities.
II06A D0672	Unable to penetrate with Avco/SSD equipment	No defects were noted
I02A D0673	1/4" wide HD ring around periphery	No defects noted on top surface, but slight color bleeding in central area of bottom
I07F D0700K	No defects	No defects
I07F D0701K	Low density ring between 3 and 2-1/2" diam.	No defects
V07 Q2315L	No defects	The top surface exhibits tiny, random scattered cavities with a 1/4" crack in the upper right corner. There was slight color bleeding along the right edge, extending approx. 1/4" toward the center with another smaller area near the mid-portion of the left edge. The bottom surface has scattered cavities ranging from .005" to .012" diam with a 1/4" surface crack along the left edge -approx. midway
VIII07 Q2317L	No defects	No defects
V07F D0703	No defects	No defects
V07F D0704	No defects	Tiny cavity on one face
V07F D0705	No defects	Peripheral crack on one face, located approx. 105° and extending into part approx. 3/8"
V07F D0706	High density inclusion and low density spot	No defects

TABLE IV-1 (CONT)

BILLET TEST DATA

Billet	Radiographic Test	Dye Penetrant
II09F D0713	Band of high density around periphery, 1/8" wide. Central is uniform and homogeneous	Two short cracks adjacent to edge on one face
V07 D0715K	No defects	No defects
V07 D0716K	No defects	Two small cavities on one face
V07 D0717K	No defects	Small cavities on both faces
V07 D0719K	No defects	One small cavity on one face
V(10)07 D0720K	No defects	No defects
V(10)07 D0721K	No defects	No defects
VIII07 D0722K	No defects	Very porous
VIII07 D0723K	No defects	One small crack 1 mil deep
VIII07 D0724K	No defects	Slight bleeding, no cracks
VIII07 D0725K	No defects	Slight bleeding, no cracks
II 10 D0726	*	No cracks, areas or porosity
III09 D0727K	*	No cracks, two shallow areas and one spongy area
VIII07 Q2345N	Uniform no defects	Too porous to be meaningful
II06B D0740K	0.035"diam. high density spot at 45° 6-1/2. No evidence of gross cracking seen visually	Cracks on both faces joining in some cases down the sides. Crack pattern is like a 2" diam. circumferential crack with spoke-like cracks radiating from it
III09F D0741	No defects	No defects
II06 D0742K	No evidence of cracking seen visually	As D0740K
II06 D0743K	0.030" diam. high density spot at grid 80° 1. No evidence of gross cracking seen visually	As D0470K
IX09F D0745K	Uniform, no defects	No defects

*Intensity of X-ray insufficient. All Hf based materials are now sent to Arnold Greene Testing Labs.

TABLE IV-1 (CONT)

BILLET TEST DATA

Billet	Radiographic Test	Dye Penetrant
IX09F D0749	Radiography not performed as its work in high density material questionable	No defects
II09F D0750	Radiography not performed as its work in high density material questionable	No defects
XIV09F D0741 Regal	Radiography not performed as its work in high density material questionable	No defects
XIV09F D0752 Regal	Radiography not performed as its work in high density material questionable	Porous with surface inclusions of foreign material
U.S. Borax Billet	Uniform, no defects	No defects
Forging Wafer A	Uniform, no defects	- - - - -
Forging Wafer B	Void, 0.75 x 0.045" wide, 1/2"	- - - - -
cut from V07 D0716K	from edge, otherwise uniform	
Thermal Stress Ring	Uniform, no defects apart from one crack	One radial crack only
II06B D0758K	Not possible	Cracked
VIII07 D0760K Regal	Uniform no defects	Uniform
VIII07 D0761K Regal	Uniform no defects	Uniform
VIII07 D0767K Regal	Uniform no defects	Uniform
VIII07 D0768K Regal	Uniform no defects	Uniform
VIII(19)(5)07 D0771 Regal	Uniform no defects	Uniform
VIII(18)(10)07 D0772 Regal	Uniform no defects	Uniform
II09F D0774K	Not possible	No surface cracking
II(5)06B D0778K	Not possible	No surface cracking
Disc C 1/16" slabs cut	Uniform no defects	Four tiny spots
Disc D from V07 D0716K	Uniform no defects	No defects
II09F D0784	No density variations noted	No defects
II(10)09F D0786	No density variations noted	No defects
V(10)07 D0788	Slightly greater density in center	No defects

TABLE IV-1 (CONT)

BILLET TEST DATA

Billet	Radiographic Test	Dye Penetrant
II06B D0790K	Uniform	Cracked
X(5)07 D0792	Uniform	No defects
X(10)07 D0793	Uniform	No defects
X(15)07 D0794	Uniform	No defects
V(5)07 D0795K	Slightly lower density in center	Short radial cracking around periphery
V(10)07 D0796K	Slightly lower density in center	No defects noted
VIII07 D0797MTFF	Uniform	Indications appear to be restricted to surface
I07 D0801	Uniform	No defects
⁻⁻III07 D0803K	Slightly lower density in center	No defects
IV09F D0804K	Uniform	No defects
XII(20)07 D0805K	Uniform	No defects
IV09F D0807K	Slightly lower density in center	No defects
IV09F D0808K	Slightly lower density in center	No defects
XII(20)07 D0809K	Slightly lower density in center	No defects
XII(20)07 D0810K	Uniform	Many small pits on surface
IV09F D0811K	Slightly lower density	No defects
XII(20)07 D0812K	Uniform	No defects
XV(20)06B D0813	Uniform	No defects
VIII07Q 2374K	Slightly lower density in center	No defects
XIV09FQ 2375K	Axially appears uniform, but top of billet is slightly greater density than bottom	No defects
III(5)09F D0815	Slightly lower in center	No defects

173

TABLE IV-1 (CONT)

BILLET TEST DATA

Billet	Radiography	Dye Penetrant
VIII07 D0803K (thin wafer)	Minor streak variations	No defects noted
I05A D0818*	No variations noted	No defects noted
I05A D0819*	No variations noted	No defects noted
I05A D0820*	No variations noted	No defects noted
I05A D0821*	1/8" low density periphery	No defects noted
IV(40)09F D0824	Not examined	No defects noted
III10A D0825	Not examined	No defects noted
V(5)05A D0828*	No variations noted	No defects noted
V(10)05A D0829*	No variations noted	No defects noted
V(15)05A D0830*	No variations noted	No defects noted
V05A D0831*	No variations noted	No defects noted
V(50)05A D0832*	No variations noted	No defects noted
XII(10)05A D0834*	No variations noted	No defects noted
XII(5)A D0835*	No variations noted	No defects noted
XII(15)05A D0837*	No variations noted	No defects noted
XII(20)05A D0838*	No variations noted	No defects noted
XII(50)05A D0839*	No variations noted	No defects noted (except very porous)
III(50)09F D0841*	Low density streaks	No defects noted
I05A D0842	Slight density variations	No defects noted
V07F D0845K	No variations noted	No defects noted
V07F D0846K	1/8" slight low density periphery	No defects noted
I05A D0848*	1/8" slight low density periphery	No defects noted
V07F D0849	1/2" slight low density periphery	No defects noted
V07F D0850K	Higher density around periphery	No abnormalities
V07F D0851K	Higher density around periphery	No abnormalities
III09F D0852K	Uniform	No abnormalities
III09F D0854K	Higher density around edge	No abnormalities
VIII(17)(15)07F D0858	Uniform	No abnormalities
VIII(19)(15)07F D0860	Uniform	No abnormalities
VIII(18)(10)07F D0861	Uniform	No abnormalities
XIV09F D0869	Uniform	No abnormalities
XIV06B D0874	Uniform	No abnormalities
XV(20)06B D0876	Uniform	No abnormalities
XV(20)06B D0886	Uniform	No abnormalities
XII(20)07F D0889K	Uniform	No Abnormalities

TABLE IV-1 (CONT)

BILLET TEST DATA

Billet	Radiography	Dye Penetrant
V07F D0955K	Uniform and homogeneous	No defects
VIII07F D0956K	Very non-uniform, HD agglomerates randomly scattered	No defects
III06B D0961K	*	No defects
III06B D0962K	*	No defects
VIII(18)(10)07F R35L	Gross LD indications throughout large LD in corner	Graphite particles at surface, no cracks
VIII07F D0965K	Both billets showed very bad mixing by visual	
VIII07F D0967K	observation and were not put through regular NDT schedule	
V07F Q2409	Low density indications scattered throughout	Not performed
VIII(18,10)07F D0973K	Uniform and homogeneous	No defects
I07F D0974K	Uniform and homogeneous	Five radial cracks on both faces
VIII07F D0975K	Lower density central area	Top surface slightly porous
VIII07 D0976K	Uniform and homogeneous	No defects
III(15)09F D1011	Not performed	No indications
I07F D1020K		No defects
III10 R52L	*	No defects
XV(20)10 D1027K	*	No defects
XV(20)10 D1031K	*	No defects
XIV(18,10)09F D1033K	*	No defects
III09F D1034K	*	No defects
III09F D1035K	*	No defects
XIV(18,10)09F D1036K	*	No defects
XIV(18,10)09F D1037K	*	No defects
XII(20)07F R56L	Slight low density region in center	No defects
XV(20)10 D1054K	*	No defects
III(5)09F D1059K	*	No defects
III(5)09F D1061K	*	No defects
XV(20)10 R62L	*	No defects
VIII(18,10)07F R40L (leading edge)	No defects	No defects
V07F R26L (leading edge)	No defects	No defects

*No radiography due to hafnium present.

TABLE IV-1 (CONT)

BILLET TEST DATA

Billet	Radiography	Dye Penetrant
XII(20)07F D0391K	Uniform	No abnormalities
XII(20)07F D0892K	Uniform	No abnormalities
VIII07F D0893K	Uniform	No abnormalities
VIII07F D0896K	Uniform	No abnormalities
VIII07F D0897K	Uniform	No abnormalities
II09F D0898	Uniform	No abnormalities
II 10 D0899	Uniform	No abnormalities
V07F D0900K	Uniform	No abnormalities
V07F D0901K	Two low density specks	No defects
V07F D0902K	No abnormalities	No defects
VIII(18)(10)07F D0904K	Uniform and homogeneous	No defects
I07F D0905K	1/2" thick band of higher density around periphery	No defects
III 10 D0906K	Not performed	No defects
III 10 D0907K	Not performed	No defects
III 10 D0908K	Not performed	No defects
II09F D0909K	Not performed	No defects
II09F D0911K	Not performed	No defects
II09F D0913K	Not performed	Pinpoint cavity
II 10 D0914K	Not performed	Minute porosity
VIII(18)(10)07F D0916K	Uniform and homogeneous	No defects
VIII(18)(10)07F D0917K	Uniform and homogeneous	No defects
VIII(18)(10)07F D0919K	Uniform and homogeneous	No defects
VIII(18)(10)07F D0920K	Uniform and homogeneous	No defects
VIII(18)(10)07F D0922K	Uniform and homogeneous	No defects
II 10 D0933K	Not performed	No defects
V07F R26L	Uniform and homogeneous	No defects
V07F R31L	Uniform and homogeneous	No defects
VIII(18)(10)07F R33L	Lower density center with high density inclusions randomly located	Porous center, different on either face
II 10 D0934K	*(see footnote)	No defects
I07F D0936K	Two low density spots located 1/2" from edge	No defects
I07F D0937K	Uniform and homogeneous	Cracked
I07F D0940K	Uniform and homogeneous	No defects
II 10 D0941K	*	No defects
II 10 D0943K	*	No defects
II 10 D0944K	*	No defects
II 10 D0945K	*	No defects
V07F D0946K	*	No defects
III 10 D0948K	*	Cracked around edge-bordered by 1/2" wide concentric ring
I07F D0950K	Uniform and homogeneous	No defects
III09F D0951K	*	No defects

TABLE IV-2

BILLET DIAMETRICAL SLICE DATA

Billet	Radiographic Test	Dye Penetrant
V02A D0612	Exhibits minute voids. One 1/2" diam. area includes all except the larger	Appears to have foreign material embedded on surface
I02A D0613	Exhibits a film density blemish and one delam. - like crack, 1/4" long	No defects noted, except "flake" indication on one surface
V02A D0614	Appears uniform and homogeneous	Porous: bleeds on both surfaces
XII(5)07 D0615 Thorn	Multiple cracking in lower central areas. Top surface has higher density that gets wider next to the edges	Severe cracks, both surfaces
V07 D0616	Two small LD areas that should be avoided if bend test specimens are to be machined	No defects noted
I07F D0628	No defects noted	No defects noted
XII07 D0629K Regal	Has an approx. 3/8" layer of HD adjacent to the top surface. The lower portion has relatively uniform appearance	Too porous for any penetrant indications that would be meaningful
XII07 D0630K Regal	There are several short LD lines parallel to the original billet faces, randomly scattered throughout the specimen	Too porous for any penetrant indications that would be meaningful
X07 D0634	Exhibits a LD biscuit-like core w/HD surrounding on 4 sides plus a slightly higher density area in the center	Crack 1/4" from edge runs full length of one face and 1/8" down the opposite
X07 D0635	Top face has an 1/16" wide HD layer: this widens to approx. 1/4" along edges	Appears to have 3 fine cracks on 3 surfaces

LD = Low Density
HD = High Density

177

TABLE IV-2 (CONT)

BILLET DIAMETRICAL SLICE DATA

Billet	Radiographic Test	Dye Penetrant
XII(5)07 D0638 Regal	No defects noted	No defects noted
XII(10)07 D0639 Regal	Exhibits fine LD lines, parallel with original faces, almost dead center. Care should be exerted if bend test specimen are planned from this part (visible on surface)	There were two cracks on one face
XII(15)07 D0641	Relatively uniform and homogeneous radiographic film density throughout	A 1/8" long crack was detected on one surface
XII(20)07 D0642 Regal	No defects were noted	No defects were noted
XII(10)07 D0667 Poco	No defects	No defects
XII(5)07 D0668 Poco	No defects	No defects
V(10)07 D0671K	No defects	No defects
II06A D0672	No defects	No defects
II09F D0713	No defects*	Laminar crack; an edge chip with cracks running parallel to the laminar crack propagating inward to join flaws that appear to start on the opposite edge, restricted to the lower half
V(10)07 D0720K	No defects	No defects
V(10)07 D0721K	No defects	No defects
III06B D0740K	+	Cracking on four billet surfaces penetrating about 1/4" into slab
III09 D0741	+	No defects
II06B D0742K	+	As in 740K
II06B D0743K	+	As in 740K

TABLE IV-2 (CONT)

BILLET DIAMETRICAL SLICE DATA

Billet	Radiography	Dye Penetrant
III(10)09F D0786	No variations noted	No defects noted
V(10)07 D0788	No variations noted	No defects noted
V(5)07 D0795K	No variations noted	No defects noted
VIII07 D0797	No variations noted	No defects noted
XII(20)07 D0805	No variations noted	No defects noted
IV09F D0808K	No variations noted	No defects noted
XV(20)06B D0813	No variations noted	No defects noted
III(5)09F D0815	No variations noted	No defects noted
II(10)A D0823K	No variations noted	No defects noted
IV(40)09F D0824	No variations	No defects
III10A D0825	No variations	No defects
III(50)09F D0841	No variations	No defects
I05A D0842[*]	No variations	No defects
I05A D0848[*]	No variations	No defects
V07F D0850K	High and low density specks	Very porous
II09F D0898	Not performed	No indications
III 10 D0899	Not performed	Ground surface porous
I07F D0940K	Slight low density in center	No indications

TABLE IV-2 (CONT)

BILLET DIAMETRICAL SLICE DATA

Billet	Radiographic Test	Dye Penetrant
IX09F D0745	+	No defects
IX09F D0749	+	One small pit on smaller face
II09F D0750	+	No defects
XIV09F D0751	+	No defects
XIV09F D0752	+	No defects

*Radiographed with the 10 mC Co^{60} isotope.

+Radiographic examination not possible for hafnium based billets.

DOCUMENT CONTROL DATA - R & D

(Security classification of title, body of abstract and indexing annotation must be entered when the overall report is classified)

1. ORIGINATING ACTIVITY (Corporate author)	2a. REPORT SECURITY CLASSIFICATION
ManLabs, Inc. 21 Erie Street Cambridge, Massachusetts 02139	UNCLASSIFIED
	2b. GROUP N/A

3. REPORT TITLE

Research and Development of Refractory Oxidation Resistant Diborides:
Part II, Volume II: Processing and Characterization

4. DESCRIPTIVE NOTES (Type of report and inclusive dates)

Technical Documentary Report, September 1967 to May 1969

5. AUTHOR(S) (First name, middle initial, last name)

Clougherty, Edward V., Hill, Russell J., Rhodes, William H., and Peters, Edward T.

6. REPORT DATE January 1970	7a. TOTAL NO. OF PAGES 195	7b. NO. OF REFS 21
8a. CONTRACT OR GRANT NO. AF33(615)-3671 b. PROJECT NO. 7350 c. Task No. 735D01 d.	9a. ORIGINATOR'S REPORT NUMBER(S) N/A 9b. OTHER REPORT NO(S) (Any other numbers that may be assigned this report)	

10. DISTRIBUTION STATEMENT This document is subject to export controls and each transmittal to foreign governments or foreign nationals may be made only with prior approval of the Metals and Ceramics Division, Air Force Materials Laboratory (MAMC), Wright-Patterson Air Force Base, Ohio 45433

11. SUPPLEMENTARY NOTES N/A	12. SPONSORING MILITARY ACTIVITY AFML(MAMC), WP-AFB, Ohio 45433

13. ABSTRACT

Zirconium and hafnium diboride were procured in several 50 to 300 pound quantities. Powder specifications were developed for hot pressing grades of ZrB_2 and HfB_2 for processing of compositions containing additions of SiC and/or C.

Several hundred 2 and 3 inch diameter billets were fabricated and characterized by destructive and nondestructive methods. Extensive thermal, physical, chemical and mechanical property measurements, thermal stress resistance tests and oxidation resistance evaluations were performed for the range of compositions and microstructural variations of grain size and porosity prepared by hot pressing. The sizes of billets fabricated by hot pressing was scaled-up to 6 inches square by 2 to 3 inches high with no reduction in physical and mechanical integrity.

A system of ceramic additives, principally SiC and/or C employed with ZrB_2 and HfB_2 produced compositions which were hot pressed to full density with fine grain sizes of 2 to 10 microns. Compositional variations of SiC and C produced structures of varying oxidation resistance, mechanical properties and thermal stress resistance. The chief effect of the addition of SiC is an improvement in oxidation resistance; the addition of C, a decrease in the bulk elastic modulus. The additions singularly and combined effected improvements in mechanical properties principally by lowering the fabrication temperature to permit full densification without appreciable grain growth. The additions reduce diboride powder specifications for hot pressing with regard principally to allowable metal oxide and carbide

DD FORM 1473 REPLACES DD FORM 1473, 1 JAN 64, WHICH IS OBSOLETE FOR ARMY USE.

DOCUMENT CONTROL DATA - R & D		
(Security classification of title, body of abstract and indexing annotation must be entered when the overall report is classified)		

1. ORIGINATING ACTIVITY (Corporate author) ManLabs, Inc. 21 Erie Street Cambridge, Massachusetts 02139	2a. REPORT SECURITY CLASSIFICATION UNCLASSIFIED
	2b. GROUP

3. REPORT TITLE

4. DESCRIPTIVE NOTES *(Type of report and inclusive dates)*

5. AUTHOR(S) *(First name, middle initial, last name)*

6. REPORT DATE	7a. TOTAL NO. OF PAGES	7b. NO. OF REFS

8a. CONTRACT OR GRANT NO. b. PROJECT NO. c. d.	9a. ORIGINATOR'S REPORT NUMBER(S) 9b. OTHER REPORT NO(S) *(Any other numbers that may be assigned this report)*

10. DISTRIBUTION STATEMENT

11. SUPPLEMENTARY NOTES	12. SPONSORING MILITARY ACTIVITY

13. ABSTRACT (CONT)

impurity content; an in-processing reduction in initial oxygen content is effected by the additives.

Limited examination of other processing procedures performed without obtaining separate powders particularly suitable for individual methods provided information relative to the utilization of methods other than hot pressing. Silicon carbide could not be retained in plasma sprayed coating nor could it be formed along with ZrB_2 as a pyrolytically deposited coating. Pressureless sintering studies carried out with small specimens suggest that additions of reactive activating agents such as zirconium hydride enhance consolidation of ZrB_2 and ZrB_2-SiC compositions. Hot isostatic pressing produced dense, fine grained structures, one half inch diameter by 2 inches long of ZrB_2 and HfB_2 with no intentional additive. Compositions containing SiC and small amounts of carbon (10 volume percent) were also consolidated to near full density with no significant grain growth. Arc casting was successfully employed to produce a structure comprised of a ZrB_2 matrix with a ZrB_2+SiC eutectic and large graphite particles; a sound billet 2 inch diameter by 4 inches long was prepared. Attempts to employ conventional hot pressing to prepare filament and fiber reinforced structures using SiC whiskers, W filaments and Thornel-25 carbon yarn reinforcements were generally unsuccessful. The best results were obtained with the Thornel yarn in a ZrB_2 matrix.

This abstract is subject to special export controls and each transmittal to foreign governments or foreign nationals may be made only with prior approval of the Air Force Materials Laboratory (MAMC), Wright-Patterson Air Force Base, Ohio 45433.

14. KEY WORDS	LINK A		LINK B		LINK C	
	ROLE	WT	ROLE	WT	ROLE	WT
Diboride						
Diboride and Carbon Compositions						
Diboride and Silicon Carbide Compositions						
Fabrication of Diboride Compositions						
Hot Pressing of Diboride Compositions						
Characterization of Diboride Compositions						
Nondestructive Testing of Diboride Compositions						
Oxidation Resistant Materials						
High Strength Ceramic Materials						